CARDIAC PHENOTYPES IN THE COLLABORATIVE CROSS: DERIVATION AND UTILITY OF CARDIAC REFERENCE RANGES FOR *MUS MUSCULUS*

A Dissertation

by

JULIA L POPP

Submitted to the Graduate and Professional School of
Texas A&M University
in partial fulfillment of the requirements for the degree of

DOCTOR OF PHILOSOPHY

Chair of Committee,	David Threadgill
Committee Members,	Ivan Rusyn
	Robert Burghardt
	Michael Criscitiello
Head of Department,	Ramesh Vemulapalli

August 2021

Major Subject: Biomedical Sciences

ABSTRACT

Contemporary approaches for developing new interventions and for pre-clinical risk evaluation include assessments for cardiovascular structure and function, frequently performed in a variety of animal and *in vitro* models, but generally lack details on normal species-specific reference ranges similar to what exists for humans. The genetically diverse Collaborative Cross (CC) mouse reference population allows for modeling genetic variability equivalent to that present in the human population. The CC population was used to develop cardiac reference values for *Mus musculus*, identify candidate genes that are associated with those phenotypes, and demonstrate inter-individual susceptibility to two known cardiotoxicants. Heart function was analyzed in males and females from 58 CC strains and C57BL/6J using high frequency ultrasound under both conscious and anesthetized conditions, as well as conscious electrocardiography to develop two standard deviation-based reference ranges for *Mus musculus* similar to what exists for humans. Additionally, genetic analysis was performed on the cardiac phenotyping data to determine candidate genes for genetic control of clinically relevant phenotypes. A subset of the 58 CC strains was also used to demonstrate inter-individual susceptibility and response to isoproterenol and chloroquine. Strain was a significant source of variability with all data sets, and associated genes not previously linked to cardiac phenotypes in mice, but those linked in humans were found. These reference ranges and genetic analysis in the CC are a novel approach to cardiovascular research, ultimately allowing more accurate diagnoses and informative safety assessments in humans.

ACKNOWLEDGMENTS

First and foremost, I would like to thank God, who has granted countless blessings, knowledge, and opportunity to me, so that I have been finally able to accomplish this dissertation..

I would like to thank my committee chair, Dr. David Threadgill, and my committee members past and present, Dr. Ivan Rusyn, Dr. Robert Burghardt, Dr. Michael Criscitiello, Dr. Roula Mouneimne, and Dr. Gonzalo Rivera for challenging me and for their guidance and support throughout the course of this research.

Thanks also go to my colleagues and the department faculty and staff for making my time at Texas A&M University a unique and fulfilling experience.

Thanks to my friends in the Ultimate Frisbee community for making College Station my home for the last 7 years.

Finally, thank you to my mother, father, older sister, and younger brother for their love and support, despite many unexpected financial burdens and emotional outbursts.

CONTRIBUTORS AND FUNDING SOURCES

Contributors

This work was supported by a dissertation committee consisting of Dr. David Threadgill of the Department of Molecular and Cellular Medicine and Dr. Ivan Rusyn of the Department of Veterinary Integrative Biosciences, Dr. Robert Burghardt of the Department of Veterinary Integrative Biosciences, and Dr. Criscitiello of the Department of Veterinary Pathobiology.

The data analyzed for Chapter 2 was provided by Professor Weihsueh Chiu.

All RNA sequencing data and expression analysis was performed by the Texas A&M Institute for Genome Sciences and Society (TIGSS).

Much of the current *in vitro* work described in Chapter 5 was performed with Krishna Patel.

All other work conducted for the dissertation was completed by the student independently.

Funding Sources

Graduate study was supported by by USEPA grant (RD83580201). This dissertation's contents are solely the responsibility of the grantee and do not necessarily represent the official views of the USEPA. Further, USEPA does not endorse the purchase of any commercial products or services mentioned in the dissertation.

NOMENCLATURE

2D	Two Dimensional
Ach	Acetylcholine
ALS	Amyotrophic Lateral Sclerosis
ANS	Autonomic Nervous System
AV	Atrioventricular
β-AR	Beta Adrenergic Receptor
BDNF	Brain-Derived Neurotrophic Factor
BPM	Beats Per Minute
CaMKII	Ca^{2+}/calmodulin-dependent protein kinase II
CC	Collaborative Cross
CO	Cardiac Output
CV	Coefficient of Variation
DO	Diversity Outbred
ECG	Electrocardiography
EDV	End Diastolic Left Ventricular Volume
EF	Ejection Fraction
EPA	Environmental Protection Agency
ESV	End Systolic Left Ventricular Volume
FS	Fractional Shortening
GLS	Global Longitudinal Strain
GWAS	Genome-wide Association Studies
HERG	Human ether-a-go-go-related gene

HF	High Frequency
HR	Heart Rate
HRV	Heart Rate Variability
IACUC	Institutional Animal Care and Use Committee
iNOS	inducible Nitric Oxide Synthase
IPA	Ingenuity Pathway Analysis
iPSC	induced Pluripotent Stem Cell
IVIVE	*In Vitro* to *In Vivo* Extrapolation
IVS	Interventricular Septum
Jax	The Jackson Laboratory
LDLR	Low-density Lipoprotein Receptor
LIF	Leukemia Inhibitory Factor
LOD	Logarithm of the Odds
LQTS	Long QT Syndrome
LV	Left Ventricle
LVID	Left Ventricular Internal Diameter
LF	Low Frequency
MI	Myocardial Infarction
MEF	Mouse Embryonic Fibroblast
MMP	Matrix Metalloproteinase
MUGA	Mouse Universal Genotyping Array
MVO_2	Myocardial Oxygen Consumption
NE	Norepinephrine
PCA	Principal Component Analysis
pNNx	Percentage of Normal consecutive N-N intervals differing by $>$x ms

QTL	Quantitative Trait Loci
QTc	QT interval Corrected
RI	Recombinant Inbred
rMSSD	Root Means Successive Square Differences
RNA	Ribonucleic Acid
ROI	Return of Investment
ROS	Reactive Oxygen Species
SA	Sinoatrial
SD	Standard Deviation
SNP	Single Nucelotide Polymorphism
SV	Stroke Volume
TIGSS	Texas A&M Institute for Genome Sciences and Society
TdP	Torsades de Pointe
TrkB	Tyrosine-Related Kinase Receptor B
TSCA	Toxic Substances Control Act
STE	Speckle-Tracking Echocardiography

TABLE OF CONTENTS

Page

LIST OF FIGURES

FIGURE Page

LIST OF TABLES

TABLE Page

1. INTRODUCTION

1.1 Overview

About 655,000 Americans die of heart disease each year, and the heart's limited ability to regenerate plays a role in leaving millions worldwide vulnerable to heart pathologies. Contemporary approaches for developing new interventions and for pre-clinical risk evaluation include assessments of cardiovascular structure and function, frequently performed in a variety of animal and *in vitro* models. Although it is well established that genetic background has an impact on susceptibility or response to external stimuli like toxicants, drugs, diet, and exercise, consideration of genetic background as a potential response modifier is usually not considered. Adverse cardiac events are the most sensitive indication for determining threshold exposure levels of xenobiotics. Yet because of the lack of considering genetic background, cardiac safety of many chemicals has been incompletely tested. Population-based animal models have become a valuable tool for evaluation inter-individual variability in response to environmental perturbations, and are well suited to improve cardiac safety testing. The most relevant for safety testing is the genetically diverse Collaborative Cross (CC) mouse reference population that allows modeling of the variability that is present in the human population.

1.2 Challenges in Cardiovascular Research

Despite major advances in cardiovascular research in the last 50 years, cardiovascular disease remains the leading cause of death globally, with lower investment compared to incidence than for other diseases like cancer, neurological disorders, or infection [1, 2]. A further complication is that translational approaches from animals are inadequate due to the limited diversity included in most studies. Additionally species differences in receptor diversity and protein function result in disparities that cannot always provide accurate targets for therapy in humans. However, the cost of larger, more translatable animals is not insignificant; the cost the same research in a dog is 37% of a chimpanzee, and a mouse is 2% of the dog [3]. Most animal cardiac assessments are

performed in acutely prepared or anesthetized animals, but anesthesia alters cardiovascular control by the autonomic nervous system and secondarily alters responses to common interventions, such as drugs [4]. This is illustrated in conflicting reports of two studies investigating the inotrope omecamtiv mecarbil to explore its risk for increased myocardial oxygen consumption MVO_2; a study performed on conscious animals found that elevated MVO_2 was not significant [5], while another study using anesthetized animals found significant increases in MVO_2 [6].

The heart itself offers unique challenges for therapeutic design as it possesses very little regenerative qualities, leaving millions vulnerable to heart failure [7]. Although most preventable deaths are the result of cardiovascular conditions [8], cardiac medical care is typically diagnostic; preventive actions are enacted with personal choices in diet, exercise, and frequent health visits. There are also sociological factors to consider as well. It is estimated that non-adherence occurs in over 60% of cardiovascular patients, with socioeconomic status having a measurable impact on cardiovascular health and treatment [9].

1.2.1 Regulatory environment for cardiovascular risk assessment

Despite major advancements in cardiovascular drug development over the last century, numerous critical challenges have arisen recently [10]: i) in all therapeutic areas, drug-induced cardiovascular toxicity occurred more frequently than hepatotoxicity [11]; ii) high cost of cardiovascular outcome trials in the current regulatory environment [2]; and iii) dependency on complicated clinically-evident cardiovascular end-points rather than using biomarkers or surrogate outcomes [2].

Cardiovascular disease is the leading cause of morbidity and mortality in the United States, and most preventive actions, when employed, are universally effective (diet, exercise, smoking cessation) [12]. Even if all preventive actions were taken, other risk factors such as environmental and occupational exposure to unknown chemicals, recreational and prescribed drug use, and comorbidity with other diseases such as diabetes, lipid metabolism disorders, and epilepsy would still contribute to cardiovascular disease. Combinations of any and all of these factors create immense challenges in cardiovascular risk assessment [13].

Cardiotoxicity testing, while necessary for both commercial chemicals and preclinical safety pharmacology, has very different regulatory requirements and available resources depending on the exposure source. For environmental chemicals, the Toxic Substances Control Act (TSCA 1976), revised in 2016, originally allowed the 62,000 chemicals already on the market to be used without safety testing. However, the Environmental Protection Agency (EPA) can now require testing of chemicals currently in use, as well as require more stringent testing for new chemicals. Only recently has the EPA adapted high throughput testing methods used in the pharmaceutical industry to test the large inventory of environmental chemicals not previously tested [14]. Considering that 33% of all drugs withdrawn from the market between 1998 and 2008 were due to cardiac complications, higher than any other organ or system [15], there is a likelihood that many untested environmental chemicals will have cardiotoxicities.

Approaches to cardiovascular risk assessment in the pharmaceutical industry have been effective for acute adverse drug effects, but long-term exposure is often not assessed, or the adverse outcome is only observed when large heterogeneous populations are exposed during clinical trials [16]. In any therapeutic area, attrition of small molecules and biologics in clinical trials due to cardiovascular complications is the most common cause; this indicates the need for more accurate preclinical cardiac risk assessment. Current cardiac safety testing of uncharacterized xenobiotics focuses mainly on electrophysiology and some ion channels of the cardiac muscle in healthy animals, despite humans commonly possessing co-morbidities or co-therapies that can affect their normal electrophysiological and ion channel function and expression [17].

While assessing cardiac safety on all drugs being developed in pharmaceutical companies is required, it is important to note that the investment in cardiovascular drug development has severely declined the last 20 years. The heart is a sensitive organ and increased testing requirements drive up the cost of development, thereby increasing investment risk and low return on investment (ROI). The current regulatory environment requires expensive tests that ironically assess clinically-evident endpoints on the least regenerative organ in the body, such as myocardial infarction (MI), hypertrophy, and ejection fraction (EF), rather investing in research for earlier, cheaper, and simpler tests

assessing biomarkers and surrogate endpoints. The need for more accurate cardiac risk assessment is essential, especially in preclinical studies, both for environmental chemicals and pharmaceuticals [2].

1.3 Mechanisms of cardiac function and cardiotoxic dysfunction

The heart is a muscle composed mostly of cardiomyocytes, endothelial cells, and fibroblasts; its key function supports blood circulation which is essential for human life. Its rhythmic waves of electrical activity ensure coordinated contraction of different regions of the heart. The heart is a dynamic organ in its ability to remodel and adapt due to exercise or injury, and yet it is unable to regenerate. Most adult human cardiomyocytes are mononucleated but polyploid and therefore unlikely to enter the cell cycle [7]. This makes the heart an especially vulnerable organ, and when it begins to fail, is very conspicuous. Unhealthy diet, lack of exercise, smoking, and obesity can all lead to heart disease. Any xenobiotic such as pharmaceuticals, illicit drugs, or environmental toxicants, in addition to these underlying diseases and complications, can also contribute to cardiovascular diseases in many uncharacterized adverse outcome pathways.

The cardiomyocytes that make up the heart are the smallest unit of contraction; they can shorten 10% in both the longitudinal and transverse directions [18]. Contraction of the heart starts from the sinoatrial (SA) node to contract the atria and then passes through the atrioventricular (AV) node causing the ventricles to contract. In healthy individuals, there is an association between the electrical and mechanical activities of the heart (Figure 1.1); the electrical activity follows a predefined cycle, while the mechanical activity is much less uniform [19].

1.3.1 Electrical and mechanical properties of the heart

The electrical activity of the heart is measured by electrocardiogram (ECG) which is a temporal recording of the changes in electrical charge in all four chambers of the heart [20]. Ionic current flows across cardiomyocytes as a result of Na^+, K^+, and Ca^{2+} ions moving across selectively permeable ion channels in the cell membrane; their movement follows the electrochemical gradient, which is maintained by active transporters. The specialized neuronal tissue, the SA node

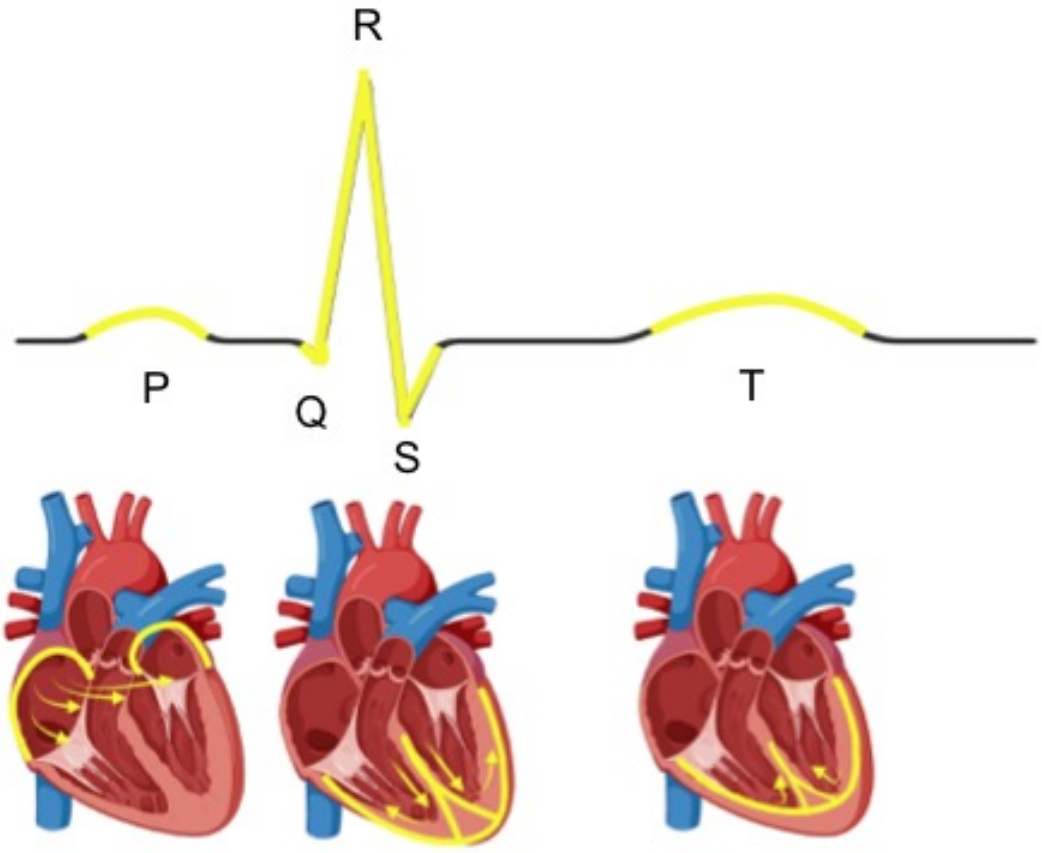

Figure 1.1: An ECG represents the electrical current moving through the heart during a heartbeat. The current's movement is divided into parts, and each part is given an alphabetic designation in the ECG.

is located in the right atrium of the heart and spontaneously and rhythmically depolarizes, causing a wave of depolarization to spread over the atria; on the ECG this manifests as the P wave. Once depolarization reaches the AV node near the basal side of the interventricular septum (IVS), the AV node slows the propagation allowing the ventricles to fill. The electrical wavefront then passes through specialized fibers to spread the depolarization throughout the lateral walls of the ventricles and IVS. The PR interval, which has very little measurable potential, is the time from AV node activation to the specialized fibers. As the current passes through the ventricles, the QRS complex is recorded as the ventricles are depolarized. The repolarization of the atria is also recorded during this time but cannot be visualized. The ST interval corresponds to the plateau phase of action

potential, and the final positive T wave corresponds to repolarization of the ventricles [20].

During the mechanical component of a cardiac cycle, from diastole to systole, the left ventricle (LV) shortens, thickens, and twists. Although each cardiomyocyte can only shorten 10% of its length, there are layers in the myocardium in which three directions of cardiomyocyte fibers reside. These layers, sliding over each other as the heart contracts, produce shear and allow the heart as a whole to shorten and twist more than 10% [21]. This myocardial deformation on the longitudinal, circumferential, and radial axes can be measured as strain and is expressed as a percentage change from the original dimension at diastole [22]. There are three perpendicular axes that can be quantified, but the most clinically relevant is global longitudinal strain (GLS), which is the earliest predictor of heart failure [23]. GLS describes the relative length change of the LV myocardium at end-diastole and end-systole, and healthy human values fall between -15.9% to -22.1% [24]. Although it is expressed as a negative value, researchers refer to the absolute value when indicating increases and decreases in GLS. Echocardiography is the most common noninvasive technique for visualizing the beating heart in real-time because of its speed and availability. Speckle-tracking echocardiography (STE), used to quantify GLS, consists of software that uses the grey-scale images to identify bright speckles present in the myocardium and tracks them frame by frame throughout the cardiac cycle [21]. This software can reveal minute changes in the myocardium due to cardiotoxicants [25], drugs [26], and infection [27], as evidenced by a lower GLS, lower ejection fraction (EF), or changes in wall thickness.

1.3.1.1 Autonomic control of the heart

While the SA node spontaneously initiates the contraction of the heart, without neuronal and hormonal influence it would consistently contract at 100 beats per minute (bpm) [28]. The body's dynamic need for oxygen and nutrients cause variability in heart rate, and in order to respond to these needs, the nervous system and hormones regulate the pacing of the SA node.

The sympathetic nervous system in the heart controls heart rate in "fight or flight" circumstances. Preganglionic nerves release acetylcholine (ACh) and postganglionic nerves release norepinephrine (NE), and these are called adrenergic fibers. The heart tissue specifically contains $\beta 1$

adrenergic receptors to receive signals from the nervous system, and their activation has a positive chronotropic effect (increase in heart rate), positive inotropic effect (increase in force of contractility), and a positive dromotropic effect (enhancement of conduction velocity). Additionally, renin release by kidneys regulates blood pressure, sodium levels, and blood volume [28].

The parasympathetic nervous system plays an antagonistic role in regulating heart function; its role is to control basal and rest state functions of the body. Preganglionic and postganglionic neurons release ACh, and in the heart, this inhibits contraction of cardiomyocytes by activating M_2 muscarinic receptors. Activation of these receptors, which are mainly in nodal and atrial tissue, has negative chronotropic, inotropic, and dromotropic effects [28].

All these features of the autonomic nervous system serve to regulate a crucial phenotype in mammals: heart rate variability (HRV). HRV is considered a surrogate parameter to evaluate the complex relationship between the brain and the heart; increased HRV indicates a dynamic and flexible relationship. Studies have shown that a higher HRV is associated with better health [29, 30, 31]. The ECG signal is used to extract autonomic functional parameters from the heart including HRV. The distances between QRS complexes is N-N. In time domain analysis, describing how the signal changes over time, important parameters include short term variation in HR via root means successive square differences (rMSSD), and cardiac parasympathetic activity via percentage of normal consecutive N-N intervals differing by >x ms (pNNx). While this method of analysis is useful, it is most often used in humans where data collection can be hours long without disturbances. Frequency domain analysis, in which the length of each N-N is transformed into waves to measure their frequency, can be performed with multiple short-term signals. The highest frequency (HF) waves is understood as a surrogate for parasympathetic activity, and low frequency (LF) reflects increased sympathetic activity. The range of values for each frequency depends on the species, and the sum of all spectra is referred to as Total Power, which estimates the total capability of the body for autonomic regulation [32].

1.3.2 Cardiotoxicity

Severe cardiotoxicity can result in arrhythmias, myocardial infarction, and myocardial hypertrophy. However, many studies show that these are conspicuous, late-stage disease endpoints, and much earlier biomarkers or other surrogate endpoints are frequently overlooked [33]. Drug-induced myocardial damage is common, and with closer monitoring of these earlier stage markers, treatments could be terminated before damage becomes irreversible. While GLS is a newly emerging phenotype to predict heart failure sooner [34], as well as perturbations in electrophysiology, the current definition of cardiotoxicity is left ventricle ejection fraction decrease of 10% to less than 55% [35].

At the cellular level, cell death occurs via apoptosis, autophagy, and necrosis. Deterioration in mitochondrial function, endoplasmic reticulum stress, calcium imbalance, and enhanced production of reactive oxygen species (ROS) are just a few of the cellular injuries that can lead to cell and tissue death [35]. Mitochondria have an essential role in cardiomyocyte homeostasis, and it has been shown that drug-induced mitochondrial dysfunction leads to cardiovascular dysfunction [36]. Rather than generating new functional heart muscle, cardiomyocyte death leads to scarring and hypertrophy and therefore myocardial dysfunction [37].

Often in toxicology, changes in electrophysiology are the earliest signs of myocardial dysfunction [20]. Electrophysiology reflects instantaneous changes in the biochemical processes of the heart that can directly influence the biophysical properties of cardiomyocytes. A pathological Q wave and ST elevation can indicate previous myocardial infarction [38], a prolonged PR interval can suggest AV block [39], changes in QRS duration or morphology can indicate delays in conduction [40], and a prolonged QT interval, corrected for heart rate, can lead to torsade de pointes (TdP), which is a dangerous form of ventricular tachycardia [41]. The QT interval is positively correlated with left ventricular mass in normotensive obese patients [42].

In terms of the whole organ, there are two types of cardiac adverse effects: functional and structural. Structural injuries can include cardiomyocyte injury, vascular injury, change in cardiac mass, and neoplasia [43]. Functional changes that can occur as a result of cardiotoxicity include change

in blood pressure, heart rate, contractility, as well as any perturbations to normal electrophysiology as evidenced by ECG [44]. Some xenobiotics can affect the integrity of the heart and induce structural changes such as myocardial injury that then cause functional changes like impaired contractility. Conversely, chronic exposure to a xenobiotic may affect the heart electrophysiologically and have adverse effects of contractile proteins, leading to remodeling [45].

1.4 Genetic control and inter-individual variability of cardiac phenotypes

Previous studies have identified a few cardiovascular traits that exhibit Mendelian inheritance. For example, the low-density lipoprotein receptor (LDLR) gene was found to have exon deletions that caused hypercholesterolemia [46]. Long QT syndrome (LQTS) [47], Marfan's syndrome [48], and severe Mendelian hypercholesterolemia [49], have single causal genes that confer large effects on the associated cardiac phenotype. However, most cardiovascular traits are more challenging to characterize as they are due to the interplay between many genetic and non-genetic factors. Identifying polygenes contributing to most cardiovascular phenotypes is challenging since many are also susceptible to environmental factors through the epigenome [50]. The functional parameters of the heart, such as ejection fraction (EF), global longitudinal strain (GLS) and QT interval, are heritable and under genetic control in humans [51, 52, 53, 54, 55].

Mapping genetic loci associated with traits involves the localization of genes underlying phenotypes on the basis of correlation with DNA polymorphisms [56]. Genetic association studies compares presence or absence of phenotypes with the genetic variants across the genome; single nucleotide polymorphisms (SNPs) are typically used to develop a catalog of common human genetic variants for association testing. Closely linked alleles tend to be inherited as a block over generations, which is called a haplotype. When phenotypic values have quantitative measures, genetic association studies are typically called quantitative trait locus (QTL) analysis. Candidate genes are then identified and usually followed by positional cloning and gene replacement to establish a functional relationship to demonstrate causality.

While various environmental factors contribute to the broad range of cardiac disorders and their causes, they have in common that the inherited DNA sequence variants play a role in conferring

risk for disease. A number of factors can influence susceptibility and severity of response: intrinsic (genetics, life stage) and extrinsic (diet, existing health conditions, co-occurring drug therapies), leading to inter-individual variability of phenotypes. Genome-wide association studies (GWAS) can identify genes responsible for potential risk, but typically do not consider extrinsic factors causing complex disease and therefore fail to estimate population-wide response variability [57]. Extrinsic factors are harder to predict and model in preclinical risk assessment.

Experimental animal models for risk assessment are the gold standard in research, but generally do not have a genome-wide representative population that is used for QTL analysis. For example, cardiac safety testing, although thorough testing is performed in different species for various routes of exposure, dose, and specific organ and cell type sensitivities, is usually only performed in homogeneous populations that lack genetic diversity seen in human populations [58]. Extrapolating animal data to humans is challenging, but the use of homogeneous, inbred animals exacerbates the ability to make inferences about human variation. Including genetic diversity should greatly enhance the translatability of experimental animal data to humans. It was previously thought that the mouse was a poor model for Ebola infection consequences since common laboratory mice did not display hemorrhagic fever. However, it was shown that with a genetically diverse panel of mice, a subset demonstrated the same frequency of hemorrhagic fever as the human population [59]. Studies using diverse strains have challenged the idea that mice or other mammals are poor models for the immune system [60], amyotrophic lateral sclerosis (ALS) [61], and toxicology [62]. Since gene-environment interactions underlie adverse toxic events, integrating genetic diversity can lead to better investigations that can identify sensitive sub-populations and quantify associated susceptibilities, as well as inform molecular pathways contributing to toxicity. Even with regard to dose-response testing, using population-level data helps eliminate bias that may occur with individual experimental models being overly sensitive or resistant. Without considering genetic variability as a factor in adverse outcome responses, risk assessment will continue to be insufficient to protect human health.

1.5 Mouse populations as a cardiovascular model

Due to the physiological similarity to humans, small size, relatively inexpensive housing costs, and short gestation and life span, the mouse model is the most commonly used mammalian model. The mouse model has the most developed genetic resources with publicly available dense SNP databases across dozens of strains [63]. It is the best genetically characterized mammalian model, and yet a single strain, the C57BL/6 mouse, is far and away the most commonly used strain in biomedical research. This includes FDA drug and EPA chemical testing requirements, inevitably leading to significant failure in translation to the genetically diverse human population. However, the C57BL/6J mouse is the gold standard in toxicity research, and yet its heart has been characterized as an abnormal, eccentric hypertrophic "athlete's heart" [64]. Interpreting data from one genome in one species to a population of another species is short-sighted and lacks the ability to distinguish small differences in phenotypes, and therefore differential adaptive responses. The use of a genetically diverse mouse population has been shown to predict and recapitulate inter-individual variability in cardiovascular health [64, 65, 66, 67], cancer[68, 69], toxicology [70], immunology [71], neuroscience [72], host-pathogen interactions [59], and diet [73].

The Collaborative Cross (CC) is a mouse genetic reference population with infinite reproducibility, randomization of variation genome-wide, and statistical power to investigate genetic networks underlying complex traits (Figure 1.2).

The types, distribution, and frequency of SNPs in the CC are comparable to those in humans, and result in high phenotypic diversity that enhances ability to map causative loci underlying complex traits. Given the complexity of cardiac physiology and disease, the use of the CC will aid in elucidating intricate genetic and correlating phenotypic networks. It can potentially identify genes associated with poorly adaptive phenotypes in response to environmental change such as disease, toxicants, and diet in a population-based context.

To provide a better model for human genetic diversity, the CC, developed to provide a better model for human genetic diversity, is as a population-based model consisting of a panel of recombinant inbred mouse strains derived from eight genetically diverse inbred strains (A/J, C57BL/6J,

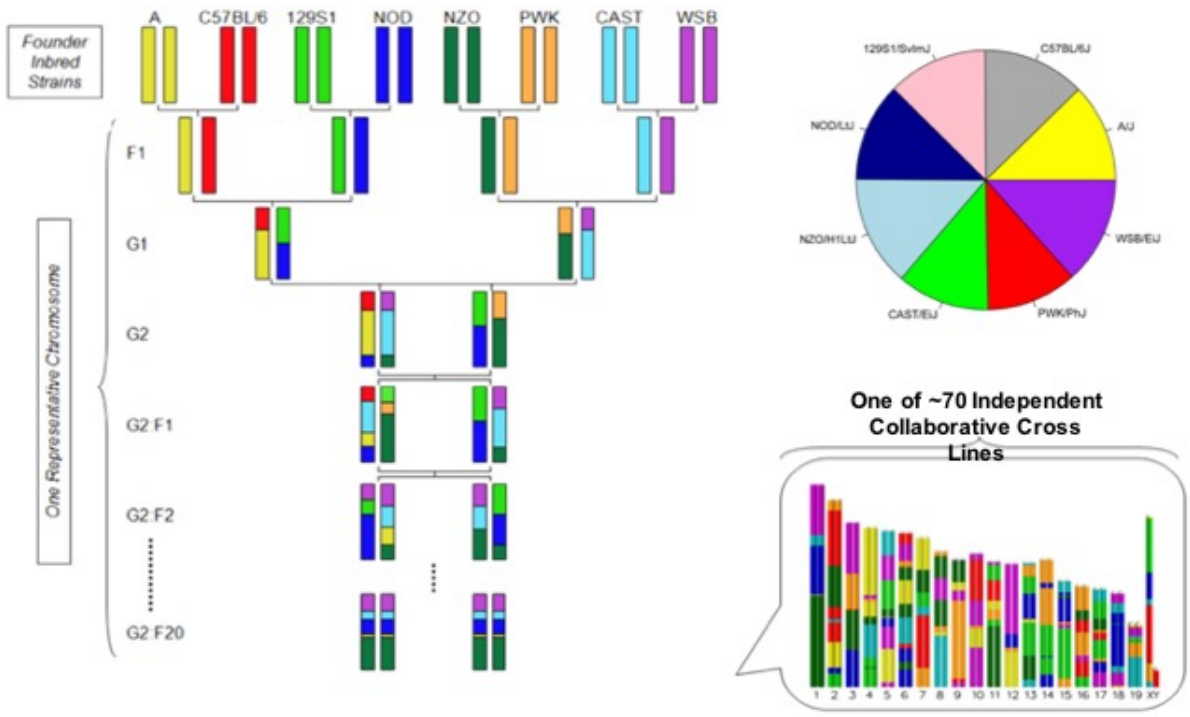

Figure 1.2: A unique funnel breeding scheme is used to derive each CC strain. This breeding approach is designed to randomize the genetic makeup of each inbred line. Each of the eight parental strains has balanced allelic frequency in CC strains.

129S1/SvImJ, NOD/LtJ, NZO/HlLtJ, CAST/EiJ, PWK/PhJ, and WSB/EiJ). Not only does this population model genetic diversity in the human population, it is infinitely replicable and supports identification of causative genetic variants contributing to complex traits, such as strain-dependent differences in cardiovascular function and toxicity responses similar to humans [57, 67].

1.6 Aims of the study

An essential prerequisite for using genetic variation in mice to model phenotypic variability in human populations, which is addressed in this dissertation, is detailed measurements of baseline cardiovascular variability across diverse mouse strains such as the CC population. Thus, the overarching goal of this study was to characterize and determine genetic drivers of cardiac phenotypes in the CC and to use the CC in a proof-of-concept study with cardiotoxicants to detect variable responses. The future of discovering therapeutic targets in this animal model, which closely resembles human variability in cardiac injury, is an important translational step between experimental

rodent cardiac studies and large-scale human clinical trials. This work will contribute to the field of heart disease research by providing key information on the cardiac reference ranges and their genetic drivers as well as cardiac injury profiles of a subset of CC.

2. DERIVATION OF CARDIAC REFERENCE RANGES FOR *MUS MUSCULUS* USING THE COLLABORATIVE CROSS AND IDENTIFICATION OF NEW CARDIAC MODELS

2.1 Introduction

Heart disease is the leading cause of death worldwide [74], with over 650,000 Americans dying of heart disease each year and accounting for 1 in 4 deaths [75]. Although the underlying causes of heart disease are multifactorial, abnormal cardiac phenotypes such as long QT, increased heart size (cardiomyopathy), and low ejection fraction (EF) are important manifestations of cardiovascular disease. Susceptibility to these abnormalities are heritable, with additional exogenous factors such as diet, exercise, metabolic disorders, environmental exposures, and drugs further increasing risk for adverse cardiac events [75]. For example, abnormalities in left ventricular (LV) structure and function are heritable [76, 77], and it has become increasingly apparent that LV function is key to heart failure [78]. With highly limited regenerative capabilities and many maladaptive processes, the heart is an especially vulnerable organ to the effect of exogenous factors. Indicative of this vulnerability, 33% of all drugs withdrawn from the market between 1998 and 2008 were due to cardiac complications [15],

Contemporary *in vivo* approaches for developing new interventions and for cardio-safety evaluation include assessments for cardiovascular structure and function, frequently performed in a variety of animal and *in vitro* models [79], but rarely include considerations of genetic background as a potential contributing risk factor. Of various animal models, non-human primates, dog, and swine are typically preferred pre-clinical species; however, they are not population-based or genetically-tractable models. By contrast, mice differ in heart physiology and electrophysiology from humans and are typically not used in pre-clinical safety studies, but have the advantage of the genetic modification tools and reference populations to study genetic causes of human disease. Even though mice are used to study cardiac pathology [80], no standard cardiac reference ranges exist for *Mus musculus* similar to that in humans. Characterization of the population diversity in

cardiac phenotypes in mice is important for identifying individuals at increased risk for adverse cardiac events and for using mice in pre-clinical safety testing.

Previous reports, such as those derived from the Framingham Heart study [81, 82], have provided a wealth of information to determine normal variation in baseline cardiac physiology in humans [83, 54]. Human data are presented as reference ranges, which are typical values within two standard deviations from the population mean. They are used to describe normal ranges of cardiac phenotypes in people and are often based on sex and age. Although previous studies have reported variable outcomes in cardiovascular disease states based on genetic factors in humans and animal models [84, 85, 86], reference ranges have not been derived for animal models that can be used to evaluate baseline cardiac risks before intervention trials. For example, the C57BL/6 mouse is one of the most commonly used strains in experimental research [87], and has been used to model cardiovascular therapies for humans [88, 89]. Yet, the hearts of C57BL/6 mice are deemed as a model for hypertrophic "athlete's heart" that is not representative of most people [64].

The role of genetic variability in disease risk is best modeled in the mouse, which has the most extensive genetic resources including dozens of strains, each potentially representing a unique risk status for heart disease development. Furthermore, nearly all environmental factors can be controlled in mouse studies, supporting detailed phenotypic and physiologic analyses. However, before the mouse can be fully exploited as a model of human population variation in cardiac physiology and disease, detailed baseline characterizations across strains and sources of measurement variation are required to properly identify models representing various risk statuses for translation to humans. To overcome the limited combinations of genetic variation present in mouse strains, the Collaborative Cross (CC) was developed as a mouse genetic reference population that has sufficient diversity to model the range of genetic diversity present in the human population [90, 91, 92].

To better understand population-based variation in cardiac phenotypes that contribute to differential disease susceptibility, and to provide a model for human population variation, this study reports detailed characterization of strain-dependent differences in baseline cardiovascular physiology, species-specific reference ranges, and sources of variation using echocardiography and elec-

trocardiography (ECG) based on the CC population. Echocardiography is used as a fast and reliable assessment of cardiac morphology and function. However, there is controversy as to whether measures on conscious or sedated mice are more reliable and representative of baseline cardiac function because stress of handling and the possibility of anesthesia inducing changes in cardiac function [93]. To compare the approaches, both conscious and isoflurane-sedated echocardiography were performed in both sexes of 58 CC mouse strains and C57BL/6J as a reference control to evaluate strain-dependent cardiac physiology. Conscious ECG was also performed to evaluate the electrical activity and autonomic regulation of heart function. Early contractile dysfunction can be detected by subtle changes in echocardiography by global longitudinal strain (GLS), EF, and LV mass, and in ECG by prolonged repolarization and depolarization of the myocardium during various intervals of the cardiac cycle, which are dependent on baseline heart function. The measures were then used to derive reference ranges for normal cardiac physiology in *Mus musculus* and to identify new models of predisposition to human cardiac conditions. Given the complexity of cardiac physiology and disease, the use of the CC will aid in elucidating genetic and associated phenotypic networks to support identification of genes underlying risk and poorly adaptive phenotypes, particularly in response to exogenous changes such as disease, toxicants, and diet in a population-based context.

2.2 Methods

2.2.1 Mice

Three male and three female adult mice, 6-9 weeks of age, from 25 CC strains were bred at the University of North Carolina Systems Genetics Core (UNC), and 33 CC strains and C57BL/6J strain were from colonies bred in house that originated from UNC for a total of 354 mice. Three is the minimum for variance analysis. Mice were provided diet 2919 (Envigo) except for CC004/TauUnc, CC007/Unc, CC008/GeniUncJ, CC009/UncJ, CC010/GeniUncJ, CC018/UncJ, CC024/GeniUncJ, CC026/GeniUnc, CC028/GeniUncJ, CC031/GeniUnc, CC033/GeniUncJ, CC038/GeniUnc, CC039/Unc, CC040/TauUnc, CC042/GeniUnc, CC045/GeniUnc, CC051/TauUnc, CC059/TauUnc, CC060/UncJ,

CC068/TauUncJ, CC071/TauUnc, CC074/Unc, CC075/UncJ, CC079/TauUncJ, CC080/TauUncJ, CC081/Unc, and CC084/TauJUnc, which were fed 8604 (Envigo) and water ad libidum using a 12-h light/dark cycle. Housing and experimentation rooms are kept consistently at 21°C-23°C. Mice were housed in cages of 2-5 mice, with clean bedding and nestlets. Strains will subsequently be referred to without the laboratory code for brevity. On Day (D) 1 and D2, mice were subjected to conscious ECG with D3 being a rest day for the mice. Anesthetized echocardiography and body weights was obtained on D4, and on D5 mice were subjected to conscious echocardiography (Figure 2.1). Mice were used for further unrelated studies, no human endpoints were necessary. No criteria were set for exclusion of any animals.The investigation conforms with the 2011 Guide for Care and Use of Laboratory Animals published by the National Institutes of Health. All experimental protocols were approved by the Institutional Animal Care and Use Committee (IACUC) of Texas A&M University (IACUC No: 2019-0435).

2.2.2 Electrocardiography

ECG recordings were obtained non-invasively using an ECGenie apparatus (Mouse Specifics). In order to eliminate circadian influences, ECG was performed between 9 am and 12 pm. Briefly, individual mice were removed from their home cage and placed on the neonate recording platform 2 minutes prior to data collection to allow for acclimation. ECG signals were acquired through disposable footpad electrodes located in the floor of the recording platform. The amplitude of the ECG signal depends on the passive nature of detecting the signals through the mouse paws that is influenced by experimental variables such as how the mouse stands, the weight of the animal, how much pressure is exerted on each paw, whether there is any moisture on the lead plate (i.e. urine and feces), and the age of the lead plate (oxidation). Consequently, amplitude differences were not used in the analysis. Approximately 20-40 raw ECG signals were analyzed per mouse using e-MOUSE software (Mouse Specifics), which employs processing algorithms for peak detection, digital filtering, and correction of baseline for motion artifacts. Heart rate (HR) was determined from R-R intervals, and HR variability was calculated as the mean difference in sequential HRs for the entire set of ECG signals analyzed. The software also determined cardiac intervals (i.e.,

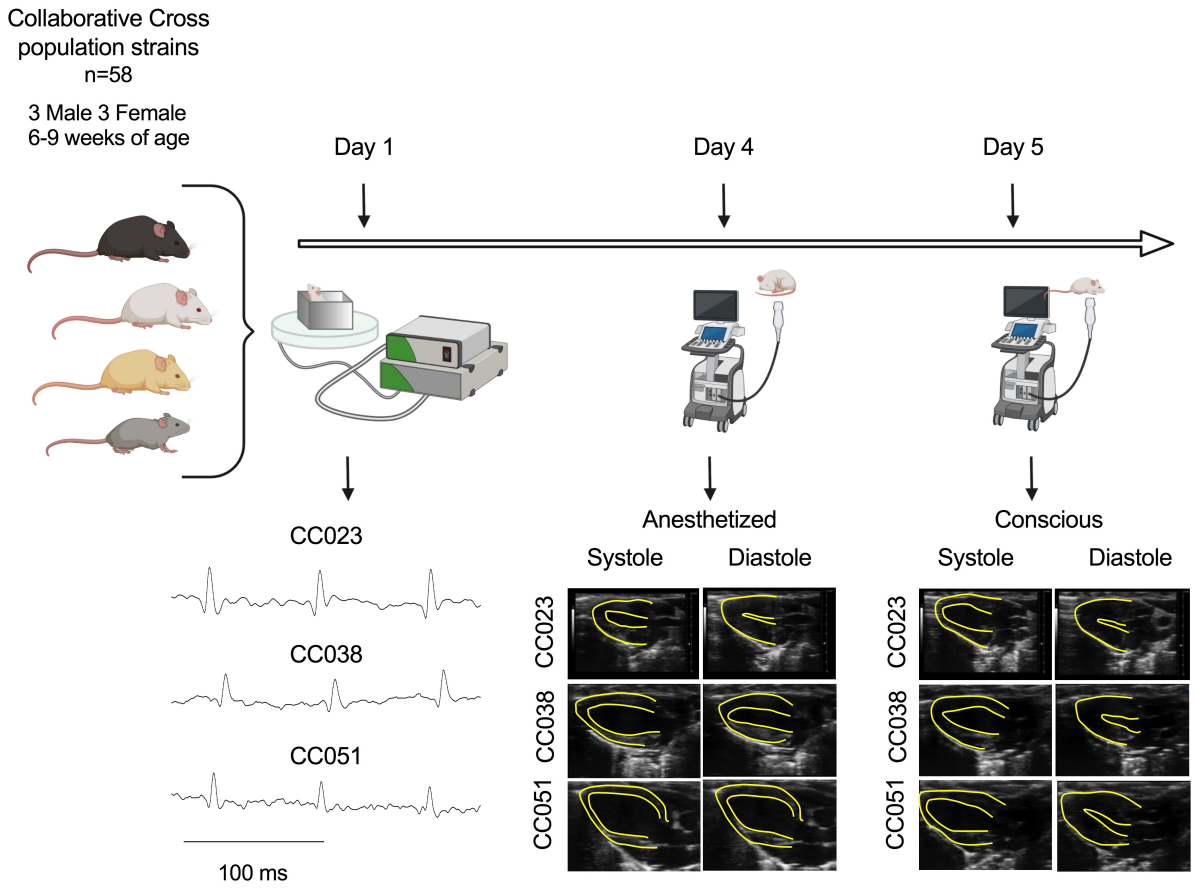

Figure 2.1: Experimental Design. Mice from 58 CC Strains and C57BL/6 were subjected to ECG (Day 1), anesthetized echocardiography (Day 4), and conscious echocardiography (Day 5).

PR, QRS, and QTc) with rejection of spurious data resulting from noise or motion. In mice, the T-wave often merges with the final part of the QRS complex [94], so the end of the T-wave of each signal was automatically defined as the point where the signal intersects the isoelectric line, denoting resting membrane potentials. All data were collected by a single operator (JLP).

2.2.3 Transthoracic Echocardiography

Cardiac morphological and functional parameters were assessed with a Vevo3100 high-frequency ultrasound imaging system (FUJIFILM VisualSonics). For anesthetized echocardiographic analysis, mice were anesthetized with 4% isoflurane in oxygen and placed in a supine position on a

temperature-controlled 39°C imaging platform under continuous supply of 1.3%-1.8% isoflurane through the mouth and nose. Ventral hair on the rostral thoracic cavity was removed at least one day prior using a hair removal cream (Nair), and pre-warmed ultrasound transmission gel was applied on the chest at the image location. Body weights were taken after anesthetized transthoracic echocardiography. Mice were allowed to rest for 24 hours before conscious echocardiography. For conscious echocardiographic analysis, mice were held firmly in the palm of one hand by the nape of the neck in the supine position with the tail held between the last two fingers. Pre-warmed ultrasound gel was placed on the chest at the image location. For two-dimensional (2D) imaging (B-mode) view along the parasternal long axis, the transducer was placed vertically to the animal body on the left side of its sternum with the notch of transducer pointing to the animal's head. After an imaging session, ultrasound gel was removed with water dampened gauze. In order to eliminate circadian influences, ultrasounds was performed between 9 am and 11 am. Measurements and calculations were performed using VevoLAB strain analysis (v3.2.6) software package (FUJIFILM VisualSonics) on three consecutive beats according to the American Society for Echocardiography [95]. Papillary muscles were excluded from the cavity in the tracing.

$$\text{EF}\% = \frac{\text{EDV - ESV}}{\text{EDV}} \times 100 \tag{2.1}$$

$$\text{GLS} = \frac{\text{LV Length - LV length}_0}{\text{LV length}_0} \times 100 \tag{2.2}$$

$$\text{FS}\% = \frac{\text{LVIDd - LVIDs}}{\text{LVId}} \times 100 \tag{2.3}$$

$$\text{SV} = \text{EDV - ESV} \tag{2.4}$$

$$\text{CO} = SV \times HR \tag{2.5}$$

HR was determined from the cardiac cycles recorded on the M-mode tracing using at least three consecutive systolic intervals. EF (Equation 2.1), GLS (Equation 2.2), FS (Equation 2.3), SV (Equation 2.4), and CO (Equation 2.5) are calculated as shown. Results are provided as reference ranges and mean $\pm$ SD of the mean for 6 mice from each strain (3 mice from each sex). All data

were collected by JLP.

2.2.4 Statistical Analysis

GLS negative values are converted to positive. Shapiro-Wilk statistic was used for normality on untransformed and log-transformed values; higher p-value was the preferred transformation. For characterizing sources of variance in this study, ANOVA was performed for each variable with factors strain, batch (nested in strain), sex, and body weight. For cross-lab comparisons, laboratory (nested in strain) was added as a factor, but because only male mice with no batch information were available, batch and sex were not included. The $\omega 2$ statistic was used as the measure of "effect size" for a factor, i.e., the fraction of variance the factor explains [96]. The overall and strain-specific variances are also calculated, as is the residual variance representing intra-strain variation. Computations were performed using R studio version 1.4.1106, with $\omega 2$ computed using the sjstats package (version 0.18.1).

2.3 Results

2.3.1 Variation in heart morphology and function across CC strains under anesthesia

Echocardiography under anesthesia is the standard approach for analyzing heart morphology and function in experimental models. Inter-strain variation was found in heart size-dependent phenotypes like EDV (36.32 μL $\pm$ 8.40), ESV (20.43 μL $\pm$ 97), diastolic LV mass (63.92 mg $\pm$ 8.30), and systolic LV mass (62.81 mg $\pm$ 8.78). In humans, these parameters are typically normalized to body surface area, for which body weight is used as a surrogate. Derived phenotypes, calculated from the primary phenotypes such as mass and volume, combine systolic and diastolic values to generate functional values of cardiac physiology. These include SV (15.88 μL $\pm$ 3.97), FS (22.08% $\pm$ 6.73), CO (6.37 mL/min $\pm$ 1.93), EF (44.77% $\pm$ 10.30), and GLS (-16.00% $\pm$ 3.65). Strain, sex, body weight, and batch within strain were analyzed for their potential contribution to measurement variation observed in the CC population. Mouse strain, or genetic background, was a significant contributor to variability ($p < 0.05$) in HR, EF, and GLS (Figure 2.2). While strain was the largest contributor to variability in the evaluated phenotypes, residual factors also contributed

to each of the three clinically relevant phenotypes. Heritability of the variation in HR, EF, and GLS were found to be high (H^2 = 0.601, 0.510, and 0.648, respectively). No significant sex effects were found.

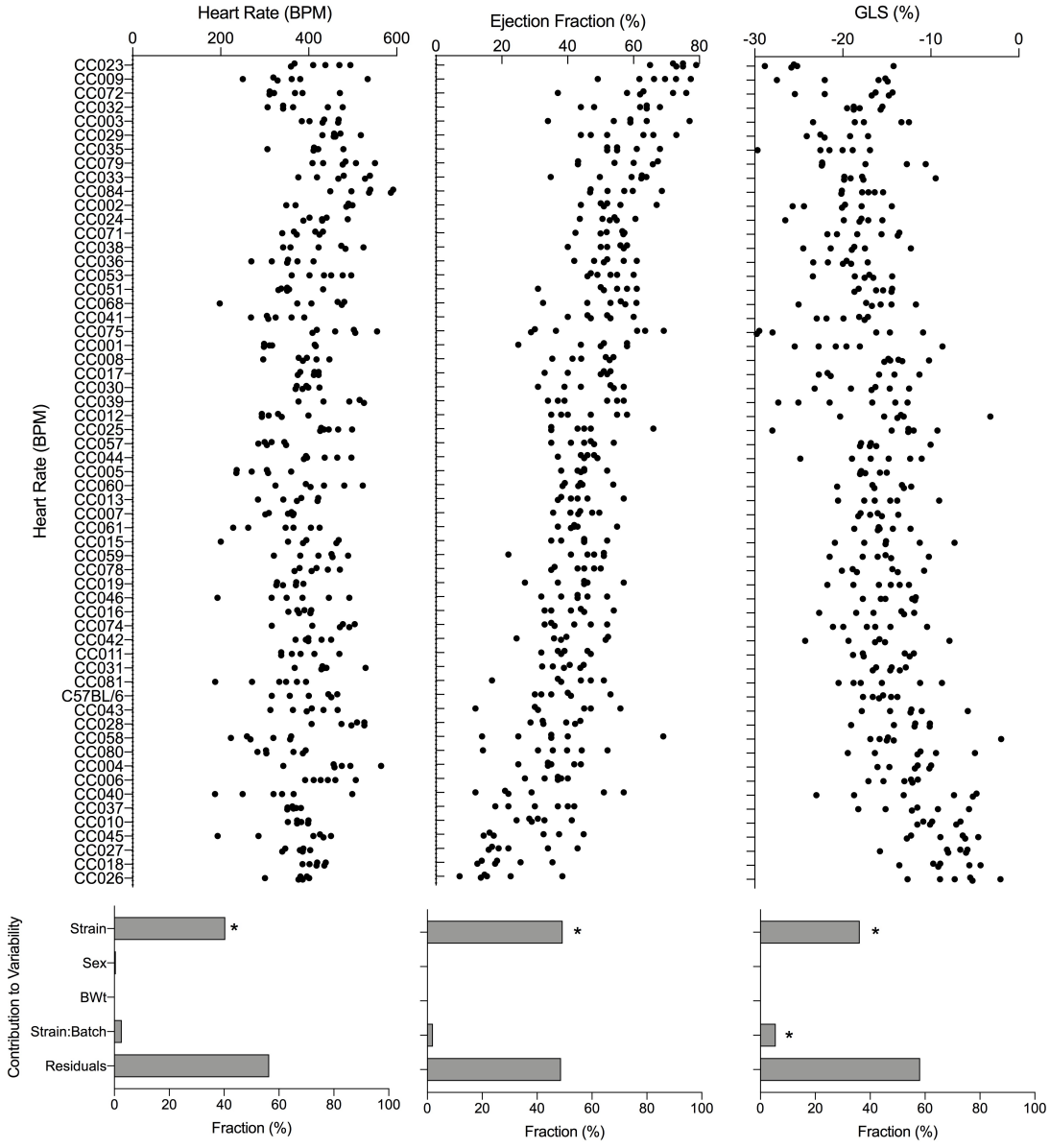

Figure 2.2: Anesthetized echocardiography elicits inter- and intra-strain variability in cardiac phenotypes. HR, EF, and GLS demonstrate variable response to anesthesia based on strain. Strain is a contributing factor to the differential response, while sex and body weight were not.

2.3.2 Differential response to anesthetized and conscious echocardiography in CC strains

The use of anesthetized mice rather than conscious mice for echocardiography has been debated in the research community [97]. To determine the impact of anesthesia on echocardiography, the same animals were analyzed under conscious and anesthetized conditions. For physiologic HR of conscious mice at rest, ranges between 450-500 beats per minute (bpm) were reported in BALB/c mice using telemetry electrocardiography [98], and to be 658 bpm $\pm$ 9 in 129S6/SvEvTac mice using conscious echocardiography [99]. Studies using anesthetized echocardiography generally keep HR in a predefined range to capture the corresponding ideal heart function as determined by EF, but in a genetically diverse population such as the CC, HR is not correlated with EF under anesthetized or conscious echocardiography (Spearmans ρ=0.2251 and 0.0833, respectively).

Across all CC strains under conscious echocardiography, HR was 682.7 bpm $\pm$ 81.38; EDV (14.64 μL $\pm$ 4.95) and ESV (4.12 μL $\pm$ 2.59); LV mass at diastole (53.69 mg $\pm$ 8.28) and systole (53.16 mg $\pm$ 10.00); and SV (10.52 μL $\pm$ 2.90), FS (47.04% $\pm$ 7.88), and CO (6.99 mL/min $\pm$ 1.80). EF (72.92% $\pm$ 7.54) and GLS (-27.34% $\pm$ 4.35) also showed differential response to conscious echocardiography across CC strains. Using an inbred strain or outbred stocks, it has been reported that anesthetics cause strain-dependent effects *in vivo* [100], depresses cardiac function [101, 97], and that sympathetic tone exerts the predominant influence on HR in conscious mice [102]. Effects on sympathetic tone was observed in the current study when comparing both methods of echocardiography. Conscious intrastrain HR variability increases as HR values decrease, indicating that sympathetic tone is strain-dependent, and at lower, more relaxed HRs, higher variability indicates more influence from other factors. Strain was a significant contributor to variability ($p < 0.05$) in the changes (Δ) of HR, EF, and GLS between anesthetized and conscious echocardiography (Figure 2.3). Heritability in conscious HR, EF, and GLS was 0.548, 0.756, and 0.738, respectively. Additionally, the heritability of the delta of these phenotypes between conscious and anesthetized echocardiography was high at 0.783, 0.624, and 0.767, respectively.

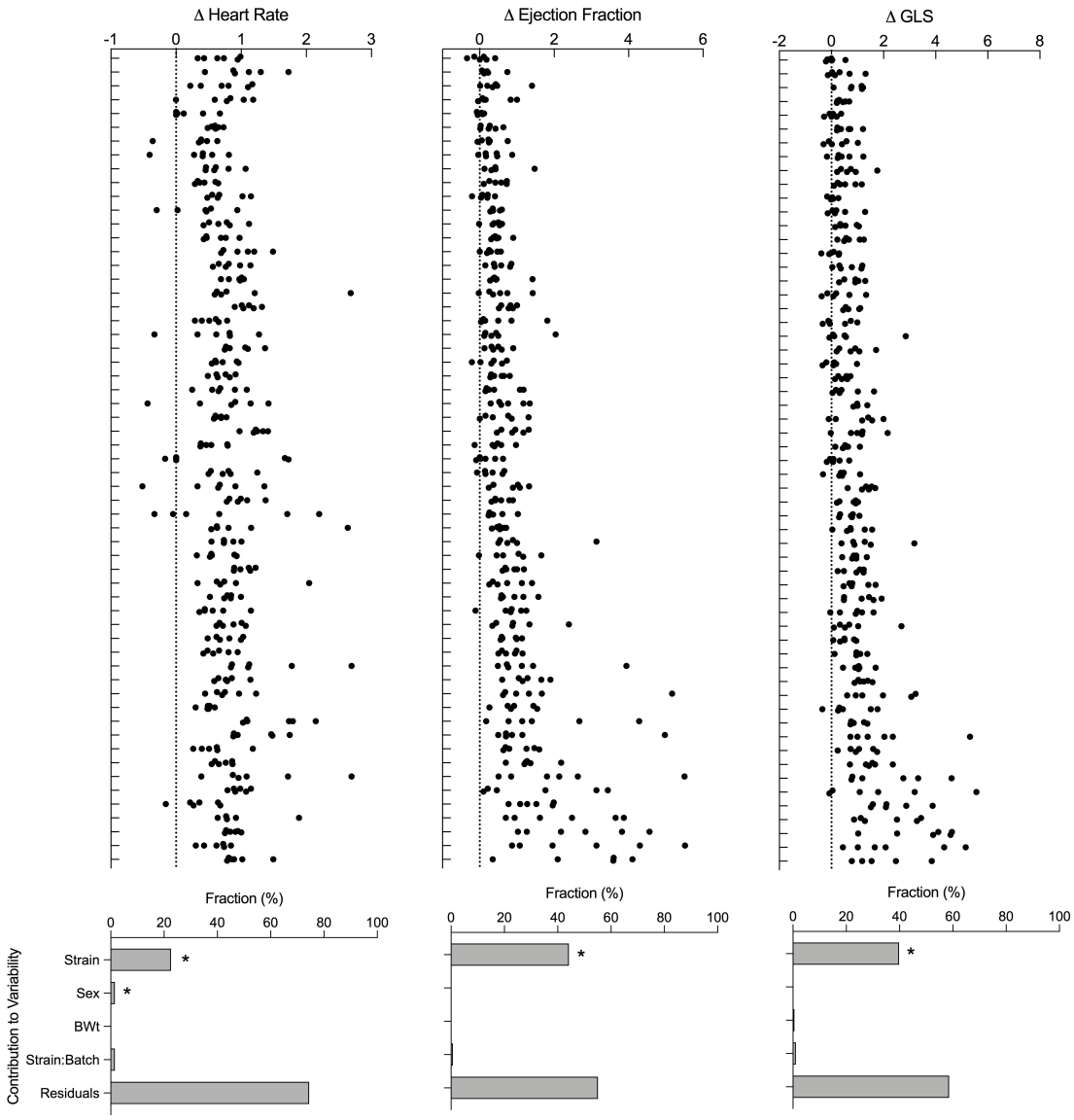

Figure 2.3: The delta between conscious and anesthetized echocardiography elicits inter- and intra-strain variability in cardiac phenotypes. HR, EF, and GLS demonstrate variable response to anesthesia based on strain. Strain is a contributing factor to the differential response, while batch, sex, and body weight were not.

2.3.3 Variation in heart electrophysiology across CC strains

Conscious ECG revealed considerable differences across strains (Figure 2.4). HR was 704.99 bpm $\pm$ 76.76. PQ (19.49 ms $\pm$ 2.48) and PR (26.44 ms $\pm$ 3.15) interval duration represent intra-atrial conduction and excitation delay within the atrioventricular (AV) node. Prolongation of these

intervals indicates AV block and is predictive of adverse outcome in humans [103, 104]. The ST interval (32.66 ms $\pm$ 4.60) pathologies include elevation, which can lead to acute myocardial infarction. The QRS complex interval (11.30 ms $\pm$ 1.43) showed wide variation across strains, and represents ventricular depolarization, and a prolongation ("wide QRS") usually indicates abnormalities in the interventricular septum due to underlying disease [105]. QTc is a HR-corrected QT interval, whose prolongation can lead to torsades de pointes or sudden cardiac death. QTc intervals (46.36 ms $\pm$ 2.92) were also variable. Strain was a significant contributor to variability ($p<0.05$) While strain was the highest characterized contributor to variability, residual factors contributed to each of HR, PR, QRS, and QTc. Heritability of HR, PR, QRS, and QTc was 0.498, 0.648, 0.680, and 0.708, respectively.

2.3.4 Reproducibility of CC mouse cardiac phenotypes

The CC are genetically reproducible and ideally, phenotypes collected under similar conditions should be comparable between laboratories. To evaluate cardiac phenotype reproducibility, the baseline data collected in this study were compared with previous studies that used a subset of CC strains. Salimova et al. assessed parameters of cardiac morphology and function using anesthetized echocardiography before and after myocardial infarction [85]. Their baseline measurements were collected at 12 weeks of age, one month older than in the current study, and revealed marked strain-dependent differences in body weight, LV mass, EF, and SV. A total of 15 strains (14 CC and one founder strain, only male mice) overlapped with the current study. The previous study performed echocardiography under 1.5% isoflurane with HRs of most strains remaining between 400 and 450 bpm. Similarly, the current study kept isoflurane anesthesia at 1.5% except for a few strains where it ranged between 1.3% and 1.8% due to differential requirements of anesthesia to maintain sedated state. Data sets were combined for analysis and evaluated for sources of variability. Even after combining data across laboratories, strain remained a significant contributor to variability ($p<0.05$) for LV mass, EF, EDV, and ESV. Body weight was a significant contributor to variability ($p < 0.05$) because LV mass, EDV, and ESV are dependent on body weight. Laboratory was also a significant factor in all four common phenotypes at ($p < 0.05$), but to a lesser extent than strain.

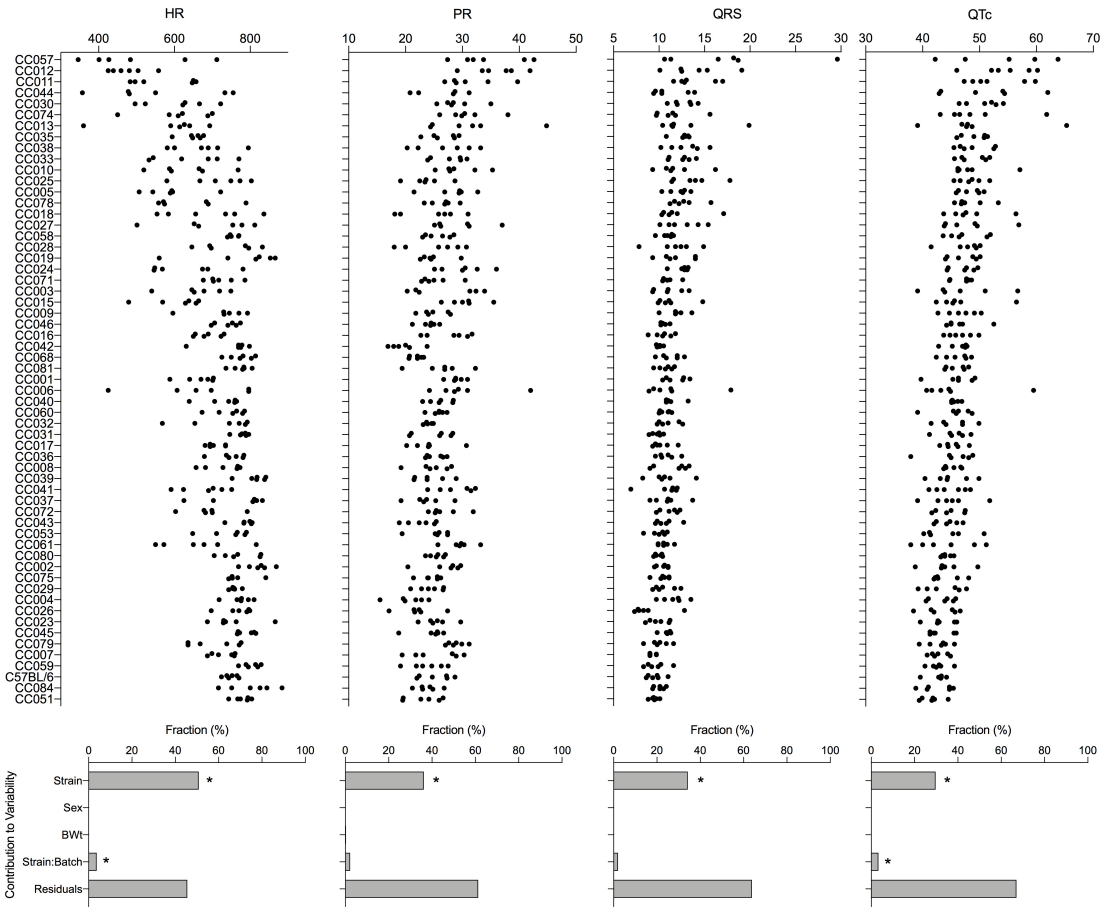

Figure 2.4: Conscious ECG elicits inter- and intra-strain variability in cardiac phenotypes. HR, PR, QRS, and QTc demonstrate variable response to anesthesia based on strain. Strain is a contributing factor to the differential response, while sex and body weight were not.

Heritability of Salimova et. al [85] data for LV Mass, EF, EDV, and ESV was 0.282, 0.479, 0.446, and 0.563, respectively, which compares well with the current study with 0.540, 0.336, 0.529, and 0.498, respectively (Figure 2.5).

The Jackson Laboratory (Jax) also reported conscious electrocardiography on 18 CC strains of both sexes at 10-12 weeks of age [106]. In those studies, data were collected using an open, elevated recording platform rather than a small neonate box, and data were collected during the first 5-10 minutes, as compared to waiting 2 minutes for the current study. Data sets were combined for analysis and evaluated for sources of variability. Strain was a significant contributor to variability ($p < 0.05$) for HR, PR interval, QRS interval, and QTc. Laboratory was also a significant factor in

three of the common phenotypes ($p<0.05$), but to a lesser extent than strain. The contribution of laboratory to HR variability is much higher than for other phenotypes, consistent with the hypothesis that HR is highly dependent on environment. In the Jax data heritability for HR, PR interval, QRS interval, and QTc was 0.535, 0.792, 0.760, and 0.776, while in the current study it was 0.695, 0.687, 0.812, and 0.907, respectively.

2.3.5 Reference ranges for *Mus musculus*

There are no established reference range values for *Mus musculus* cardiac measurements similar to what exists for humans and other pre-clinical species. To develop mouse-specific values, data across CC strains were used to develop reference ranges for cardiac measures in anesthetized (Table 2.1) and conscious (Table 2.2) mice. Because there were no sex specific differences, male and female data were combined to have 6 mice for each strain. Because human reference ranges exclude patients with outlying values of blood pressure, glomerular filtration rate, and cholesterol, and history of hypertension and diabetes, strains that fall outside of the population reference range are excluded for the normal mouse reference range. Reference ranges were calculated to be 2 standard deviations on either side of the population mean for each phenotype. Coefficient of variation (CV) of normal mouse means were also compared with available official human data from the American Society of Echocardiography (Table 2.3) [24].

2.3.5.1 Anesthetized echocardiography cardiac phenotypes

In anesthetized mice, average HR is 396 ± 52.53 bpm, and the HR normal reference range of anesthetized mice is 291 bpm - 501 bpm; CC005 and CC058 have very low HRs under anesthesia at about 286 and 298 bpm, respectively, whereas CC039 and CC084 have an average HR of 497 and 533 bpm, respectively. EF normal reference range under isoflurane anesthesia is 26.7% - 62.8%, far wider than the 50% to 65% previously reported using individual inbred strains or outbred populations lacking the diversity present in the CC [99, 107]. CC026 and CC018 are below the population range at an average of 18.7% and 20.7%, respectively. Conversely, CC023 and CC009 are above the population range at 73.2% and 66.2%, respectively. Interestingly, CC005, a very low

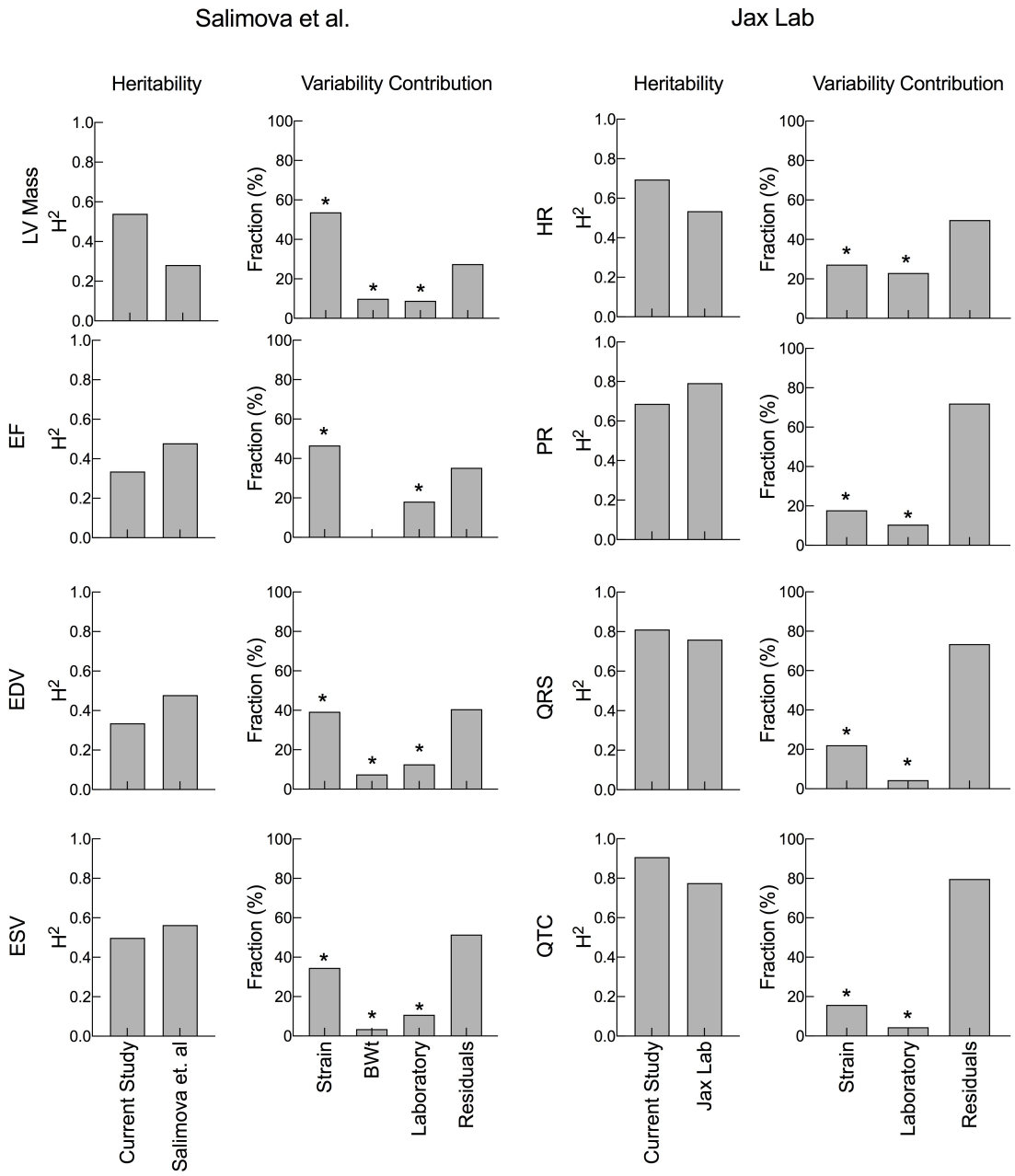

Figure 2.5: Comparison of data sets between laboratories reveals variability to reproducibility. Baseline cardiac phenotype data collected in this study was compared with previous studies that used a subset of CC strains. Salimova et al. assessed parameters of cardiac morphology and function using anesthetized echocardiography. Jax Lab performed conscious electrocardiography on another subset of strains present in this study. Heritability (H^2) and assessment of variability contribution by population characteristics.

Parameter	Mean ± SD	2-SD Range	Lower Limit Outlier Strains	Upper Limit Outlier Strains
EDV (μL)	35.22 ± 7.98	19.26-51.17	N/A	CC031, CC007, CC018
ESV (μL)	20.03 ± 5.94	8.15-31.91	CC023	CC018, CC031
EDLVM (mg)	64.26 ± 10.14	43.98-84.54	CC033	N/A
ESLVM (mg)	62.48 ± 9.79	42.91-82.05	N/A	CC018
EF (%)	44.78 ± 9.03	26.72-62.83	CC026, CC018	CC023, CC009
GLS (%)	-16.14 ± 3.93	-24.00- -8.27	CC023	CC026, CC027
SV (μL)	15.87 ± 4.34	7.18-24.55	CC027, CC026	CC084, CC007
FS (%)	21.58 ± 5.69	10.20-32.97	CC026	CC023, CC009
CO (mL/min)	6.17 ± 2.04	2.09-10.25	N/A	CC084, CC031
HR_{echo} (bpm)	396.35 ± 52.53	291.29-501.41	CC005	CC084

Table 2.1: Anesthetized *Mus musculus* echocardiography reference ranges. SD = standard deviation

Parameter	Mean ± SD	2-SD Range	Lower Limit Outlier Strains	Upper Limit Outlier Strains
EDV (μL)	13.87 ± 4.99	3.90-23.85	N/A	CC005, CC007, CC010
ESV (μL)	3.91 ± 2.16	0-8.23	N/A	CC005
EDLVM (mg)	53.12 ± 9.48	34.16-72.08	N/A	CC008, CC018
ESLVM (mg)	52.36 ± 9.02	34.31-70.40	N/A	CC008, CC018
EF (%)	73.58 ± 10.24	53.10-94.06	CC005, CC060	N/A
GLS (%)	-27.34 ± 4.35	-18.64- -36.03	N/A	N/A
SV (μL)	10.22 ± 3.70	2.82-17.61	N/A	CC007, CC010
FS (%)	47.04 ± 11.53	23.98-70.09	N/A	N/A
CO (mL/min)	6.89 ± 2.38	2.12-11.66	N/A	CC007
HR_{echo} (bpm)	704.24 ± 51.90	600.43-808.04	CC005, CC010 CC003, CC001 CC035, CC061 CC012	CC039
HR_{ECG} (bpm)	712.58 ± 60.30	591.97-833.19	CC012, CC057	N/A
PR (ms)	26.54 ± 3.33	19.88-33.21	CC004	N/A
QRS (ms)	11.30 ± 1.45	8.39-14.20	N/A	N/A
QTc (ms)	46.36 ± 3.34	39.69-53.04	N/A	N/A

Table 2.2: Conscious *Mus musculus* echocardiography and ECG reference ranges. SD = standard deviation

Parameter	Anesthetized %CV	Conscious %CV	Parameter	Men %CV	Women %CV
EDV (μL)	22.65	35.95	EDV (mL)	20.75	19.74
ESV (μL)	29.66	55.30	EDV (mL)	24.39	25.00
EDLVM (mg)	15.78	17.85			
ESLVM (mg)	15.66	17.23			
EF (%)	20.16	13.92	EF (%)	8.06	7.81
GLS (%)	24.36	15.91			
SV (μL)	27.64	27.53			
FS (%)	26.53	26.33			
CO (mL/min)	33.05	34.66			
HR_{echo} (bpm)	13.25	8.59			

Table 2.3: Comparison of *Mus musculus* and human reference ranges

HR strain, still maintains an intermediate EF at 44%. GLS normal reference range under the same conditions was -24.0% to -8.3%. Outlier strain CC023 has a high level of myocardial deformation at -25.2%, whereas strains with less deformation, which can be an early predictor of heart failure [108], are CC026 and CC027 at -7.0% and -8.4%, respectively.

2.3.5.2 Conscious echocardiography phenotypes

The normal reference range for conscious HR is 575 - 812 bpm with CC005 and CC010 having the lowest HRs at an average of 412 and 505 bpm, respectively. For conscious EF, the normal reference range is 53.1% - 94.1%, slightly wider than the 65% - 84% previously reported using individual inbred strains or outbred populations [109, 99]. CC005 and CC060 have low EF at an average of 52.0% and 56.6%, respectively. Although EF of a few individual mice fall above the population reference range, no strain averages are above the population range, albeit C57BL/6J, CC072, and CC041 fall close to the high end of the reference range at 84.5%, 85.3%, and 86.8%, respectively. GLS normal reference range is -36.0% to -18.6%.

2.3.5.3 Electrophysiology cardiac phenotypes

The normal reference range for HR during conscious ECG is 591 - 833 bpm. CC012 and CC057 had an average HR of 478 and 500 bpm, respectively, while no strain averages fell above

the population reference range. The PR interval normal reference range is 19.9 - 33.2 ms. Strains CC042 and CC004 are below the population reference range at 19.7 and 20.6 ms, respectively, while CC012 and CC057 are 35.9 and 34.6 ms, respectively. The normal reference range for QRS complex is 8.4 - 14.2 ms. Strains CC057 and CC012 are above the population range at 17.5 ms. While CC026 still falls in the population range at 8.78 ms, this strain had the shortest QRS complex. QTc normal reference range is 39.7 - 53.0 ms. No strains are below this population range, but CC057, CC012, and CC011 fall above the population range at 56.6, 54.3, and 52.6 ms, respectively.

2.3.6 Mouse models of extreme cardiac phenotypes

The differences in cardiac parameters amongst the strains may be exploited as models for various disease-like cardiac phenotypes. Based on the echocardiography findings, several CC strains show disease-like phenotypes observed in humans (Table 2.1). From the anesthetized echocardiography data, CC018 has dilated EDV and ESV, and low EF, hallmarks of dilated cardiomyopathies. CC027 has relatively normal EF but decreased GLS, which can be seen in patients with early signs of cancer therapy-related cardiac dysfunction. CC026 has decreased SV, EF, and GLS and are similar to patients with systolic cardiomyopathies such as late stage cancer therapy-related cardiac dysfunction. CC031 has dilated EDV, and increased SV and CO, which can be seen in "athlete's heart" similar to C57BL/6J. CC084 has increased SV, CO, and HR, which can be seen in acute high CO states such as anemia or sepsis. From the conscious echocardiography data, CC005 strain may be considered as a model for dilated cardiomyopathies with its dilated EDV and ESV, and reduced EF. CC010 has dilated EDV, increased SV and decreased HR, which are often seen in "athlete's hearts".

2.4 Discussion

In the present study, cardiac physiology was evaluated in 58 strains of the CC and C57BL/6J, a classical inbred strain that is widely used as a single-strain reference. Overall, our findings demonstrate that there are marked differences in cardiac physiology and response to anesthesia

among strains, and that these differences are due to genetic background. While including genetic diversity adds to the scale of the study, defining what is "normal" for mouse cardiac function can better inform selection of strains as models as has been successfully done previously for cancer [110, 111], toxicology [70, 62, 112], immunology [71, 113], neuroscience [72], and reproduction [114].

The first key finding of this study was the large amount of variation in cardiac phenotypes under normal echocardiography conditions. All traits monitored in this study were highly heritable. Anesthetized echocardiography was slightly more heritable than conscious echocardiography, likely due to anesthesia minimizing some uncharacterized sources of variation. This naturally occurring variation more closely models that seen in the human population, redefining what "normal" means for mouse models and method of echocardiography [51]. The anesthetized volume parameters %CV are comparable to those seen in humans, while conversely the conscious functional parameter, EF, is more similar to humans. This indicates that primary measurements are perhaps more accurately measured under anesthesia in mice. However the effect of anesthesia can drastically change functional parameters, and those values should be recorded when the mouse is conscious.

The second finding was that anesthesia and stress of conscious mouse handling can differentially influence echocardiographic phenotypes based on genetic background. While residual effects contribute to a large portion of the overall variability seen across strains in EF, GLS, and especially HR, the strain effects are also highly significant and account for the largest source of variation. Residual influence is smaller in anesthetized mice, which supports that conscious echocardiography is inherently noisier and likely due to experimental variables such as the level of stress, physical scruffing, and background noise. EF has been the most common and established method for assessment of LV function in humans, but in recent years GLS has shown to be more sensitive to LV dysfunction at earlier diagnostic stages [115], and has improved reproducibility [116] and precision.[115] The American Society of Echocardiography and the European Association of Cardiovascular Imaging have agreed that deformity changes precede ventricular dysfunction, and GLS

has become a routine diagnostic for cardiotoxicity prediction in cancer patients [34]. In normal and dilated human hearts, EF is related to GLS by a factor of approximately 3 [117]. However, in human diseases where the ratio of SV to LV cavity size can be preserved, such as in chronic kidney disease [23] or recently emerging heart failure with preserved EF, EF is not informative and is not related to GLS [118].

It is noteworthy that the differential response to anesthesia, which affects EF or GLS measurements or both, is also evident in the data from this study. CC023, CC003, CC002 have almost no change in EF and GLS between anesthesia and conscious echocardiography, whereas CC026, CC018, CC027 are drastically different by a factor of more than 2.5. Strains with a lower EF under anesthesia seem to maintain the highest intrastrain variability, indicating that a high and healthy baseline EF is more reproducible. In animals with preexisting cardiac pathology or experimentally-induced cardiac pathology, reduced myocardial contractility and autonomic nervous system suppression via anesthesia can exaggerate cardiac pathologies and confound interpretation [99]. Of note is the dramatically lower EF under anesthesia in a few strains; while most experts would consider this heart failure, the method of anesthesia was the same for each individual. Mice were breathing normally and recovered normally, even at these values. While strain is a factor influencing variability, higher H^2 values of phenotypes when conscious indicate that anesthesia reduces residual effects that have a genetic contribution. Under both conscious and anesthetized echocardiography, outlier strains outside the established reference ranges are potential models of human cardiac disease. Some strains that are models of, for example, dilated cardiomyopathy under anesthesia are not the same strains that present as models under conscious echocardiography. This indicates that not only does genetic background need to be taken into account when defining models for human cardiac disease, but the method of echocardiography does as well. The outlying strains listed as potential models for various cardiac disease states are a useful tool for researchers looking for naturally pre-disposed models of cardiac phenotypes, in both conscious and anesthetized echocardiography.

The third key finding was that genetic background influences cardiac electrophysiology, and

the redefinition of normal cardiac electrophysiological intervals in mice. Residual effects have a large contribution to the variability seen across strains, but strain differences still contribute significantly. It is still a matter of debate whether the mouse is an acceptable model for studies of human cardiac electrophysiology [119, 20]. The extrapolation to humans of the T wave, methods that induce diseases such as myocardial ischemia and Brugada syndrome [119], and overall cardiac morphology are a few reasons why this must be done with caution. Mice are typically not used for their electrophysiological traits in drug safety evaluation, but are used in studies of chemical toxicity, and therefore still need to be characterized and optimized to be the most accurate model. Under anesthesia, the C57BL/6J mouse appears to be an average mouse as this strain was in the top three strains for highest conscious EF, and yet under anesthesia was a more intermediate strain at 14th lowest. Heritability of HR during ECG was high (H^2=0.498), although not as high as other phenotypes, indicating environmental factors, and therefore sympathetic tone, play a large role in maintaining beat rate. Other significant ECG phenotypic variances were generally smaller within than between strains, indicative of elevated trait heritabilities. The C57BL/6J mouse is used most commonly when comparing mouse electrophysiology to humans, especially in risk assessment research. The duration of action potential, as indicated by QTc, is an important interval for both congenital and induced pathologies, especially for cardiotoxicity. Although the C57BL/6J mouse does fall within the reference range, it is remarkable that this strain has among the shortest QTc of the 59 mouse strains analyzed, and therefore even less accurately represents the "normal" human. This raises concerns for this strain's abundant use in mouse cardiac studies and general representation of human heart health.

The fourth key finding is the amount that environment affects HR, even in a diverse population, indicating that an average HR is relative and cannot be reduced to one value. Sex contributes significantly to variability of HR difference between anesthetized and conscious echocardiography, indicating that male and female mice respond differently to stressors of conscious and anesthetized echocardiography. HRs in anesthetized echocardiography, conscious echocardiography, and ECG were significantly different ($p<0.0001$). While some strains maintained their outlier state among

strain ranking for HR values, others had more scattered rankings. For example CC005 had the 5th lowest HR for ECG and lowest for conscious and anesthetized echocardiography, while CC002 was ranked 3rd for lowest HR in conscious echocardiography and 43rd and 50th in HR from ECG and anesthetized echocardiography, respectively. HRs were among the least heritable traits, and yet the change in HR from conscious to anesthetized mice was heritable, indicating that the response of HR to anesthesia is heritable. Strains like CC005 have one of the lowest HRs under anesthesia, and yet maintain intermediate level EF values, further demonstrating that HR is not necessarily the constant variable by which to evaluate anesthetized echocardiography phenotypes. Consistent with these observation, some humans can have resting HR that are up to 70 bpm different from other individuals [120].

The fifth key finding is the identification of new, natural models of human cardiac disease predisposition. There is a pressing need to understand the molecular mechanisms of cardiovascular disease, and understanding even baseline genetic differences can have implications for response to toxicants, drugs, and environmental exposures. Indeed a recent study found differential response to doxorubicin-induced cardiotoxicty [62], and yet the susceptible strains still do not correlate with the current study's at risk strains. Baseline phenotypes might not be directly informative for predicting outcomes of drugs or chemicals, but to elucidate the molecular mechanisms underlying cardiac pathologies the depth of baseline diversity must first be explored. The current study's models have advantages compared to cardiac models prepared with genetically engineered mice, xenobiotic-induced remodeling, or surgical intervention. Transgenic mice are complicated and expensive to engineer; manipulating the mouse at the genetic level will not always develop into a disease that is comparable to humans. Genetic engineering is not entirely foolproof and sometimes the work needs to be repeated to obtain the desired result. Unwanted side-effects from drug or xenobiotic cannot be avoided, and established doses may underestimate or overestimate doses needed to produce the desired result in a diverse population. Surgical models of cardiac disease involve rapid induction of the stressor, whereas the current study's models develop more naturally over the course of the mouse's life, similar to humans.

While the current study has strengths in terms of the number of strains, time of data collection, and the use of standard echocardiographic techniques; several limitations must be acknowledged. Intrastrain variance in some strains was high with some strains being more differentially susceptible to external stressors, indicating that reproducibility is in itself a phenotype that must be acknowledged. This can also be observed in inter-laboratory differences contributing to variability. We did not observe any sex differences in the functional phenotypes, most likely due to the low number of replicas per strain. The echocardiographic and electrocardiographic software analysis were designed based on data from only a few inbred strains, which could lead to inaccuracies in analysis when the software assumes similar heart tissue density and shape across all animals. To conclude, this study reports the largest cardiac phenotyping analysis performed in a genetically diverse mouse reference population that has supported the development of cardiac reference ranges for *Mus musculus* and identification of new mouse models for cardiac disease predisposition.

3. GENETIC ANALYSIS OF MOUSE CARDIAC PHENOTYPES

3.1 Introduction

Heart disease is the leading cause of death in the United States, accounting for 665,000 deaths per year [75]. The financial burden of heart disease is also a major concern, at about $219 billion a year [121]. A risk factor for heart disease is variation in cardiac structure. Increased LV mass and hypertrophy, for example, are predictive of coronary heart disease [122]. The diagnosis of heart failure is primarily based on imaging the structural and functional parameters of the heart, as well as electrophysiological assessment [54]. The impact of exogenous risk factors such as diet, smoking, exercise, and drug abuse are well recognized, but the genetic architecture underlying susceptibility is still being explored. Most heart disorders are polygenic, so identifying the combination of linked and unlinked genes contributing to their phenotypes is challenging, especially when including possible epigenetic influences [50].

Genome-wide association studies (GWAS) in humans have been used to identify risk loci for cardiac diseases, but numerous genes, each imparting a small genetic effect that cumulatively affect disease risk presents, challenges the statistical analysis used to find "hits" when compared to monogenic diseases. This analysis also usually explores loci associated with traits as binary rather than continuous. Additionally, because human cardiac phenotypes evolve in concert with environmental factors, there is little control over the amount or type of genetic contribution driving these phenotypes. As a compliment, animal models support controlled experimental conditions to explore genetic factors contributing to cardiac phenotypes, and, unlike humans, support phenotypic replicability across genetically identical individuals. The mouse has the most developed genetic resources of mammalian models, but most studies using mouse models of complex diseases or traits focus on only a single strain to explore molecular mechanisms underlying disease phenotypes, which contains limited genetic diversity [63]. The Collaborative Cross (CC) was developed as a mouse genetic reference population that has sufficient diversity to model genetic diversity present

in the human population [90, 91, 92]. The CC are a panel of recombinant inbred (RI) strains derived from eight founder strains, A/J, C57BL/6J, 129S1/SvImJ, NOD/LtJ, NZO/H1LtJ, CAST/EiJ, PWK/PhJ, and WSB/EiJ, using a funnel breeding scheme to generate an infinitely reproducible, yet randomized model to ascribe causality to genes using the resultant large phenotypic diversity [91]. The eight founder inbred strains represent three subspecies of *Mus musculus*, including three wild-derived strains allowing for more genetic diversity than in previous RI panels. The CC panel captures 90% of the known allelic diversity present in the laboratory mouse genome, and its broad and continuous distribution of many phenotypes accurately represents that seen in the human population [92, 123, 124, 59]. It also provides a platform to identify genetic networks underlying complex phenotypes, and is therefore ideal for analysis of complex traits underlying cardiac physiology.

Echocardiography and electrocardiography are the standard noninvasive approaches for exploring cardiac form and function. Echocardiography is typically performed under anesthesia in mice, although it is well known that anesthetics depress cardiac function [125], which can result in an underestimation of LV function [101]. To prevent these effects, studies have also used conscious echocardiography, but the stress of handling and its effects on cardiac function are not insignificant [126]. The autonomic nervous system controls the differences that are seen in these two types of echocardiography; high sympathetic activity regulates conscious echocardiographic heart function, while low sympathetic and high parasympathetic regulates cardiac function that is demonstrated in anesthetized echocardiography [125]. It is likely that genetic control of the autonomic nervous system plays a role in conscious cardiac phenotypes. Similarly, functional parameters of the heart, such as ejection fraction (EF), global longitudinal strain (GLS), and QT interval, are heritable in humans [51, 127], and are under genetic control [53, 54, 55]. Previous work in this lab demonstrated high heritability in these phenotypes, indicating genetic control for cardiac phenotypes in response to anesthesia or restraint in the CC population.

This study used the CC and its associated genetic resources to identify quantitative trait loci (QTL) and candidate genes for cardiac phenotypes, in anesthetized and conscious echocardiogra-

phy, and conscious electrocardiography (ECG). Understanding the genetic determinants of cardiac physiology in mice, particularly in a genetically diverse population, while using multiple methods of assessment, can support more accurate translation of mouse cardiac research to humans to identify populations at risk, and provide novel targets for therapy and prevention.

3.2 Methods

3.2.1 gQTL

QTL mapping was performed using gQTL [128], a web accessible, simple graphical user interface application based on the DOQTL platform in R to perform QTL mapping using data from CC mice. Log of the odds ratio (LOD) was the reported mapping statistic. Briefly, gQTL uses regression modeling using trait as a response, and generates significance thresholds through permutation analysis. The significance thresholds for QTL were calculated using 10,000 permutations. CC084 was removed from analysis because it is newer than other strains and its standard genome is not well characterized.

3.2.2 Correlation of gene expression with cardiac phenotypes

Using gene expression data in a subset of total strains analyzed [85], the coefficient of determination, r^2, was used to identify the genes whose expression is highly associated with clinically relevant phenotypes of CC mice described above. Expression data was collected from uninjured male mice at 6 weeks of age in the study performed by Salimova et al [85].

3.3 Results

3.3.1 Genetic control of functional echocardiography parameters measured under anesthesia

To identify genetic loci associated with cardiac phenotypes as well as explore the contribution of founder alleles, independent quantitative trait locus (QTL) analyses was performed by interrogating 150,000 SNPs across the genome. This analysis identified one significant and two suggestive QTLs associated with anesthetized echocardiographic phenotypes (Figure 3.1). The position

of the significant GLS peak SNP was at 90.38 Mb on Chromosome (Chr) 17. To identify the CC founder contribution to this phenotype, parental allele-specific tests were performed indicating that the 129S1/SvImJ founder haplotype on Chr 17 contributed to the longitudinal axis displacement of the left ventricle. One candidate gene was identified in this region where 129S1/SvImJ was polymorphic compared to the other seven founders: *Mettl4*. *Mettl4* is a known regulator DNA methylation [129]. N6-adenosine methylation (m6A) of RNA transcripts is the most prevalent modification found in many classes of RNA [130], and has been shown to be regulated by the protein METTL4 in mouse failing hearts. While its normal biological processes are still being explored, a recent report found that m6a hypermethylation has been associated with cardiac hypertrophy, contraction, and sarcomere dynamics [131]. GLS is a direct measurement of cardiac contractility.

Expression data associated with anesthetized GLS QTL analysis revealed *Gpr139* (r^2=0.708) and *Fyn* (r^2=0.674) on the smaller peaks of Chr 7 and Chr 10, respectively. Anesthetized GLS was associated in the literature *Csrp3* (r^2=0.723), which is involved in cardiac mechanosensory processes, and human mutations cause cardiomyopathy and heart failure [132, 133]. *Akap10* (r^2=0.729) is implicated in in heart rhythm regulation, and *Klf4* (r^2=0.699) is crucial for transcriptional control of cardiac mitochondrial homeostasis [134].

The same haplotype analysis was performed across all suggestive loci for HR as well. The position of the suggestive HR peak SNP was at 77.15 Mb on Chr 6. 129S1/SvImJ also appeared to be driving this phenotype, and *Reg2* was the only coding gene present in the interval that had 129S1/SvImJ specific polymorphisms.

Expression data associated with anesthetized HR QTL analysis revealed *Ypel5* (r^2=0.725) and *Tcte3* (r^2=0.693) and *Pbx2* (r^2=0.686) on the smaller peaks of Chr 17. Anesthetized HR was associated in the literature with the cardiac sodium channel gene *Scn5a* (r^2=0.809), a channel whose disruption leads to slowed conduction and ventricular tachycardia, that is suggested to play a central role in normal heart rate and AV conduction [135]. *Mest* (r^2=0.73) is widely expressed in the mouse embryo, but has been shown to specifically direct cardiac development [136]. *CAV3*

(r^2=0.726) in humans has been associated with long QT syndrome (LQTS), but also expression of *Cav3* in mice is necessary for cardiac protection [137].

The position of the suggestive EF peak SNP was at 138.11 Mb on Chr 3. PWK/PhJ appeared to be driving this phenotype, with *Zgrf1* and *Casp6* being the only coding genes with PWK/PhJ unique polymorphisms present in the QTL interval. A gene associated with EF in the literature was *Pde4a* (r^2=0.658), is crucial in the control of 3'-5'-cyclic adenosine monophosphate (cAMP) signaling in rodent cardiac myocytes.

3.3.2 Genetic control of functional echocardiography parameters measured while conscious

Conscious echocardiography has environmental factors that may differentially affect heart function as compared to anesthetized echocardiography. Only EF had a suggestive peak on Chr 13 (Figure 3.2). 129S1/SvImJ was driving this phenotype, and the only gene with 129S1/SvImJ unique polymorphisms in the QTL interval is *Cenpk*. There are no known links of *Cenpk* to heart function. Chr 15 was not analyzed further since the QTL interval encompassed the whole chromosome.

Expression data associated with anesthetized EF QTL analysis revealed *Epha1* (r^2=0.684) on Chr 6. Conscious EF was associated the expressed genes *Gnat3* (r^2=0.849), *Rock1* (r^2=0.792), and *Ncdn* (r^2=0.693). *GNAT3* has been found to be associated with metabolic syndrome in Mexican-Americans [138], which is a cluster of conditions like hypertension, abnormal cholesterol levels, high blood sugar, and excess body fat around the waist that lead to increased risk of heart disease. ROCK1 is involved in cardiac fibrosis [139], and diastolic dysfunction is exacerbated by Rock1 deficiency [140]. Variants of *Rock1* knock-out in mouse hearts exhibits decreased cofilin-2, which is associated with abnormal actin pattern, lack of proper orientation, and a poorly organized sarcomere [141].

Conscious HR was associated with *Prkca* (r^2=0.750), *Gngt2* (r^2=0.756), *Rcan2* (r^2=0.700), and *Casc1* (r^2=0.713). In recent literature, PRKCA has been associated with cardiovascular disease in humans [142, 143], and is a downstream regulator of β_1-adrenergic receptor (β_1-AR). Notably, PRKCA is a key regulator of cardiac contractility and Ca^{2+} homeostasis in mouse cardiomyocytes

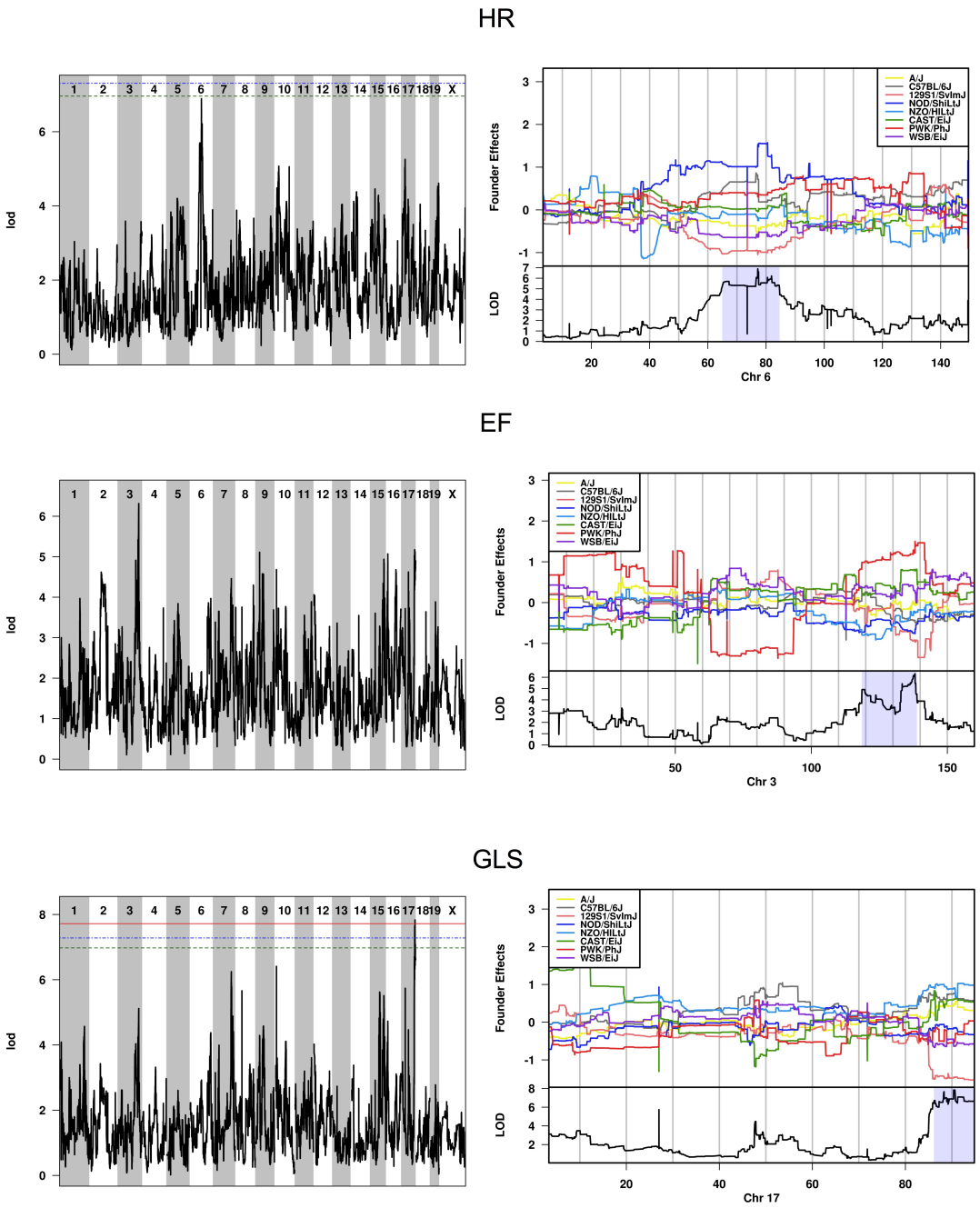

Figure 3.1: Manhattan plot and founder allele effect plot demonstrate suggestive peaks for anesthetized HR_{echo}, EF, and GLS. The horizontal lines indicate the significance threshold at p=0.15 (green), p=0.1 (blue), p=0.05 (red).

[144]. *Gngt2* has links to the sympathetic nervous system [145], and *Rcan2* has links to the heart as well [146]. *CASC1* has been directly linked to resting heart rate in humans using genome-

wide association meta-analysis [147]. *HMGB1* is also associated with heart development and heart failure [148].

Conscious GLS was associated with *Ppid* (r^2=0.809), *G3bp2* (r^2=0.663), *Ncdn* (r^2=0.621), and *Mmp11* (r^2=0.661). *PPID* encodes the protein CYP40, which is implicated in heart development and cardiac function [149]; Cyp40 knockout in mice post-myocardial infarction versus wild-type mice demonstrated better LV systolic function and attenuated LV dilatation [150]. G3bp2 is linked to isoproterenol-induced cardiac hypertrophy [151]. Mmp11 is a matrix metalloproteinase (MMP), and MMPs are involved in cardiac remodeling and are biomarkers in delineating cardiovascular risk [152].

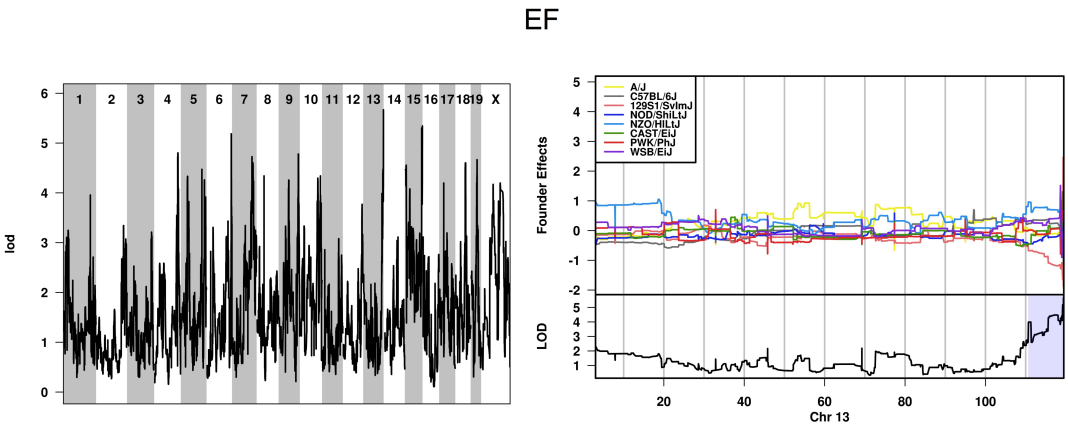

Figure 3.2: Manhattan plot and founder allele effect plot demonstrate suggestive peaks for conscious EF.

3.3.3 Genetic control of conscious electrophysiological parameters

One significant and two suggestive QTLs were associated with ECG phenotypes (Fig. 3.3). The position of the significant peak for PR interval was at 49.53 Mb on Chr 4. PR represents intra-atrial conduction and excitation delay within the atrioventricular (AV) node. CAST/EiJ and NOD/LtJ are both potential drivers of this phenotype, and when each are exclusively polymorphic, candidate genes include *Fancg* and *Trim14* (CAST/Ei), and *1700022I11Rik*, *Unc13b* and *Cd72* (NOD/LtJ).

Unc13b has not been directly linked with autonomic regulation of heart rate but has been connected with the nervous system [153, 154]. In humans, UNC13B is involved in neurotransmitter release by acting in synaptic vesicle priming [155]. *Pex13* (r^2=0.749) was also associated with QTL analysis of the PR interval.

QTc interval had two suggestive peaks as well, on Chr 2 and 4 at 169.47 Mb and 47.78 Mb, respectively. A/J is driving the phenotype seen on the distal portion of Chr 2, and when exclusively polymorphic, presents 3 candidate genes: *Prdm11*, *Bdnf*, and *Ppp1r14d*. NOD/LtJ is driving the locus of significance on Chr 4, and is the same region as was shown with the PR interval; this therefore presents the same candidate genes *1700022I11Rik*, *Unc13b* and *Cd72*. *Bdnf* (Brain-derived neurotrophic factor) is a known regulator of cardiovascular homeostatis [156]. It binds the tyrosine-related kinase receptor B (TrkB) and triggers downstream signaling. It is primarily a regulator of synaptic transmission and plasticity at adult synapses in the autonomic nervous system, but recent evidence highlights that the BDNF/TrkB pathway is expressed in the cardiovascular system and closely associated with the development and outcome of coronary artery disease, heart failure, and cardiomyopathy [156]. A study reported that BDNF enhanced normal cardiomyocyte Ca^{2+} cycling, contractility, and relaxation via regulating Ca^{2+}/calmodulin-dependent protein kinase II (CaMKII) signals [157]. BDNF also maintains cardiac contraction force through TrkB.T1, and disruption of TrkB.T1 caused dysregulated calcium signaling in the heart [158]. Expression data associated with QTc QTL analysis revealed *Retsat* (r^2=0.743) and *Olfr176* (r^2=0.700) in the small peak on Chr 6 and 7 respectively.

3.4 Discussion

In the present study, genetic control of functional cardiac phenotypes was established, and candidate genes were identified. Anesthetized functional echocardiography and conscious ECG phenotypes presented significant and suggestive QTLs, and conscious echocardiography had suggestive QTLs. Using microarray expression data [85], highly associated genes were connected with phenotypes of interest. Candidate genes with links to heart function or autonomic nervous system regulation were explored, and *Mettl4* and *Bdnf* are implicated as new genes associated with

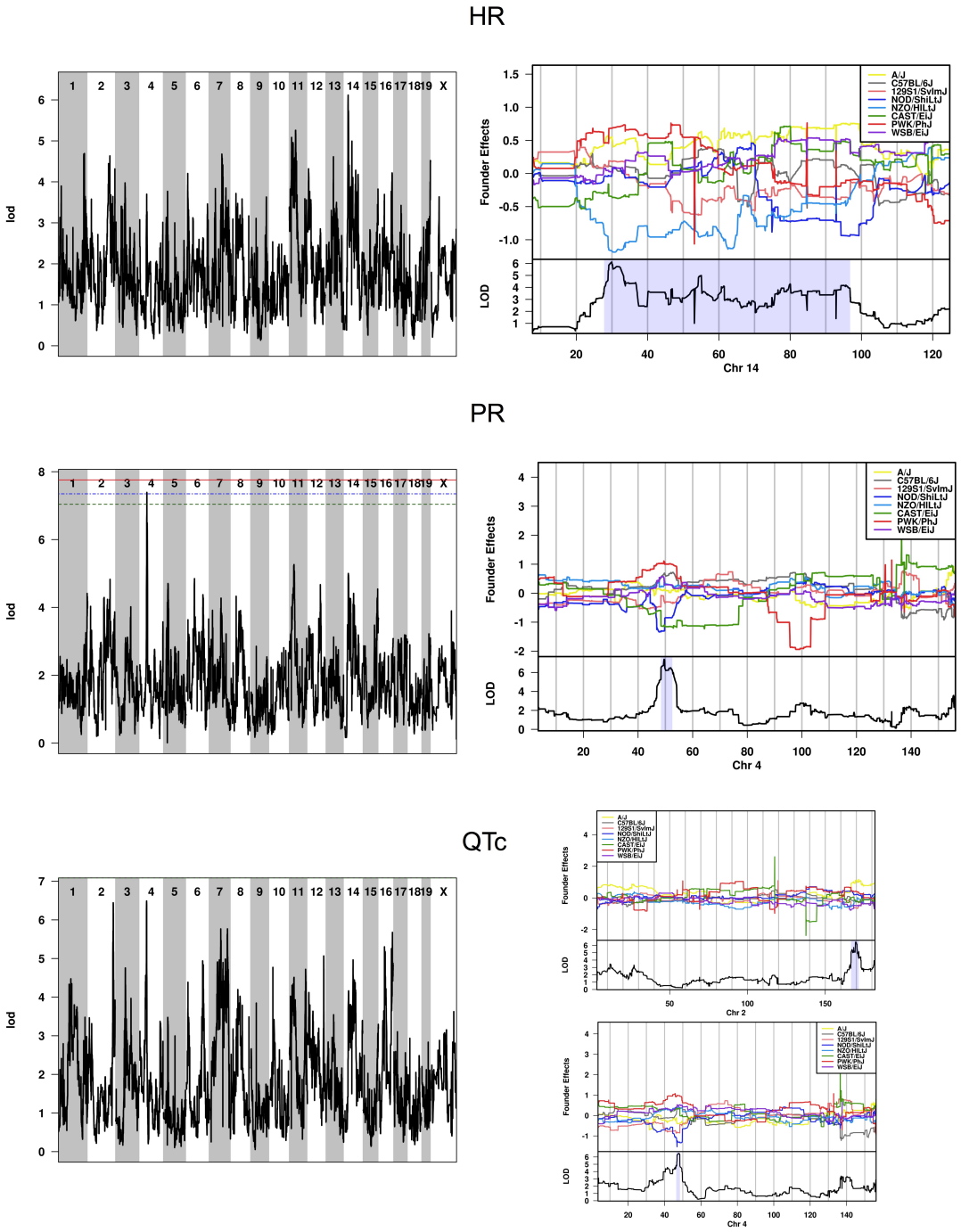

Figure 3.3: Manhattan plot and founder allele effect plot demonstrate suggestive peaks for HR_{ECG}, PR interval, and QTc interval. The horizontal lines indicate the significance threshold at p=0.15 (green), p=0.1 (blue), p=0.05 (red).

mouse GLS and QTc intervals, respectively.

The first key finding was that *Mettl4* has been established as a candidate gene for anesthetized GLS. The epigenetic changes that METTL4 facilitates lead to regulation of contractility and therefore are an essential part of normal heart function (Figure 3.4). Understanding what leads to increased contractility efficiency could potentially present therapeutic targets in cases where GLS is high, such as during systolic dysfunction and heart failure.

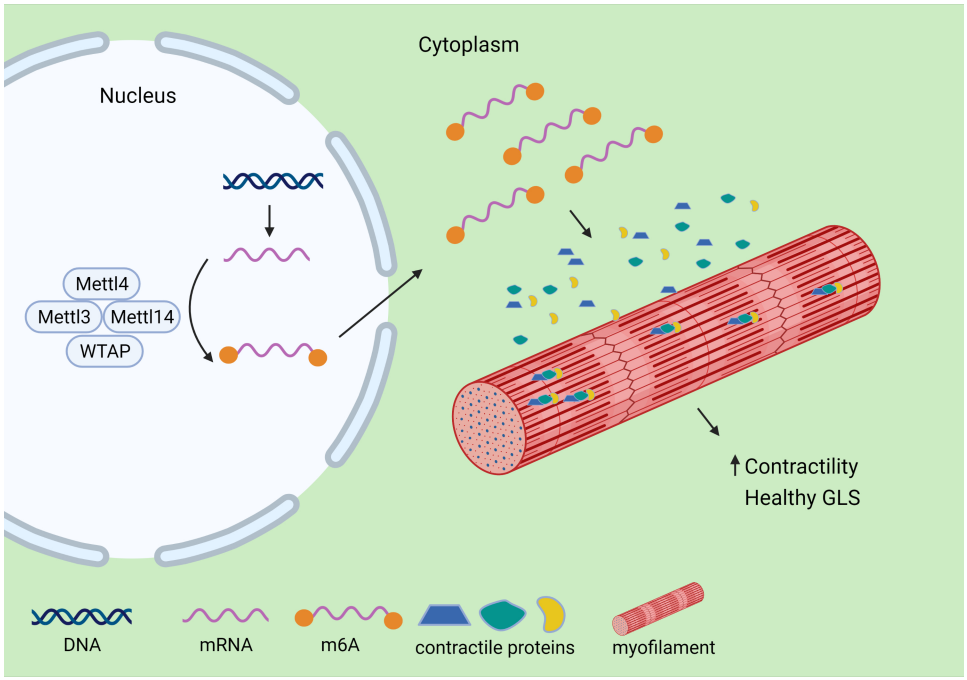

Figure 3.4: Graphic depicting proposed pathway of Mettl4 effect on GLS.

The second key finding was that *Bdnf* was also established as a candidate gene for QTc. In humans it has been confirmed that the most common types of LQTS is caused by heterozygous mutations in the K^+ channel subunits KvLQT1 or Human ether-a-go-go-related gene (HERG) [159, 160]. Although ion channels between humans and mice are conserved, there are differences; mice have much higher heart rates than humans, requiring shorter action potentials, and different repolarizing K^+ currents [161]. Mice also do not have a defined T wave in the ECG output, but physiologically still experience ventricular depolarization and repolarization [119]. Telemetric

assessment of ECG is preferred, but many electrophysiology studies are still performed in sedated animals, and many QT interval models are based on these studies [162]. This introduces *Bdnf* as a potential new regulator of the QT interval, or for these purposes, ventricular depolarization and repolarization, either as a potential therapy target or to establish a new mouse model of the QT interval.

The third key finding was that conscious echocardiography phenotypes revealed genetic similarities to human cardiac phenotypes. Conscious HR had common genes that are highly associated with human HR, that were not as highly significant in anesthetized HR. Anesthetized echocardiography is the traditional method for non-invasive cardiac assessment in mice [163], and yet conscious echocardiography is translatable to humans as well. Interestingly, finding links in literature to the heart for the genes associated with the anesthetized functional phenotypes, EF and GLS was more challenging than with conscious phenotypes.

The range of each phenotype across the 58 CC strains is wider than seen in previous studies exploring cardiac physiology in commonly used mouse strains [67]. To our knowledge this is the largest CC population to be used for cardiac analysis, but some limitations must be acknowledged. The number of biological replicates could have been increased; due to the fact that no sex differences were found across the phenotypes, male and female data was combined for QTL analysis. Any sex-linked polygenes associated with cardiac physiology would not have been detected in this study. Conscious echocardiography inherently involves more environmental factors than anesthesia or ECG, so determining genetic control of those phenotypes was challenging. Scruffing the mouse in the supine position, background noise of the echocardiography machine or even imaging imperfections due to micro movements of the mouse can explain some of this. The anesthetic agent used, isoflurane, is a negative inotrope and chronotrope, and suppresses the autonomic nervous system. This explains why EF and GLS are both less robust and variable in anesthetized conditions, allowing for simpler genetic analysis. Isoflurane inherently removes many environmental stimuli, which increases detection of associations between sympathetic nervous stimulation and cardiac function, but also that the conscious state is more complex. These environmental stimuli can stim-

ulate the sympathetic nervous system and affect blood pressure, heart rate, contractility, which all influence EF and GLS.

Genetic analysis of CC cardiac phenotypic data presented two new targets for genetic control of cardiac physiology as well as validate conscious ehcocardiography as unique yet complimentary method to anesthetized echocardiography for murine cardiac physiology. Several of the clinically relevant phenotypes did not show significant or suggestive associations, which indicates that the gene x environment interactions have to be better characterized or they are controlled my many small effect alleles. Two genes not previously associated with their respective phenotypes were identified and have been associated with cardiac physiology. Overall this study provides new perspectives on the genetic control of GLS and QTc interval not previously known, potentially providing new therapeutic targets or future transgenic mouse models.

4. CARDIAC TOXICITY MODELS IN THE COLLABORATIVE CROSS

4.1 Introduction

Identifying susceptible individuals, both for drug development and environmental protection, is an important part of risk assessment. The therapeutic use of chemicals is limited by their capacity to induce toxicity, which can lead to adverse reactions and even death. Cardiotoxicity is one of the top reasons for attrition in preclinical and clinical development as well as market withdrawal of drugs [164, 165]. Approaches to cardiovascular risk assessment in the pharmaceutical industry have been effective for acute adverse drug effects, but long-term exposure is often not assessed, or the adverse outcome is only observed when large heterogenous populations are exposed during clinical trials [16]. In addition to the risk of developing known chemicals into drugs, uncharacterized chemicals can be linked to 23% of cardiovascular disease cases [166]; additionally a large number of chemical agents currently in use have not been adequately tested for toxicity [167]. Particular care must be paid to cardiovascular adverse drug reactions due to the limited ability of the heart to regenerate. Cardiac damage is often lifelong, or can only be repaired with major surgery [165]. Cardiovascular toxicity is a common cause of attrition of small molecules and biologics in drug development, as well as presence of cardiovascular disease from environmental chemicals; this indicates a dire need for more accurate preclinical cardiac risk assessment.

A critical component of evaluating risk for decision-making is determining how humans will respond, and when using *in vitro* models to answer this, accurate translation across species is crucial. However, there are uncertainties when translating cardiac data from mammalian models to humans, and while there is a considerable level of homology, metabolic rate, receptor diversity, scale, ion channel differences, in addition to behavioral differences add challenges for extrapolation to humans. The extrapolation of accurate animal data to humans is challenging, especially since it largely relies on studies performed using models with a homogenous genetic background [168]. With this model, the response may fall outside the range of human response, whereas with a

genetically diverse population, similar to that of humans, the chance of seeing a range of response similar to that of humans increases.

Surprisingly little is known about potential strain-specific susceptibilities towards cardiac remodeling and ventricular arrhythmias *in vivo*. The role of genetic variability in disease risk is best modeled in the mouse, which has the most advanced genetic resources including dozens of strains, each potentially representing a unique risk status for toxicity development. The Collaborative Cross (CC) mice are a genetically diverse mouse population that is comparable to the human population, but with randomized genetic variation. This means that a smaller cohort of mice can be used to gather useful data than a human epidemiologic study. The advantages of this population over a panel of inbred strains is that it can support analysis of human diseases with complex etiologies originating through interactions between unique allele combinations and the environment. The CC recombinant inbred population originated from eight founder strains of inbred strains: NOD/ShiLtJ, NZO/HILtJ, A/J, C57BL/6J, 129S1/SvImJ, CAST/EiJ, PWK/PhJ, and WSB/EiJ. The use of a genetically diverse mouse population has been shown to predict and recapitulate inter-individual variability in cardiovascular health [64, 65, 66, 67], cancer [68, 69], toxicology [70], immunology [71], neuroscience [72], host-pathogen interactions [59], and diet [73].

As known cardiotoxicants above therapeutic doses, isoproterenol and chloroquine have been well documented for their therapeutic and toxic potential, and are suitable models to demonstrate inter-individual cardiac response. This study reports detailed characterization of strain-dependent differences in cardiac response to isoproterenol, at the dose commonly used for induction of myocardial injury in mice, and chloroquine at therapeutic levels to evaluate differential cardiac response in CC strains using echocardiography and electrocardiography (ECG). As a non-selective β-adrenergic receptor (β-AR) agonist, isoproterenol is a positive inotrope and chronotrope, and it causes injury to cardiomyocytes via calcium overload, depletion of energy stores, and excessive production of free radicals [52]. Mice typically develop hypertrophy, dilation, and ventricular dysfunction after two weeks of daily injections [169]. Since genetic background has been shown to

play a significant role in susceptibility to isoproterenol-induced cardiac injury, this study was designed to explore its effects in the CC population whose randomized recombinant genetic variation captures more diversity of the mouse genome than common inbred strains [170, 171, 172].

Chloroquine is a quinoline compound typically used to treat malaria, but more recently has been used to treat pro-inflammatory diseases such as rheumatoid arthritis [173]. The exact mechanism of action is still being explored, but it can inhibit inducible nitric oxide synthase (iNOS) as well as interfere with normal iron metabolism. In humans, complications are varied, and cardiovascular adverse side effects include conduction disorders, hypertrophy, and hypertension [174]. Chloroquine was chosen due to the high degree of response variability seen in human induced pluripotent stem cell-derived cardiomyocytes [79]. A therapeutic dose was selected to explore pharmacological safety based on genetic background-dependent early cardiac response.

To provide a unique perspective on drug-perturbed heart function, conscious echocardiography was performed in both sexes of eight CC strains to evaluate strain-dependent cardiac toxicity. Anesthetized cardiac assessment was not used since anesthesia can affect cardiac function [97], and is not typcially used in humans. Conscious electrocardiography (ECG) was also performed to evaluate the electrical activity and autonomic regulation of heart function. Early adverse events can be detected by subtle changes in echocardiography by global strain, ejection fraction, and ventricular mass, and in ECG by prolonged repolarization and depolarization of the myocardium during various intervals of the cardiac cycle, which are dependent on baseline heart function. Given the complexity of cardiac physiology and disease, the use of the CC will aid in elucidating intricate genetic and associated phenotypic networks to support identification of genes underlying risk and poorly adaptive phenotypes, particularly in response to toxicants.

4.2 Methods

4.2.1 Mice and exposures

Three adult male and three female mice, 7-8 weeks of age, from eight CC strains, CC006/TauUnc, CC012/GeniUncJ, CC013/GeniUncJ, CC019/TauUncJ, CC024/GeniUncJ, CC027/GeniUncJ, CC041/

TauUnc, and CC043/GeniUncJ, were from colonies bred in house that originated from UNC. Mice were provided 2919 diet (Envigo) and water *ad libidum* using a 12 hour light/dark cycle. Strains will subsequently be referred to without the laboratory code. Isoproterenol (isoprenaline hydrochloride, Millipore-Sigma) was dissolved in sterile saline daily and was injected intraperitoneally (60 mg/kg/day) once daily for 14 days. Chloroquine (Chloroquine phosphate, Millipore-Sigma) was dissolved in sterile saline daily and injected intraperitoneally (50 mg/kg/day) once daily for 14 days. The investigation conforms with the 2011 Guide for Care and Use of Laboratory Animals published by the National Institutes of Health. All experimental protocols were approved by the Institutional Animal Care and Use Committee (IACUC) of Texas A&M University (IACUC No: 2019-0435).

4.2.2 Electrocardiography

Electrocardiography (ECG) recordings were obtained non-invasively using an ECGenie apparatus (Mouse Specifics, Inc.). Briefly, on days 0, 1, 7, and 14, individual mice were removed from their home cage and placed on the neonate recording platform 2 minutes prior to data collection to allow for acclimation. ECG signals were acquired through disposable footpad electrodes located in the floor of the recording platform. The amplitude of the ECG signal depends on the passive nature of detecting the signals through the mouse paws that is influenced by experimental variables such as how the mouse stands, the weight of the animal, how much pressure is exerted on each paw, whether there is any moisture on the lead plate (i.e. urine and feces), and the age of the lead plate (oxidation of the silver). Consequently, no amplitude was used in analysis. Approximately 20-30 raw ECG signals were analyzed per mouse using e-MOUSE software (Mouse Specifics), which employs processing algorithms for peak detection, digital filtering, and correction of baseline for motion artifacts. Heart rate (HR) was determined from R-R intervals, and HR variability was calculated as the mean difference in sequential HRs for the entire set of ECG signals analyzed. The software also determined cardiac intervals (*i.e.*, PR, QRS, and QTc) with rejection of spurious data resulting from noise or motion. In mice the T-wave often merges with the final part of the QRS complex [94], so the end of the T-wave of each signal was defined as the point where the signal

intersects the isoelectric line. All data were collected by the same person.

4.2.3 Transthoracic echocardiography

Cardiac morphological and functional parameters were assessed with a Vevo3100 high-frequency ultrasound imaging system (FUJIFILM VisualSonics Inc.). Chest hair was removed using a hair removal cream (Nair) before being allowed to rest for 24 hours before echocardiography. For echocardiographic analysis, mice were held firmly in the palm of one hand by the nape of the neck in the supine position with the tail held between the last two fingers. Pre-warmed ultrasound gel was placed on the chest at the image location. For two-dimensional (2D) imaging (B-mode) view along the parasternal long axis, the transducer was placed vertically to the animal body on the left side of its sternum with the notch of transducer pointing to the animal's head. After an imaging session, ultrasound gel was removed with water dampened gauze. In order to eliminate circadian influences, ultrasound was performed between 9 am and 11 am. Measurements and calculations were performed using VevoLAB strain analysis (v3.2.6) software package (FUJIFILM VisualSonics Inc.) on three consecutive beats according to the American Society for Echocardiography [95]. Heart rate was determined from the cardiac cycles recorded on the M-mode tracing, using at least three consecutive systolic intervals. All data were collected by the same person.

4.2.4 Cardiac gene expression analysis

CC013 hearts were placed in individual tubes and frozen at -80°C until ribonucleic acid (RNA) sequencing could be performed. All molecular work was performed in the Molecular Genomics Core of the Texas A&M Institute for Genome Sciences and Society (TIGSS). The following protocol is adapted from the Molecular Genomics Core, and TIGSS personnel aided in data acquisition and plot generation. Hearts were homogenized in Trizol and an aliquot taken for analysis. RNA samples were quantified with a Qubit Fluorometer (Life Technologies) with a broad range RNA assay and concentrations were normalized for library preparation. RNA quality from the hearts were verified on an Agilent TapeStation with a broad range RNA ScreenTape. Total RNA sequencing libraries were prepared using the Illumina TruSeq Stranded mRNA-seq preparation kit.

Barcoded libraries were pooled at equimolar concentrations and sequenced on an Illumina NovaSeq 6000 2x150 S4 flow cell. RNA-seq libraries were trimmed to remove adapter sequences and low-quality bases using TrimGalore version 0.6.6, with Cutadapt version 3.0 and FastQC version 0.11.9. Trimmed reads were mapped with Tophat2 version 2.1.1 to the CC013 pseudogenome from UNC. Coordinate alignments were converted to the mm10 genome using Lapels version 1.1.1. Differential expression was conducted in R using the DESeq2 package. The resulting gene expression values were uploaded to Ingenuity Pathways (QIAGEN, enlo, Netherlands; www.ingenuity.com Application Build 261899, Content Version 18030641) for biological pathway analysis.

4.2.5 Sequencing analysis

CC013 livers were shipped to Neogen for sequencing analysis. Mouse Universal Genotyping Array (MUGA), MiniMUGA, an array-based genetic QC platform with over 11,000 probes was used.

4.2.6 Statistical Analysis

Statistical tests used were Wilcoxon matched pairs rank sum test, and then Kruskal-Wallis for comparing strain differences. Dunn's posthoc test was also performed on phenotypes with strain differences.

4.3 Results

4.3.1 Isoproterenol results in cardiac remodeling in all eight CC strains

After isoproterenol exposure, changes in EDV (p=0.0078), ESV (p=0.0078), diastolic LV mass (p=0.0156), and systolic LV mass (p=0.0156) indicated that mice experienced significant cardiac remodeling (Figure 4.1). HR during echocardiography before treatment was also significantly different compared to after treatment (p=0.0391). Although EF was not significant (p=0.7422), GLS was (p=0.0234) supporting findings that GLS is the earliest predictor of heart disease [108], especially in cases of cardiotoxicity [34]. When comparing strain-dependent responses to isoproterenol by echocardiography, ΔHR was significantly different between strains (p=0.0045), and Dunn's multiple comparison test revealed that CC024 echocardiography ΔHR is significantly different

from both CC019 (p=0.0092) and CC027 (p=0.0172).

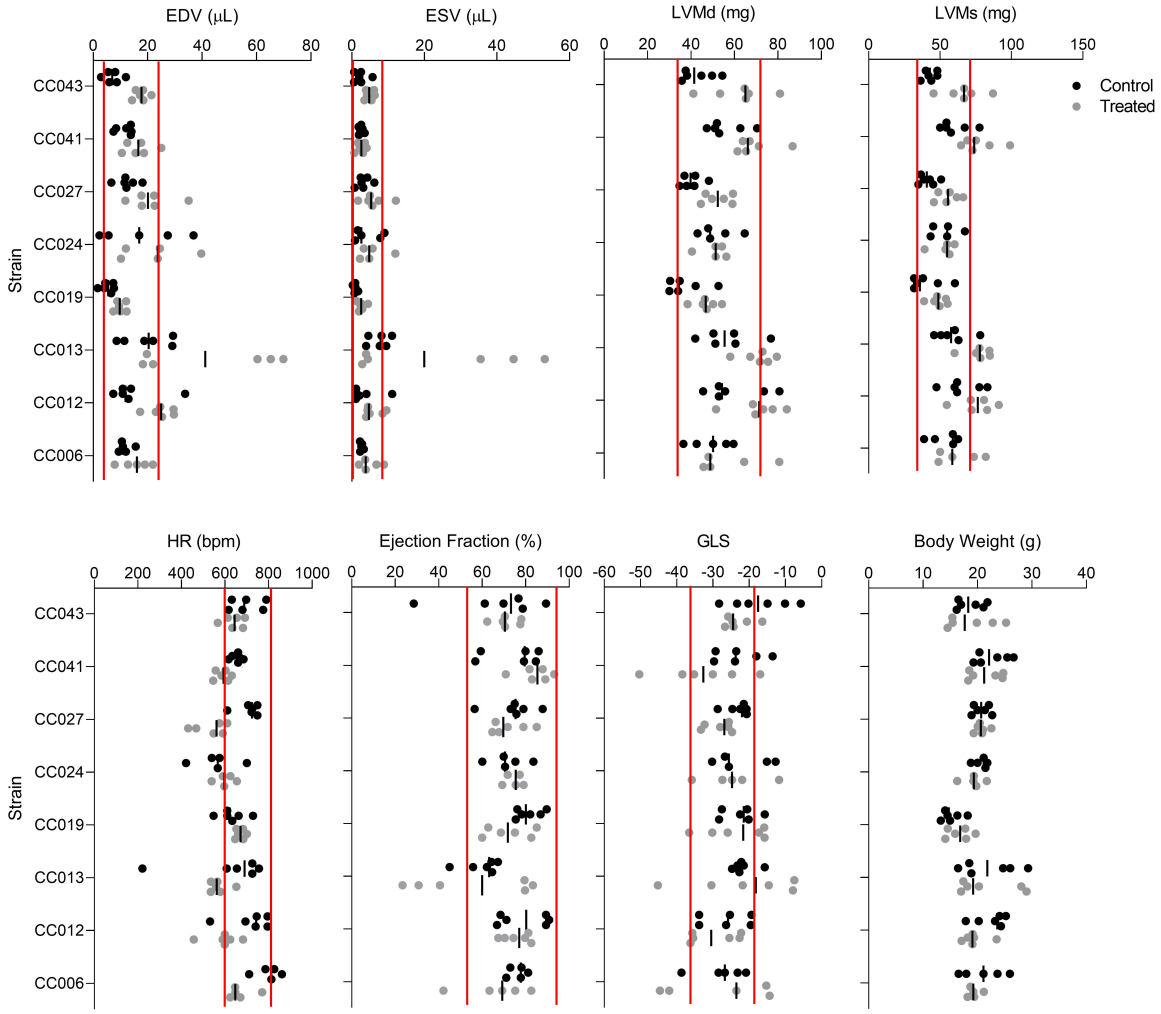

Figure 4.1: Scatterplots of echocardiographic phenotypes and body weight for control and isoproterenol treated mice. Horizontal bars represent median values for each strain.

4.3.2 Differential electrophysiological response in CC strains to isoproterenol

Contrary to HR determined by echocardiography, HR during electrocardiography was not significantly different between control and isoproterenol treated mice (p=0.9435) (Figure 4.2). Neither were the other intervals of interest: PR (p=0.8438), QRS (p=0.7422), QTc (p=0.999). When

comparing strain-dependent responses to isoproterenol, only ΔHR and ΔQTc interval were significantly different (p=0.0028 and 0.0262, respectively). Similar to observations by echocardiography, Dunn's multiple comparison test revealed that CC024 ECG ΔHR is significantly different from both CC019 (p=0.0044) and CC027 (p=0.0066). No significant posthoc comparisons were found for ΔQTc.

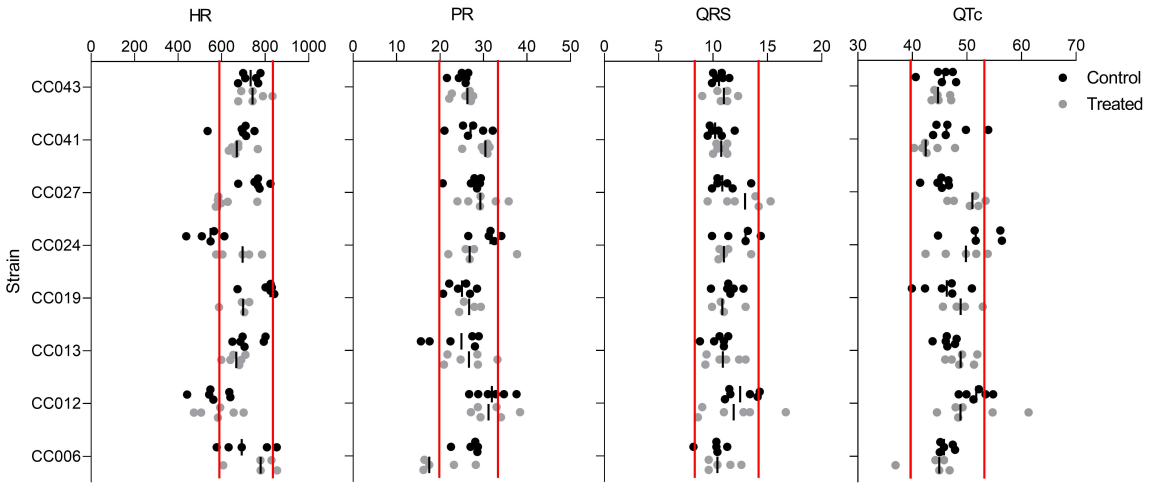

Figure 4.2: Scatterplots of ECG phenotypes for control and isoproterenol treated mice. Horizontal bars represent median values for each strain.

4.3.3 Bimodal response of CC013 to isoproterenol reveals differentially expressed genes

Three of the six CC013 mice demonstrated dilated cardiomyopathy. To gain insight into molecular mechanisms behind why an inbred line would react bimodally to the same experimental conditions, RNAseq was performed on the six CC013 mice revealing 275 differentially expressed genes (Fold change 1.0 and p-value=0.01). Principal component analysis (PCA) analysis showed clustering of the three mice that experienced dilated cardiomyopathy (379, 386, and 387) (Figure A.1). Genes expressed at higher levels in mice with larger LV volume as compared to normal mice included genes previously associated with with cellular remodeling and dilated cardiomyopathy such as *Mmp12*, *Col81a*, *Hspa1b*, *Ccr3*, and *Runx1* [175, 176, 177, 178, 179]. Additionally,

decreased levels of *Bcl6* and *Gstk1*, as shown in the mice with dilated cardiomyopathy, are associated with increased remodeling [180, 181]. Using Ingenuity Pathway Analysis (IPA) we found that the 275 differentially expressed genes were enriched in pathways associated with remodeling and inflammation (Figure 4.3).

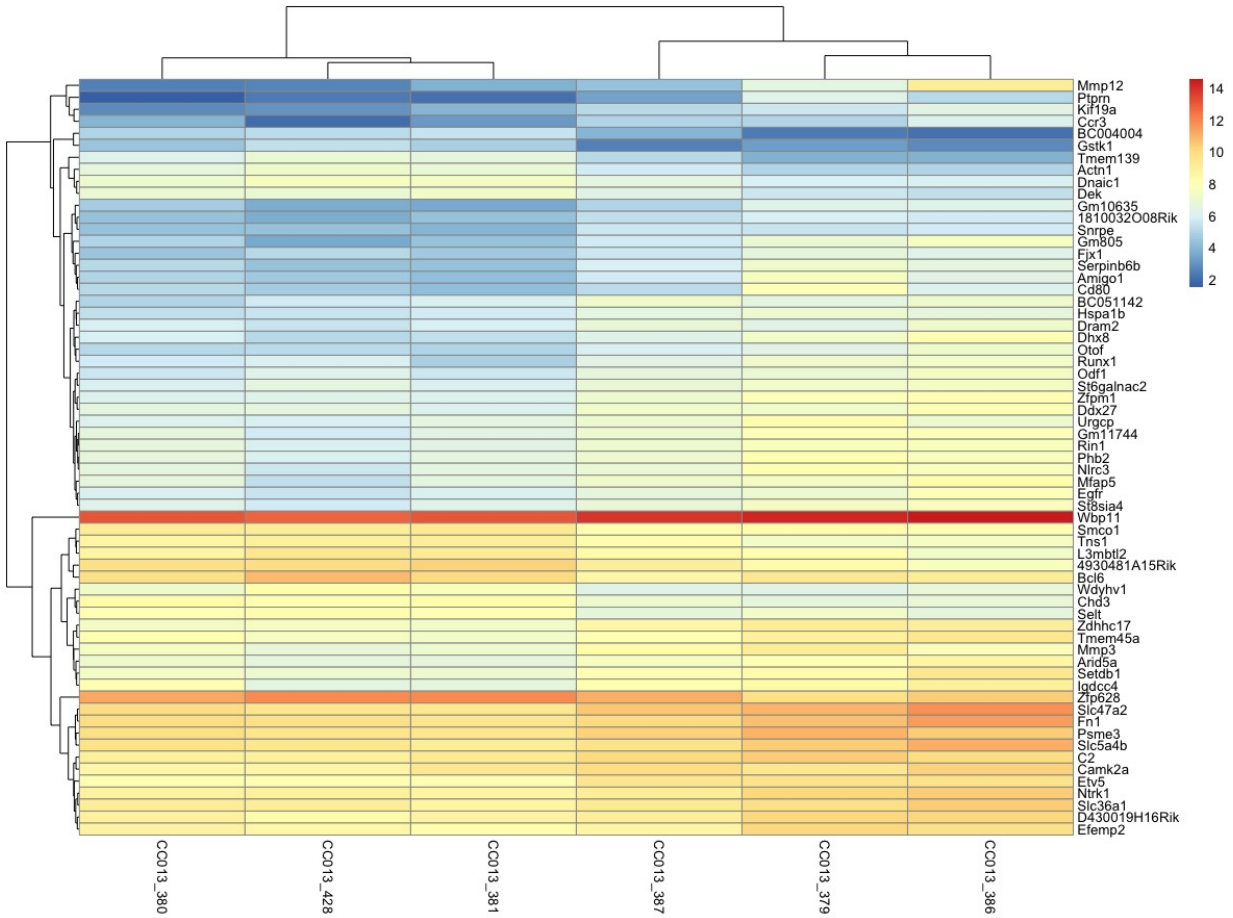

Figure 4.3: Heatmap of differentially expressed genes in gastric tissue between CC013 380, CC013 428, CC013 381 and CC013 387, CC013 379, CC013 386. (fold-change 1.0 and adjusted p<0.01). Red indicates higher expression and blue indicates lower expression.

Genotyping revealed no SNPs differentially expressed between the normal and dilated cardiomyopathic mice.

4.3.4 Differential remodeling response in CC strains to chloroquine

Chloroquine demonstrated no significant differences between control and treated populations in any echocardiographic parameter ($p>0.05$) (Figure 4.4). However, when examining strain-dependent differential response of chloroquine on echocardiographic phenotypes, ΔEDV ($p=0.0309$), as well as Δdiastolic ($p=0.018$) and Δsystolic ($p=0.057$) LV mass were different, indicating that some strains experienced cardiac remodeling while others did not. Posthoc tests revealed that CC019 and CC041 had significantly different ΔLV mass at diastole ($p=0.0032$) and systole ($p=0.0161$).

4.3.5 Differential electrophysiological response in CC strains to chloroquine

Chloroquine demonstrated significant differences between control and treated populations in QRS ($p=0.0391$) and QTc ($p=0.0469$) intervals. When comparing strain differences, only ΔQRS was significant ($p=0.0226$) (Figure 4.5).

4.4 Discussion

In the present study, differential response to known disruptors of cardiac physiology were evaluated in eight strains of the CC population. The findings demonstrate genetic background plays a crucial role in response to characterized cardiotoxicants, even at therapeutic levels. While genetic diversity is an important part of this study, conscious assessment of cardiac phenotypes provides a unique perspective on cardiac function, without the impact of anesthesia, which is known to depress cardiac function [97, 101].

The first key finding of this study was isoproterenol, although an established model for induction of cardiac injury, the only differences in interstrain response were electrophysiological. As a population, baseline and treated groups were significantly different. It is also important to consider that conscious echocardiography could be eliminating responses in cardiac function due to stress of handling, or that anesthetized echocardiography exaggerates the disease phenotype. It is not known whether LV function in healthy and diseased mice responds differently to restraint or anesthesia. Previous studies have reported differential response based on genetic background, but echocardiography was performed under anesthesia [172]. Additionally, isoproterenol had no

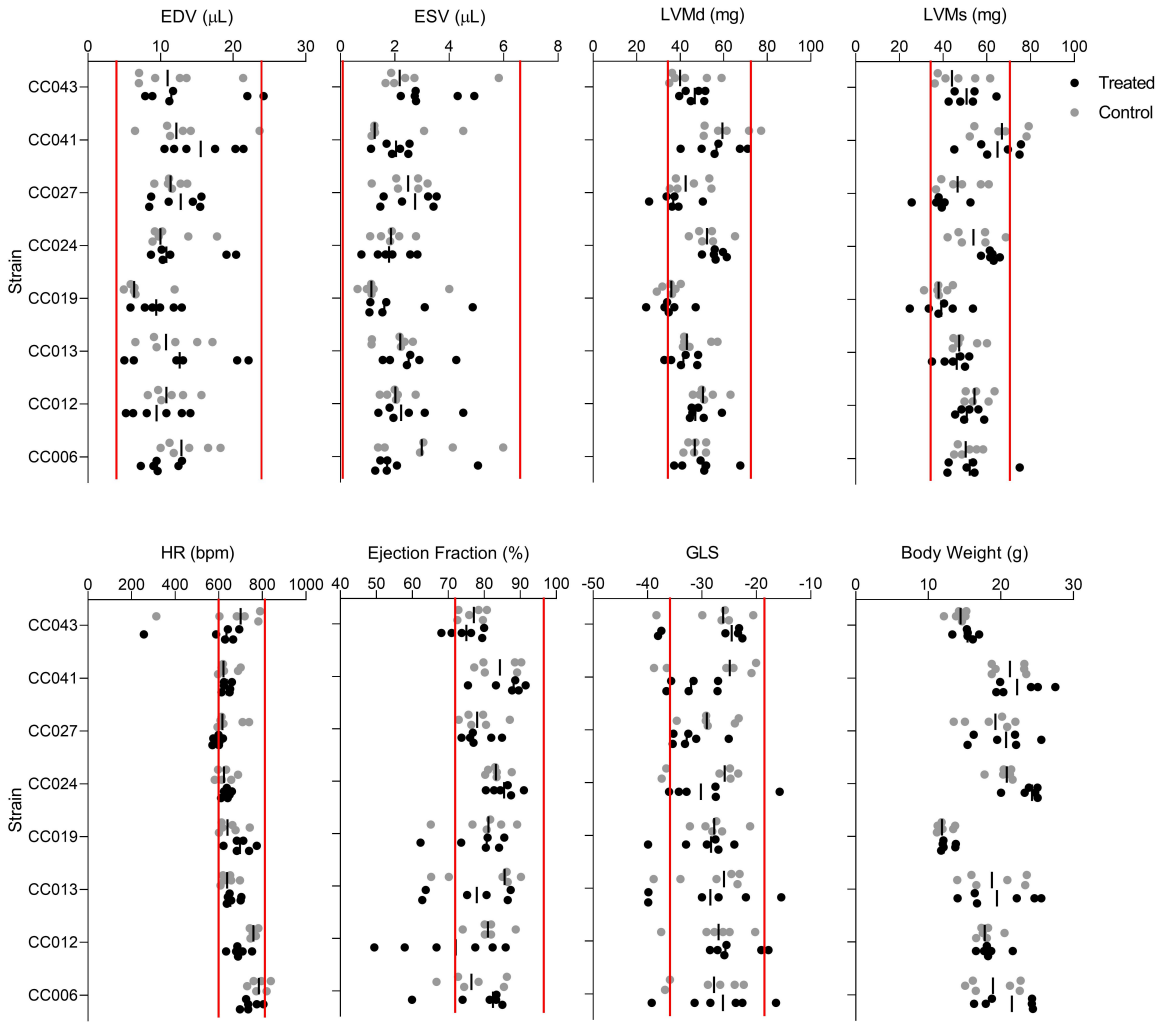

Figure 4.4: Scatterplots of echocardiographic phenotypes and body weight for control and chloroquine treated mice. Horizontal bars represent median values for each strain.

differentially expressed phenotypes between strains except for QTc. For example, most individuals of the strains CC041 and CC024 decreased their QTc interval, while strains like CC013 and CC027 have a prolonged QTc interval as compared to other strains (Figure A.2). This is interesting because isoproterenol is typically used to treat Torsades de Pointes TdP.

The second key finding were the intrastrain differences in CC013 in response to isoproterenol. Interestingly, the bimodal response did not cluster by sex. While RNAseq revealed key differential gene expression between the two groups, genetic sequencing revealed no reported segregation in

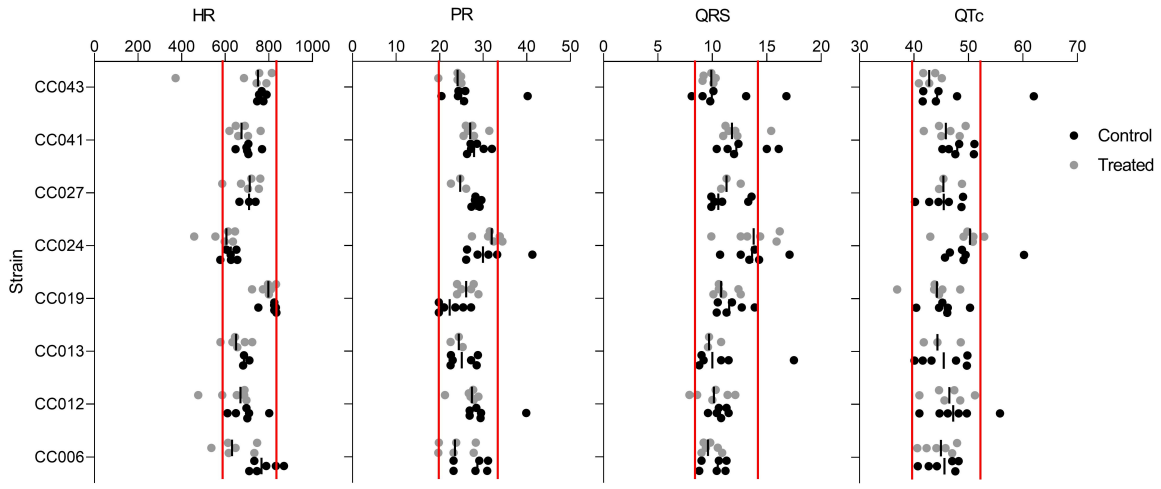

Figure 4.5: Scatterplots of ECG phenotypes for control and chloroquine treated mice. Horizontal bars represent median values for each strain.

any areas of SNP differences, thereby epigenetic or another source of variation are causing the differences in cardiac physiology. Isoproterenol is a β-AR agonist and chronic administration is followed by downregulation of β-AR. Strain-dependent β-AR downregulation and uncoupling has been shown in C57BL/6 mice versus A/J, indicating this process is subject to genetic regulation. It is likely that the severe remodeling occurring in the dilated cardiomyopathy subset of CC013 is due to the lack of downregulation of this receptor with chronic exposure. A gene encoding the alpha isozyme Calcinuerin A is a known target of β-AR signaling and isoproterenol induced cardiac injury [182].

The third key finding was that there were few differences in population response to chloroquine, but many interstrain differences in response to the drug, emphasizing the importance of characterizing differences in baseline phenotypes. Electrophysiology parameters were significantly changed after treatment, which is unsurprising considering the early response to environmental stimuli, biochemical changes such as alterations in calcium homeostasis and electrophysiology occur. Remodeling is occurring in some strains as well as both lengthening and shortening of the QRS complex. This reiterates human cases that report variation of adverse reactions is inter-individual,

demonstrating the CC as an appropriate model of human disease.

The current study was strengthened by the genetic diversity of the CC, but several limitations must be acknowledged. The bimodal response of CC013 to the characterized chemical isoproterenol is an indicator that the strain is not inbred. While this can help to identify regions in the genome affecting response, it prevents the use of biological replicates and reproducibility in this strain. It is also clear that conscious assessment of cardiac phenotypes is affected by handling; HR in conscious echocardiography via scruffing was not significantly different after treatment, while HR in ECG was significantly different. This indicates that the stress of scruffing is masking potential positive chronotropic effects of isoproterenol.

Conscious assessment of these phenotypes provides a unique perspective on how the autonomic nervous system can influence assessment of response to known perturbors of cardiac physiology and future studies will include exploration of genetic networks underlying these diverse phenotypes. Overall the utility of this study is its demonstration of differential response to cardiotoxicants.

5. SIGNIFICANCE, LIMITATIONS, AND FUTURE DIRECTIONS

5.1 Significance

Heart damage occurs as a result of genetic and environmental factors and can lead to death. Mice are the most genetically developed mammalian model and can be translatable to humans. Their small size and short lifespan are financially advantageous and allow researchers to follow disease progression at an accelerated rate, but also from humans in contractile function. Inclusion of genetic variability can overcome some of these limitations that provide species-species reference ranges. Reference ranges for clinically relevant cardiac phenotypes in humans guide physicians in their cardiac diagnoses. In this dissertation, we sought to characterize and understand the genetic control of mouse cardiac phenotypes in a diverse population by developing *Mus musculus* specific cardiac reference ranges. Furthermore, we sought to understand how conscious assessment of cardiac phenotypes might influence response to known cardiac toxicants.

In Chapter 2, we investigated inter-individual variability in cardiac phenotypes using the Collaborative Cross population-based mouse model. We established reference ranges, based upon a level of genetic diversity similar to that in humans, for mice. We observed marked inter- and intra-strain differences in baseline phenotypes, in both conscious and unconscious echocardiography and conscious electrocardiography measurements. Importantly, using the new reference ranges, this study also identified several natural models of various heart conditions. The advantage of these natural models is that they do not require surgery or genetic manipulation, and are predicted to progress naturally over the mouse's lifetime, which leads these models to be more translatable to humans. Consequently, this work addressed a critical gap in normal variation in *Mus musculus*. Overall this research established cardiac reference ranges for *Mus musculus* similar to what exists for humans and the identification of sources of variation, of which strain accounted for the largest source, as well as natural models of heart pathologies.

In Chapter 3, we investigated genetic control of the clinically relevant cardiac phenotypes de-

scribed in Chapter 2. Overall this research discovered two previously unknown genes associated with mouse cardiac physiology, as well as verified conscious echocardiography as a valid method for mouse cardiac assessment. While QTL analysis was most successful with anesthetized echocardiographic data, which is inherently less variable, r^2 of conscious phenotypes with expression data revealed associated mouse genes related to human cardiac phenotypes. Overall this research was a complex assessment of genetic factors controlling mouse cardiac phenotypes; it presents new targets for possible future research and therapeutic intervention as well as validated methods for mouse cardiac assessment.

In Chapter 4 we investigated cardiac response to both isoproterenol and chloroquine using conscious measurements. Depending on the phenotype, we observed differences before and after treatment, and also differential response to treatment based on strain. Isoproterenol had no differentially expressed phenotypes except for QTc. For example, most individuals of the strains CC041 and CC024 decreased their QTc interval, while strains like CC013 and CC027 have a prolonged QTc interval, putting them at risk for TdP. This is interesting and somewhat unexpected because isoproterenol is typically used to treat TdP. Isoproterenol has been well characterized in dozens of inbred and a few traditional recombinant inbred strains> However the effect of isoproterenol has not been explored in a conscious state where there would be no interaction with anesthetics [171, 172]. Chloroquine has not been explored in a genetically diverse population, but host genetics have been shown to play a role in malaria and malaria drug resistance [183, 184].

The heart's primary clinical phenotypes are complex traits, resulting from an interaction between genes and the environment. The heart is also part of an integrated physiological system with complex interactions with other organ systems. Although efforts have been made to study the heart and its function using reductionist approaches, many systems-level phenotypes cannot currently be modeled or studied using these approaches; each of these reductionist approaches has advantages and disadvantages (Table 5.1). The cardiomyocyte monolayer can be used in a variety of settings, such as drug discovery phase of drug development to screen for chemicals that might disrupt Ca^{2+} signaling. The cardiac spheroid is a 3D aggregate of differentiated cardiomyocytes from stem

cells, and can more accurately mimic the microenvironment of a heart than a monolayer. The heart on a chip most accurately mimics the natural habitat of the heart cells, as well as provides more techniques of cardiomyocyte assessment. Each of these *in vitro* heart models can be created with primary cells or stem cell-derived cells.

	Advantages	Disadvantages
cardiomyocyte monolayer	high cell yield, easily expandable	less mature differentiation than 3D culture
	homogenous cells (less diversity = more reproducibility)	2D excludes important signaling that occurs when cells are in a 3D matrix or 3D structure
	uniform exposure to chemicals and media	
cardiac spheroid	3D structure allows for 3D signaling involved in scaffolding	cells can differentiate heterogenously
	3D environment better represents organ microenvironment	limited drug permeability
	can contain various cell types such as vascular and stromal cells	more difficult than monolayer to scale up for high throughput
		Difficult to measure parameters like pressure and force of contraction, only electrical activity
heart on a chip	can control differentiation of vascular cells and stromal cells	microfluidics do not necessarily mimic the human body
	provide fluid flow cells	difficult to scale up
	provide separate access to various organ compartments, also means control	for high-throughput studies
	can measure kinetics and electrical activity of the tissue	

Table 5.1: Advantages and disadvantages of various *in vitro* models of the human heart

In vivo, rat models have dominated research into heart damage for small animals; they share the low cost of housing and ease of handling with mice, but their larger size facilitates surgeries and post surgery procedures more easily than mice. Mouse models are still used, however, for

atherosclerosis, hypercholesterolemia, and heart failure due to their low procedure costs, and the ease of manipulation of the mouse genome [185]. Large animal models, although the time between exposure and observable change is longer than in small animal models, have anatomical similarities to humans that small animals cannot reproduce. For example the porcine model of heart failure is the most similar to humans, both in heart structure and organization of coronary vessels as well as arteries exiting heart chambers [185]. Large animal studies require much more expensive and specialized equipment, as well as dedicated facilities.

No single model perfectly recreates human cardiac pathologies, and there are always considerations of cost, trained personnel, and available facilities and equipment. One aspect often not considered in most of these models, is genetic diversity. Humans are genetically diverse, and in the era of personalized medicine, understanding the network of genes and various polymorphisms leading to disease is essential. Outbred stocks are available in most animal models, but the resources available to interpret the genetic basis for the phenotypic differences that are seen in these populations are limited. The mouse model has the most developed genetic resources with publicly available dense SNP databases across dozens of inbred and reproducible strains [63], positioning it for this study's blend of genotypic and clinically relevant phenotypic cardiac data.

As a model, the Collaborative Cross (CC) is well suited to mimic a complex organ system *in vivo* including genetic variation that can impact interpretation of functional changes. As a mouse population, it contains a level of genetic diversity not present in other models, and unlike the related Diversity Outbred (DO), the CC is reproducible, allowing QTL mapping to be performed without genotyping each individual and supporting replication of data between labs. The capability of the CC to model both complex organ physiology and genetic diversity makes the model more clinically comparable to humans. This positions the CC to uniquely support unraveling the complex network between molecular components and cardiac function. Overall this research was a novel use application of the broad spectrum of capabilities of the CC, in the context of normal and cardiotoxic cardiac phenotypes.

5.2 Limitations

This work explored the impact of genetic diversity in *Mus musculus* on cardiovascular traits for which reference ranges are derived in humans, but did not use exclusion criteria such as blood pressure, cholesterol, low density lipoprotein to high density lipoprotein ratio, glomerular filtration rate, impaired fasting glucose, exercise capacity, creatinine, or triglycerides that are considered clinically relevant to heart health [24]. Future mouse studies can explore these traits in the CC to better understand their impact on cardiovascular health.

Additionally, conscious assessment of cardiac phenotypes increases environmental influences on some cardiac physiology phenotypes, but removes potential interactions with anesthesia that may otherwise complicate interpretations. While this is not necessarily a disadvantage, it must be acknowledged and addressed in future studies. Conscious functional phenotypes are more complex than those derived under anesthetized; no significant echocardiographic functional phenotype had statistically significant correlations with strain-specific gene expression. Indeed, even effects of acute chronotropic effects of isoproterenol are not observed in conscious mice [125]. Increasing the number of biological replicates could help to limit the intra-strain variability seen in conscious echocardiographic measurements.

Although chapter 4 does start to address the need for advanced recombinant strains to understand the underlying genetic basis for response to drugs, several limitations must be acknowledged. To have significant mapping power to identify genes controlling differential response to both drugs, more strains would be needed. Additional information may also be obtained from investigating the relationship between multiple time points, concentrations, and cardiovascular endpoints such as histopathological scoring and early biomarkers of toxicity.

Interestingly, none of the genes that appear to drive the phenotypes using QTL analysis appear in previously published microarray expression datasets. This is likely due to less strains being used for r^2 analysis. There is also a smaller range of data with less strains. Microarray expression data with all 58 strains would likely match QTL analysis more accurately.

Overall the CC is well suited for combining genetic network elucidation with clinically rele-

vant cardiac traits, but some limitations must be acknowledged. The fact that reproducibility, or intrastrain variation, is also a phenotype presents challenges. Statistically significant results, precision, and uncharacterized environmental factors can all lead to the high intrastrain variability and limited reproducibility seen in each chapter. Working with live organisms is challenging, but the strain effect was still highly significant, as was the related measure of heritability. The CC are 95% homozygous, and humans are much more heterozygous. This means there is also substantial genetic information from non-additive effects of more heterozygotic animals, such as those in the DO.

5.3 Future Directions

Although adding additional strains increases power to estimate QTL more than adding biological replicates [186], the total number of CC strains available currently is 70 and therefore an n=3 can be increased for higher resolution mapping of cardiac phenotypes.

Because eight strains limit our ability to map isoproterenol and chloroquine response phenotypes, adding additional strains to the study in Chapter 4 can aid in our ability to characterize the genetic control of those phenotypes. Additionally, exploring individual strain dose-response curves in this CC population could help to more accurately develop a population dose response curve to determine the threshold dose. Future studies using QTL analysis can also improve mapping resolution and exploration of the genetic basis of pharmacological and toxicological inter-individual response.

Animal models have been the gold standard for risk assessment, and in addition to the uncertainty in the accuracy of translation to humans, they are costly, can take many years, and are not amenable to high-throughput screening. While strides have been made in developing *in vitro* models, they have yet to be validated directly *in vivo*. While the work is ongoing, we are designing a panel of CC induced pluripotent stem cell (iPSC)-derived cardiac spheroids that are genetically identical to CC mice, and can validate the *in vitro* to *in vivo* extrapolation (IVIVE) paradigm. While baseline measurements from human cardiomyocytes and their matched donor have shown to be predictive [187], this cannot be performed in humans for an *in vitro* toxicity response due to

ethical reasons.

Contracting cardiomyocytes have been shown to accurately assess chemicals for drug-induced arrhythmia [188, 79]. Cardiomyocytes in the context of an embryoid body (EB) mimic cardiac tissue in both form and function, and cardiac spheroids display various cell types present in the heart (Fig 5.1), as well as electrophysiological properties [189]. While primary cardiomyocytes are useful, they cannot replicate and would need to be harvested for every experiment. iPSCs are an immortal cell line and can be derived from a variety of somatic cell types and reproducibly induced into cardiomyocytes.

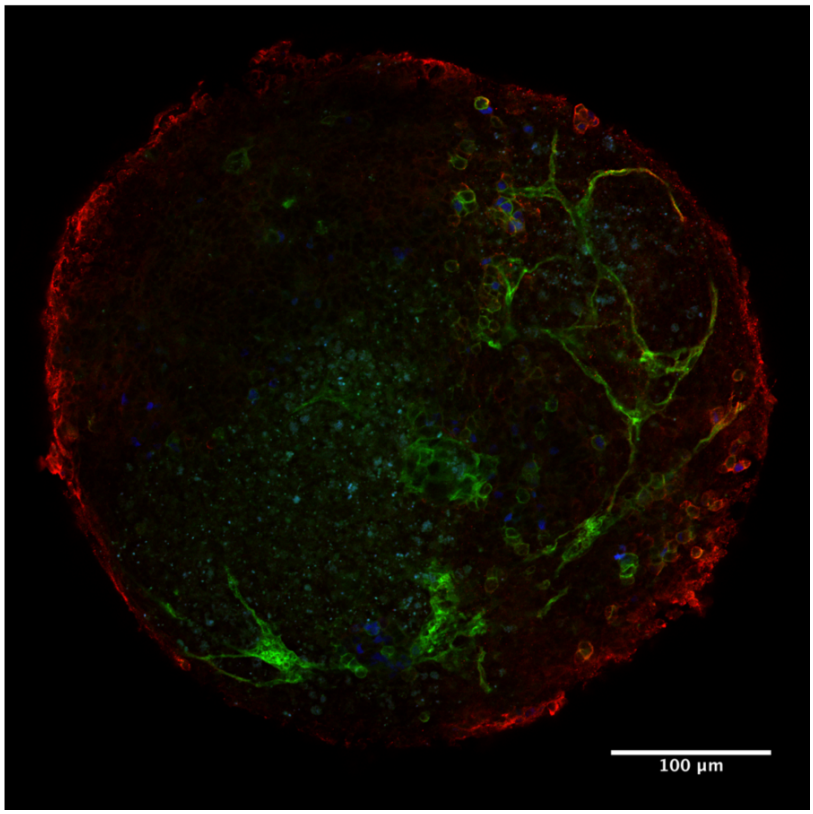

Figure 5.1: Representative confocal image of immunofluorescent cardiac spheroid. Spheroids were labeled for sarcomeric α-actinin (red), CD31 (green), and Oct4 (blue).

Previous work in the lab has shown that Sendai virus vectors can be used for the reprogramming of CC-derived mouse embryonic fibroblasts (MEFs) to iPSCs. The Sendai Virus delivers the four

Yamanaka factors as human transgenes, *OCT4*, *SOX2*, *KLF4*, and *MYC*, into the cell to replicate in the cytoplasm [190]. Its ability to infect many different host cells, and its non-integration into the genome of host cells allow for differentiation later and leave the genomic DNA of the cell undamaged. After 10-15 passages, depending on the CC strain, the Sendai Virus is cleared (Figure 5.2), and cells express endogenous mouse orthologs (Figure 5.3)

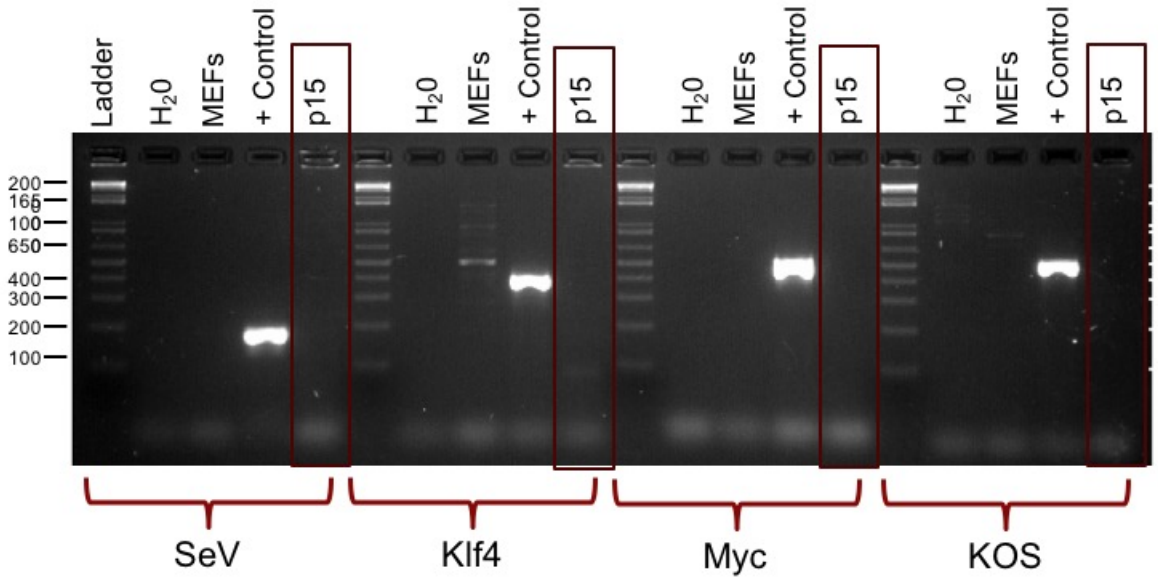

Figure 5.2: PCR analysis demonstrates clearing of the Sendai virus at passage 15 (outlined in red).

During this time, cells were cultured with GSK3B inhibitor CHIR99201 (Millipore-Sigma), MEK inhibitor PD0325901 (Millipore-Sigma), and Leukemia Inhibitory Factor (LIF) (Millipore-Sigma) to inhibit differentiation. Once iPSCs were cleared of the Sendai virus and expressing endogenous mouse pluripotent genes, cells were aggregated into embryoid bodies to be differentiated into cardiac spheroids. Cells were placed in Aggrewell^{TM} system (STEMCELL Technologies Inc.) for 72 hours, and subsequently placed into a spinner flask to differentiate for 10-14 days, with media exchange and filtration every other day. Currently, 6 CC cell lines have been successfully reprogrammed into iPSCs and differentiated into cardiac spheroids.

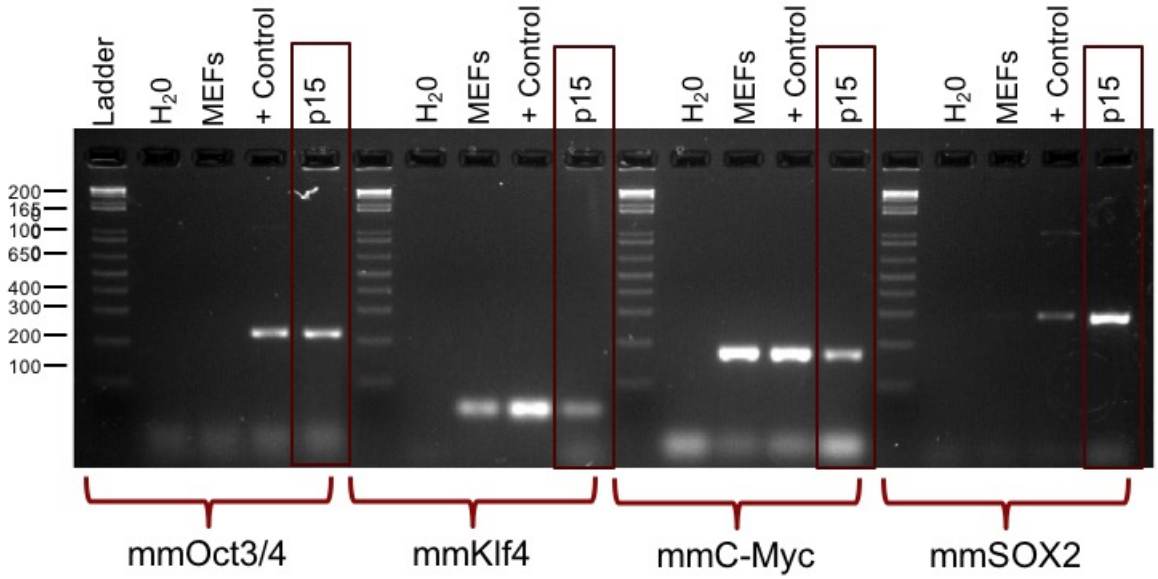

Figure 5.3: PCR analysis demonstrates expression of the mouse endogenous Yamanaka factors passage 15 (outlined in red).

Future work with these cells could include, as a proof of concept, high-throughput screening of known cardiotoxicants to validate *in vivo* mouse chemical exposures. Following validation of IVIVE, cardiac spheroids can be used to test uncharacterized chemicals and their metabolites, with altered doses and altered duration of exposure.

REFERENCES

[1] WHO, "Cardiovascular diseases (cvds)," 2017.

[2] C. B. Fordyce, M. T. Roe, T. Ahmad, P. Libby, J. S. Borer, W. R. Hiatt, M. R. Bristow, M. Packer, S. M. Wasserman, N. Braunstein, B. Pitt, D. L. DeMets, K. Cooper-Arnold, P. W. Armstrong, S. D. Berkowitz, R. Scott, J. Prats, Z. S. Galis, N. Stockbridge, E. D. Peterson, and R. M. Califf, "Cardiovascular drug development: is it dead or just hibernating?," *J Am Coll Cardiol*, vol. 65, no. 15, pp. 1567–82, 2015.

[3] T. A. Fitzgerald, "Comparison of research cost: man–primate animal–other animal models," *J Med Primatol*, vol. 12, no. 3, pp. 138–45, 1983.

[4] S. F. Vatner and E. Braunwald, "Cardiovascular control mechanisms in the conscious state," *N Engl J Med*, vol. 293, no. 19, pp. 970–6, 1975.

[5] Y. T. Shen, F. I. Malik, X. Zhao, C. Depre, S. K. Dhar, P. Abarzua, D. J. Morgans, and S. F. Vatner, "Improvement of cardiac function by a cardiac myosin activator in conscious dogs with systolic heart failure," *Circ Heart Fail*, vol. 3, no. 4, pp. 522–7, 2010.

[6] J. P. Bakkehaug, A. B. Kildal, E. T. Engstad, N. Boardman, T. Naesheim, L. Ronning, E. Aasum, T. S. Larsen, T. Myrmel, and O. J. How, "Myosin activator omecamtiv mecarbil increases myocardial oxygen consumption and impairs cardiac efficiency mediated by resting myosin atpase activity," *Circ Heart Fail*, vol. 8, no. 4, pp. 766–75, 2015.

[7] K. Kikuchi and K. D. Poss, "Cardiac regenerative capacity and mechanisms," *Annu Rev Cell Dev Biol*, vol. 28, pp. 719–41, 2012.

[8] G. Danaei, E. L. Ding, D. Mozaffarian, B. Taylor, J. Rehm, C. J. Murray, and M. Ezzati, "The preventable causes of death in the united states: comparative risk assessment of dietary, lifestyle, and metabolic risk factors," *PLoS Med*, vol. 6, no. 4, p. e1000058, 2009.

[9] W. M. Schultz, H. M. Kelli, J. C. Lisko, T. Varghese, J. Shen, P. Sandesara, A. A. Quyyumi, H. A. Taylor, M. Gulati, J. G. Harold, J. H. Mieres, K. C. Ferdinand, G. A. Mensah, and L. S. Sperling, "Socioeconomic status and cardiovascular outcomes: Challenges and interventions," *Circulation*, vol. 137, no. 20, pp. 2166–2178, 2018.

[10] M. McClellan, N. Brown, R. M. Califf, and J. J. Warner, "Call to action: Urgent challenges in cardiovascular disease: A presidential advisory from the american heart association," *Circulation*, vol. 139, no. 9, pp. e44–e54, 2019.

[11] H. Laverty, C. Benson, E. Cartwright, M. Cross, C. Garland, T. Hammond, C. Holloway, N. McMahon, J. Milligan, B. Park, M. Pirmohamed, C. Pollard, J. Radford, N. Roome, P. Sager, S. Singh, T. Suter, W. Suter, A. Trafford, P. Volders, R. Wallis, R. Weaver, M. York, and J. Valentin, "How can we improve our understanding of cardiovascular safety liabilities to develop safer medicines?," *Br J Pharmacol*, vol. 163, no. 4, pp. 675–93, 2011.

[12] M. J. Pletcher and A. E. Moran, "Cardiovascular risk assessment," *Med Clin North Am*, vol. 101, no. 4, pp. 673–688, 2017.

[13] C. Kendir, M. van den Akker, R. Vos, and J. Metsemakers, "Cardiovascular disease patients have increased risk for comorbidity: A cross-sectional study in the netherlands," *Eur J Gen Pract*, vol. 24, no. 1, pp. 45–50, 2018.

[14] C. Rovida, S. Asakura, M. Daneshian, H. Hofman-Huether, M. Leist, L. Meunier, D. Reif, A. Rossi, M. Schmutz, J. P. Valentin, J. Zurlo, and T. Hartung, "Toxicity testing in the 21st century beyond environmental chemicals," *ALTEX*, vol. 32, no. 3, pp. 171–81, 2015.

[15] J. S. MacDonald and R. T. Robertson, "Toxicity testing in the 21st century: a view from the pharmaceutical industry," *Toxicol Sci*, vol. 110, no. 1, pp. 40–6, 2009.

[16] B. R. Berridge, P. Hoffmann, J. R. Turk, F. Sellke, G. Gintant, G. Hirkaler, K. Dreher, A. E. Schultze, D. Walker, N. Edmunds, W. Halpern, J. Falls, M. Sanders, and S. D. Pettit, "Integrated and translational nonclinical in vivo cardiovascular risk assessment: gaps and opportunities," *Regul Toxicol Pharmacol*, vol. 65, no. 1, pp. 38–46, 2013.

[17] P. Ferdinandy, I. Baczko, P. Bencsik, Z. Giricz, A. Gorbe, P. Pacher, Z. V. Varga, A. Varro, and R. Schulz, "Definition of hidden drug cardiotoxicity: paradigm change in cardiac safety testing and its clinical implications," *Eur Heart J*, vol. 40, no. 22, pp. 1771–1777, 2019.

[18] C. Yu, K. Liu, S. Tang, and S. Ding, "Chemical approaches to cell reprogramming," *Curr Opin Genet Dev*, vol. 28, pp. 50–6, 2014.

[19] F. W. Prinzen, C. H. Augustijn, M. A. Allessie, T. Arts, T. Delhaas, and R. S. Reneman, "The time sequence of electrical and mechanical activation during spontaneous beating and ectopic stimulation," *Eur Heart J*, vol. 13, no. 4, pp. 535–43, 1992.

[20] A. K. Farraj, M. S. Hazari, and W. E. Cascio, "The utility of the small rodent electrocardiogram in toxicology," *Toxicol Sci*, vol. 121, no. 1, pp. 11–30, 2011.

[21] C. Johnson, K. Kuyt, D. Oxborough, and M. Stout, "Practical tips and tricks in measuring strain, strain rate and twist for the left and right ventricles," *Echo Res Pract*, vol. 6, no. 3, pp. R87–R98, 2019.

[22] P. P. Sengupta, J. Korinek, M. Belohlavek, J. Narula, M. A. Vannan, A. Jahangir, and B. K. Khandheria, "Left ventricular structure and function: basic science for cardiac imaging," *J Am Coll Cardiol*, vol. 48, no. 10, pp. 1988–2001, 2006.

[23] R. Krishnasamy, N. M. Isbel, C. M. Hawley, E. M. Pascoe, M. Burrage, R. Leano, B. A. Haluska, T. H. Marwick, and T. Stanton, "Left ventricular global longitudinal strain (gls) is a superior predictor of all-cause and cardiovascular mortality when compared to ejection fraction in advanced chronic kidney disease," *PLoS One*, vol. 10, no. 5, p. e0127044, 2015.

[24] R. M. Lang, L. P. Badano, V. Mor-Avi, J. Afilalo, A. Armstrong, L. Ernande, F. A. Flachskampf, E. Foster, S. A. Goldstein, T. Kuznetsova, P. Lancellotti, D. Muraru, M. H. Picard, E. R. Rietzschel, L. Rudski, K. T. Spencer, W. Tsang, and J. U. Voigt, "Recommendations for cardiac chamber quantification by echocardiography in adults: an update from the american society of echocardiography and the european association of cardiovascular imaging," *Eur Heart J Cardiovasc Imaging*, vol. 16, no. 3, pp. 233–70, 2015.

[25] H. Sawaya, I. A. Sebag, J. C. Plana, J. L. Januzzi, B. Ky, T. C. Tan, V. Cohen, J. Banchs, J. R. Carver, S. E. Wiegers, R. P. Martin, M. H. Picard, R. E. Gerszten, E. F. Halpern, J. Passeri, I. Kuter, and M. Scherrer-Crosbie, "Assessment of echocardiography and biomarkers for the extended prediction of cardiotoxicity in patients treated with anthracyclines, taxanes, and trastuzumab," *Circ Cardiovasc Imaging*, vol. 5, no. 5, pp. 596–603, 2012.

[26] A. M. Maceira, C. Ripoll, J. Cosin-Sales, B. Igual, M. Gavilan, J. Salazar, V. Belloch, and D. J. Pennell, "Long term effects of cocaine on the heart assessed by cardiovascular magnetic resonance at 3t," *J Cardiovasc Magn Reson*, vol. 16, p. 26, 2014.

[27] N. Akuzawa and M. Kurabayashi, "Native valve endocarditis due to escherichia coli infection: a case report and review of the literature," *BMC Cardiovasc Disord*, vol. 18, no. 1, p. 195, 2018.

[28] R. Gordan, J. K. Gwathmey, and L. H. Xie, "Autonomic and endocrine control of cardiovascular function," *World J Cardiol*, vol. 7, no. 4, pp. 204–14, 2015.

[29] G. Ogliari, S. Mahinrad, D. J. Stott, J. W. Jukema, S. P. Mooijaart, P. W. Macfarlane, E. N. Clark, P. M. Kearney, R. G. J. Westendorp, A. J. M. de Craen, and B. Sabayan, "Resting heart rate, heart rate variability and functional decline in old age," *CMAJ*, vol. 187, no. 15, pp. E442–E449, 2015.

[30] M. Omerbegovic, "Linear short-term heart rate variability parameters of subjects tobacco cigarette smokers and subjects nonsmokers in preoperative period," *Med Arch*, vol. 71, no. 1, pp. 12–15, 2017.

[31] S. B. Fadaee, K. S. Beetham, E. J. Howden, T. Stanton, N. M. Isbel, and J. S. Coombes, "Oxidative stress is associated with decreased heart rate variability in patients with chronic kidney disease," *Redox Rep*, vol. 22, no. 5, pp. 197–204, 2017.

[32] G. Ernst, "Heart-rate variability-more than heart beats?," *Front Public Health*, vol. 5, p. 240, 2017.

[33] R. M. Califf, "Biomarkers, putative surrogates, surrogates, and decision making," *Circ Cardiovasc Imaging*, vol. 6, no. 1, pp. 6–7, 2013.

[34] E. A. Gripp, G. E. Oliveira, L. A. Feijo, M. I. Garcia, S. S. Xavier, and A. S. Sousa, "Global longitudinal strain accuracy for cardiotoxicity prediction in a cohort of breast cancer patients during anthracycline and/or trastuzumab treatment," *Arq Bras Cardiol*, vol. 110, no. 2, pp. 140–150, 2018.

[35] W. Ma, S. Wei, B. Zhang, and W. Li, "Molecular mechanisms of cardiomyocyte death in drug-induced cardiotoxicity," *Front Cell Dev Biol*, vol. 8, p. 434, 2020.

[36] Z. V. Varga, P. Ferdinandy, L. Liaudet, and P. Pacher, "Drug-induced mitochondrial dysfunction and cardiotoxicity," *Am J Physiol Heart Circ Physiol*, vol. 309, no. 9, pp. H1453–67, 2015.

[37] M. J. Foglia and K. D. Poss, "Building and re-building the heart by cardiomyocyte proliferation," *Development*, vol. 143, no. 5, pp. 729–40, 2016.

[38] J. A. Barrabes, J. Figueras, C. Moure, J. Cortadellas, and J. Soler-Soler, "Q-wave evolution of a first acute myocardial infarction without significant st segment elevation," *Int J Cardiol*, vol. 77, no. 1, pp. 55–62, 2001.

[39] S. Bidstrup, M. Salling Olesen, J. Hastrup Svendsen, and J. Bille Nielsen, "Role of pr-interval in predicting the occurrence of atrial fibrillation," *J Atr Fibrillation*, vol. 6, no. 4, p. 956, 2013.

[40] G. Bagliani, J. Brugada, R. De Ponti, G. Viola, P. Berne, and F. M. Leonelli, "Qrs variations during arrhythmias: Mechanisms and substrates. toward a precision electrocardiology," *Card Electrophysiol Clin*, vol. 11, no. 2, pp. 315–331, 2019.

[41] J. Duan, J. Tao, M. Zhai, C. Li, N. Zhou, J. Lv, L. Wang, L. Lin, and R. Bai, "Anticancer drugs-related qtc prolongation, torsade de pointes and sudden death: current evidence and future research perspectives," *Oncotarget*, vol. 9, no. 39, pp. 25738–25749, 2018.

[42] R. Mukerji, B. E. Terry, J. L. Fresen, M. Petruc, G. Govindarajan, and M. A. Alpert, "Relation of left ventricular mass to qtc in normotensive severely obese patients," *Obesity (Silver Spring)*, vol. 20, no. 9, pp. 1950–4, 2012.

[43] D. A. Watkins, B. Hasan, B. Mayosi, G. Bukhman, J. A. Marin-Neto, A. Rassi Jr, A. Rassi, and R. K. Kumar, *Structural Heart Diseases*. 2017.

[44] P. J. O'Brien, "Cardiac troponin is the most effective translational safety biomarker for myocardial injury in cardiotoxicity," *Toxicology*, vol. 245, no. 3, pp. 206–18, 2008.

[45] G. Hanton, "Preclinical cardiac safety assessment of drugs," *Drugs R D*, vol. 8, no. 4, pp. 213–28, 2007.

[46] M. A. Lehrman, W. J. Schneider, T. C. Sudhof, M. S. Brown, J. L. Goldstein, and D. W. Russell, "Mutation in ldl receptor: Alu-alu recombination deletes exons encoding transmembrane and cytoplasmic domains," *Science*, vol. 227, no. 4683, pp. 140–6, 1985.

[47] M. E. Curran, I. Splawski, K. W. Timothy, G. M. Vincent, E. D. Green, and M. T. Keating, "A molecular basis for cardiac arrhythmia: Herg mutations cause long qt syndrome," *Cell*, vol. 80, no. 5, pp. 795–803, 1995.

[48] H. C. Dietz, G. R. Cutting, R. E. Pyeritz, C. L. Maslen, L. Y. Sakai, G. M. Corson, E. G. Puffenberger, A. Hamosh, E. J. Nanthakumar, S. M. Curristin, and et al., "Marfan syndrome caused by a recurrent de novo missense mutation in the fibrillin gene," *Nature*, vol. 352, no. 6333, pp. 337–9, 1991.

[49] M. Abifadel, M. Varret, J. P. Rabes, D. Allard, K. Ouguerram, M. Devillers, C. Cruaud, S. Benjannet, L. Wickham, D. Erlich, A. Derre, L. Villeger, M. Farnier, I. Beucler, E. Bruckert, J. Chambaz, B. Chanu, J. M. Lecerf, G. Luc, P. Moulin, J. Weissenbach, A. Prat, M. Krempf, C. Junien, N. G. Seidah, and C. Boileau, "Mutations in pcsk9 cause autosomal dominant hypercholesterolemia," *Nat Genet*, vol. 34, no. 2, pp. 154–6, 2003.

[50] D. E. Arking and A. Chakravarti, "Understanding cardiovascular disease through the lens of genome-wide association studies," *Trends Genet*, vol. 25, no. 9, pp. 387–94, 2009.

[51] H. Choquet, K. K. Thai, C. Jiang, D. K. Ranatunga, T. J. Hoffmann, A. S. Go, A. C. Lindsay, M. G. Ehm, D. M. Waterworth, N. Risch, and C. Schaefer, "Meta-analysis of 26 638 individuals identifies two genetic loci associated with left ventricular ejection fraction," *Circ Genom Precis Med*, vol. 13, no. 4, p. e002804, 2020.

[52] V. Khan, S. Sharma, U. Bhandari, N. Sharma, V. Rishi, and S. E. Haque, "Suppression of isoproterenol-induced cardiotoxicity in rats by raspberry ketone via activation of peroxisome proliferator activated receptor-alpha," *Eur J Pharmacol*, vol. 842, pp. 157–166, 2019.

[53] D. K. Arnett, R. B. Devereux, D. Kitzman, A. Oberman, P. Hopkins, L. Atwood, A. Dewan, D. C. Rao, and G. Hypertension Genetic Epidemiology Network Study, "Linkage of left ventricular contractility to chromosome 11 in humans: The hypergen study," *Hypertension*, vol. 38, no. 4, pp. 767–72, 2001.

[54] N. Aung, J. D. Vargas, C. Yang, C. P. Cabrera, H. R. Warren, K. Fung, E. Tzanis, M. R. Barnes, J. I. Rotter, K. D. Taylor, A. W. Manichaikul, J. A. C. Lima, D. A. Bluemke, S. K. Piechnik, S. Neubauer, P. B. Munroe, and S. E. Petersen, "Genome-wide analysis of left ventricular image-derived phenotypes identifies fourteen loci associated with cardiac morphogenesis and heart failure development," *Circulation*, vol. 140, no. 16, pp. 1318–1330, 2019.

[55] C. Newton-Cheh, M. G. Larson, D. C. Corey, E. J. Benjamin, A. G. Herbert, D. Levy, R. B. D'Agostino, and C. J. O'Donnell, "Qt interval is a heritable quantitative trait with evidence of linkage to chromosome 3 in a genome-wide linkage analysis: The framingham heart study," *Heart Rhythm*, vol. 2, no. 3, pp. 277–84, 2005.

[56] D. Altshuler, M. J. Daly, and E. S. Lander, "Genetic mapping in human disease," *Science*, vol. 322, no. 5903, pp. 881–8, 2008.

[57] L. Zeise, F. Y. Bois, W. A. Chiu, D. Hattis, I. Rusyn, and K. Z. Guyton, "Addressing human variability in next-generation human health risk assessments of environmental chemicals," *Environ Health Perspect*, vol. 121, no. 1, pp. 23–31, 2013.

[58] I. Rusyn, D. M. Gatti, T. Wiltshire, S. R. Kleeberger, and D. W. Threadgill, "Toxicogenetics: population-based testing of drug and chemical safety in mouse models," *Pharmacogenomics*, vol. 11, no. 8, pp. 1127–36, 2010.

[59] A. L. Rasmussen, A. Okumura, M. T. Ferris, R. Green, F. Feldmann, S. M. Kelly, D. P. Scott, D. Safronetz, E. Haddock, R. LaCasse, M. J. Thomas, P. Sova, V. S. Carter, J. M. Weiss, D. R. Miller, G. D. Shaw, M. J. Korth, M. T. Heise, R. S. Baric, F. P. de Villena, H. Feldmann, and M. G. Katze, "Host genetic diversity enables ebola hemorrhagic fever pathogenesis and resistance," *Science*, vol. 346, no. 6212, pp. 987–91, 2014.

[60] D. Masopust, C. P. Sivula, and S. C. Jameson, "Of mice, dirty mice, and men: Using mice to understand human immunology," *J Immunol*, vol. 199, no. 2, pp. 383–388, 2017.

[61] T. Hatzipetros, L. P. Bogdanik, V. R. Tassinari, J. D. Kidd, A. J. Moreno, C. Davis, M. Osborne, A. Austin, F. G. Vieira, C. Lutz, and S. Perrin, "C57bl/6j congenic prp-tdp43a315t mice develop progressive neurodegeneration in the myenteric plexus of the colon without exhibiting key features of als," *Brain Res*, vol. 1584, pp. 59–72, 2014.

[62] C. J. Zeiss, D. M. Gatti, O. Toro-Salazar, C. Davis, C. M. Lutz, F. Spinale, T. Stearns, M. B. Furtado, and G. A. Churchill, "Doxorubicin-induced cardiotoxicity in collaborative cross (cc) mice recapitulates individual cardiotoxicity in humans," *G3 (Bethesda)*, vol. 9, no. 8, pp. 2637–2646, 2019.

[63] J. R. Wang, F. P. de Villena, H. A. Lawson, J. M. Cheverud, G. A. Churchill, and L. McMillan, "Imputation of single-nucleotide polymorphisms in inbred mice using local phylogeny," *Genetics*, vol. 190, no. 2, pp. 449–58, 2012.

[64] B. D. Hoit, S. Kiatchoosakun, J. Restivo, D. Kirkpatrick, K. Olszens, H. Shao, Y. H. Pao, and J. H. Nadeau, "Naturally occurring variation in cardiovascular traits among inbred mouse strains," *Genomics*, vol. 79, no. 5, pp. 679–85, 2002.

[65] J. J. Avila, S. K. Kim, and M. P. Massett, "Differences in exercise capacity and responses to training in 24 inbred mouse strains," *Front Physiol*, vol. 8, p. 974, 2017.

[66] M. S. Barnabei, N. J. Palpant, and J. M. Metzger, "Influence of genetic background on ex vivo and in vivo cardiac function in several commonly used inbred mouse strains," *Physiol Genomics*, vol. 42A, no. 2, pp. 103–13, 2010.

[67] K. Moreth, R. Fischer, H. Fuchs, V. Gailus-Durner, W. Wurst, H. A. Katus, R. Bekeredjian, and M. Hrabe de Angelis, "High-throughput phenotypic assessment of cardiac physiology in four commonly used inbred mouse strains," *J Comp Physiol B*, vol. 184, no. 6, pp. 763–75, 2014.

[68] K. M. Reilly, "The effects of genetic background of mouse models of cancer: Friend or foe?," *Cold Spring Harb Protoc*, vol. 2016, no. 3, p. pdb top076273, 2016.

[69] P. Wang, Y. Wang, S. A. Langley, Y. X. Zhou, K. Y. Jen, Q. Sun, C. Brislawn, C. M. Rojas, K. L. Wahl, T. Wang, X. Fan, J. K. Jansson, S. E. Celniker, X. Zou, D. W. Threadgill, A. M. Snijders, and J. H. Mao, "Diverse tumour susceptibility in collaborative cross mice: identification of a new mouse model for human gastric tumourigenesis," *Gut*, vol. 68, no. 11, pp. 1942–1952, 2019.

[70] L. Lewis, B. Borowa-Mazgaj, A. de Conti, G. A. Chappell, Y. S. Luo, W. Bodnar, K. Konganti, F. A. Wright, D. W. Threadgill, W. A. Chiu, I. P. Pogribny, and I. Rusyn, "Population-based analysis of dna damage and epigenetic effects of 1,3-butadiene in the mouse," *Chem Res Toxicol*, vol. 32, no. 5, pp. 887–898, 2019.

[71] J. B. Graham, J. L. Swarts, M. Mooney, G. Choonoo, S. Jeng, D. R. Miller, M. T. Ferris, S. McWeeney, and J. M. Lund, "Extensive homeostatic t cell phenotypic variation within the collaborative cross," *Cell Rep*, vol. 21, no. 8, pp. 2313–2325, 2017.

[72] R. T. Molenhuis, H. Bruining, M. J. V. Brandt, P. E. van Soldt, H. J. Abu-Toamih Atamni, J. P. H. Burbach, F. A. Iraqi, R. F. Mott, and M. J. H. Kas, "Modeling the quantitative nature of neurodevelopmental disorders using collaborative cross mice," *Mol Autism*, vol. 9, p. 63, 2018.

[73] W. T. Barrington, P. Wulfridge, A. E. Wells, C. M. Rojas, S. Y. F. Howe, A. Perry, K. Hua, M. A. Pellizzon, K. D. Hansen, B. H. Voy, B. J. Bennett, D. Pomp, A. P. Feinberg, and D. W. Threadgill, "Improving metabolic health through precision dietetics in mice," *Genetics*, vol. 208, no. 1, pp. 399–417, 2018.

[74] WHO, "The top 10 causes of death," 2020.

[75] S. S. Virani, A. Alonso, E. J. Benjamin, M. S. Bittencourt, C. W. Callaway, A. P. Carson, A. M. Chamberlain, A. R. Chang, S. Cheng, F. N. Delling, L. Djousse, M. S. V. Elkind, J. F. Ferguson, M. Fornage, S. S. Khan, B. M. Kissela, K. L. Knutson, T. W. Kwan, D. T. Lackland, T. T. Lewis, J. H. Lichtman, C. T. Longenecker, M. S. Loop, P. L. Lutsey, S. S. Martin, K. Matsushita, A. E. Moran, M. E. Mussolino, A. M. Perak, W. D. Rosamond, G. A. Roth, U. K. A. Sampson, G. M. Satou, E. B. Schroeder, S. H. Shah, C. M. Shay, N. L. Spartano, A. Stokes, D. L. Tirschwell, L. B. VanWagner, C. W. Tsao, E. American Heart Association Council on, C. Prevention Statistics, and S. Stroke Statistics, "Heart disease and stroke statistics-2020 update: A report from the american heart association," *Circulation*, vol. 141, no. 9, pp. e139–e596, 2020.

[76] Y. Jin, T. Kuznetsova, M. Bochud, T. Richart, L. Thijs, D. Cusi, R. Fagard, and J. A. Staessen, "Heritability of left ventricular structure and function in caucasian families," *Eur J Echocardiogr*, vol. 12, no. 4, pp. 326–32, 2011.

[77] W. S. Post, M. G. Larson, R. H. Myers, M. Galderisi, and D. Levy, "Heritability of left ventricular mass: the framingham heart study," *Hypertension*, vol. 30, no. 5, pp. 1025–8, 1997.

[78] P. Ponikowski, A. A. Voors, S. D. Anker, H. Bueno, J. G. F. Cleland, A. J. S. Coats, V. Falk, J. R. Gonzalez-Juanatey, V. P. Harjola, E. A. Jankowska, M. Jessup, C. Linde, P. Nihoyannopoulos, J. T. Parissis, B. Pieske, J. P. Riley, G. M. C. Rosano, L. M. Ruilope, F. Ruschitzka, F. H. Rutten, and P. van der Meer, "2016 esc guidelines for the diagnosis and treat-

ment of acute and chronic heart failure," *Rev Esp Cardiol (Engl Ed)*, vol. 69, no. 12, p. 1167, 2016.

[79] S. D. Burnett, A. D. Blanchette, F. A. Grimm, J. S. House, D. M. Reif, F. A. Wright, W. A. Chiu, and I. Rusyn, "Population-based toxicity screening in human induced pluripotent stem cell-derived cardiomyocytes," *Toxicol Appl Pharmacol*, vol. 381, p. 114711, 2019.

[80] B. R. Berridge, V. Mowat, H. Nagai, A. Nyska, Y. Okazaki, P. J. Clements, M. Rinke, P. W. Snyder, M. C. Boyle, and M. Y. Wells, "Non-proliferative and proliferative lesions of the cardiovascular system of the rat and mouse," *J Toxicol Pathol*, vol. 29, no. 3 Suppl, pp. 1S–47S, 2016.

[81] P. S. Wild, J. F. Felix, A. Schillert, A. Teumer, M. H. Chen, M. J. G. Leening, U. Volker, V. Grossmann, J. A. Brody, M. R. Irvin, S. J. Shah, S. Pramana, W. Lieb, R. Schmidt, A. V. Stanton, D. Malzahn, A. V. Smith, J. Sundstrom, C. Minelli, D. Ruggiero, L. P. Lyytikainen, D. Tiller, J. G. Smith, C. Monnereau, M. R. Di Tullio, S. K. Musani, A. C. Morrison, T. H. Pers, M. Morley, M. E. Kleber, J. Aragam, E. J. Benjamin, J. C. Bis, E. Bisping, U. Broeckel, S. Cheng, J. W. Deckers, M. F. Del Greco, F. Edelmann, M. Fornage, L. Franke, N. Friedrich, T. B. Harris, E. Hofer, A. Hofman, J. Huang, A. D. Hughes, M. Kahonen, K. Investigators, J. Kruppa, K. J. Lackner, L. Lannfelt, R. Laskowski, L. J. Launer, M. Leosdottir, H. Lin, C. M. Lindgren, C. Loley, C. A. MacRae, D. Mascalzoni, J. Mayet, D. Medenwald, A. P. Morris, C. Muller, M. Muller-Nurasyid, S. Nappo, P. M. Nilsson, S. Nuding, T. Nutile, A. Peters, A. Pfeufer, D. Pietzner, P. P. Pramstaller, O. T. Raitakari, K. M. Rice, F. Rivadeneira, J. I. Rotter, S. T. Ruohonen, R. L. Sacco, T. E. Samdarshi, H. Schmidt, A. S. P. Sharp, D. C. Shields, R. Sorice, N. Sotoodehnia, B. H. Stricker, P. Surendran, S. Thom, A. M. Toglhofer, A. G. Uitterlinden, R. Wachter, H. Volzke, A. Ziegler, T. Munzel, W. Marz, T. P. Cappola, J. N. Hirschhorn, G. F. Mitchell, N. L. Smith, E. R. Fox, *et al.*, "Large-scale genome-wide analysis identifies genetic variants associated with cardiac structure and function," *J Clin Invest*, vol. 127, no. 5, pp. 1798–1812, 2017.

[82] C. Andersson, A. D. Johnson, E. J. Benjamin, D. Levy, and R. S. Vasan, "70-year legacy of the framingham heart study," *Nat Rev Cardiol*, vol. 16, no. 11, pp. 687–698, 2019.

[83] E. R. Fox, S. K. Musani, M. Barbalic, H. Lin, B. Yu, K. O. Ogunyankin, N. L. Smith, A. Kutlar, N. L. Glazer, W. S. Post, D. N. Paltoo, D. L. Dries, D. N. Farlow, C. W. Duarte, S. L. Kardia, K. J. Meyers, Y. V. Sun, D. K. Arnett, A. A. Patki, J. Sha, X. Cui, T. E. Samdarshi, A. D. Penman, K. Bibbins-Domingo, P. Buzkova, E. J. Benjamin, D. A. Bluemke, A. C. Morrison, G. Heiss, J. J. Carr, R. P. Tracy, T. H. Mosley, H. A. Taylor, B. M. Psaty, S. R. Heckbert, T. P. Cappola, and R. S. Vasan, "Genome-wide association study of cardiac structure and systolic function in african americans: the candidate gene association resource (care) study," *Circ Cardiovasc Genet*, vol. 6, no. 1, pp. 37–46, 2013.

[84] J. R. Golbus, M. J. Puckelwartz, J. P. Fahrenbach, L. M. Dellefave-Castillo, D. Wolfgeher, and E. M. McNally, "Population-based variation in cardiomyopathy genes," *Circ Cardiovasc Genet*, vol. 5, no. 4, pp. 391–9, 2012.

[85] E. Salimova, K. J. Nowak, A. C. Estrada, M. B. Furtado, E. McNamara, Q. Nguyen, L. Balmer, C. Preuss, J. W. Holmes, M. Ramialison, G. Morahan, and N. A. Rosenthal, "Variable outcomes of human heart attack recapitulated in genetically diverse mice," *NPJ Regen Med*, vol. 4, p. 5, 2019.

[86] B. J. Maron and J. J. Mulvihill, "The genetics of hypertrophic cardiomyopathy," *Ann Intern Med*, vol. 105, no. 4, pp. 610–3, 1986.

[87] M. M. Simon, S. Greenaway, J. K. White, H. Fuchs, V. Gailus-Durner, S. Wells, T. Sorg, K. Wong, E. Bedu, E. J. Cartwright, R. Dacquin, S. Djebali, J. Estabel, J. Graw, N. J. Ingham, I. J. Jackson, A. Lengeling, S. Mandillo, J. Marvel, H. Meziane, F. Preitner, O. Puk, M. Roux, D. J. Adams, S. Atkins, A. Ayadi, L. Becker, A. Blake, D. Brooker, H. Cater, M. F. Champy, R. Combe, P. Danecek, A. di Fenza, H. Gates, A. K. Gerdin, E. Golini, J. M. Hancock, W. Hans, S. M. Holter, T. Hough, P. Jurdic, T. M. Keane, H. Morgan, W. Muller, F. Neff, G. Nicholson, B. Pasche, L. A. Roberson, J. Rozman, M. Sanderson,

L. Santos, M. Selloum, C. Shannon, A. Southwell, G. P. Tocchini-Valentini, V. E. Vancollie, H. Westerberg, W. Wurst, M. Zi, B. Yalcin, R. Ramirez-Solis, K. P. Steel, A. M. Mallon, M. H. de Angelis, Y. Herault, and S. D. Brown, "A comparative phenotypic and genomic analysis of c57bl/6j and c57bl/6n mouse strains," *Genome Biol*, vol. 14, no. 7, p. R82, 2013.

[88] S. McLaughlin, B. McNeill, J. Podrebarac, K. Hosoyama, V. Sedlakova, G. Cron, D. Smyth, R. Seymour, K. Goel, W. Liang, K. J. Rayner, M. Ruel, E. J. Suuronen, and E. I. Alarcon, "Injectable human recombinant collagen matrices limit adverse remodeling and improve cardiac function after myocardial infarction," *Nat Commun*, vol. 10, no. 1, p. 4866, 2019.

[89] S. Lee, D. H. Lee, B. W. Park, R. Kim, A. D. Hoang, S. K. Woo, W. Xiong, Y. J. Lee, K. Ban, and H. J. Park, "In vivo transduction of etv2 improves cardiac function and induces vascular regeneration following myocardial infarction," *Exp Mol Med*, vol. 51, no. 2, pp. 1–14, 2019.

[90] D. W. Threadgill, K. W. Hunter, and R. W. Williams, "Genetic dissection of complex and quantitative traits: from fantasy to reality via a community effort," *Mamm Genome*, vol. 13, no. 4, pp. 175–8, 2002.

[91] G. A. Churchill, D. C. Airey, H. Allayee, J. M. Angel, A. D. Attie, J. Beatty, W. D. Beavis, J. K. Belknap, B. Bennett, W. Berrettini, A. Bleich, M. Bogue, K. W. Broman, K. J. Buck, E. Buckler, M. Burmeister, E. J. Chesler, J. M. Cheverud, S. Clapcote, M. N. Cook, R. D. Cox, J. C. Crabbe, W. E. Crusio, A. Darvasi, C. F. Deschepper, R. W. Doerge, C. R. Farber, J. Forejt, D. Gaile, S. J. Garlow, H. Geiger, H. Gershenfeld, T. Gordon, J. Gu, W. Gu, G. de Haan, N. L. Hayes, C. Heller, H. Himmelbauer, R. Hitzemann, K. Hunter, H. C. Hsu, F. A. Iraqi, B. Ivandic, H. J. Jacob, R. C. Jansen, K. J. Jepsen, D. K. Johnson, T. E. Johnson, G. Kempermann, C. Kendziorski, M. Kotb, R. F. Kooy, B. Llamas, F. Lammert, J. M. Lassalle, P. R. Lowenstein, L. Lu, A. Lusis, K. F. Manly, R. Marcucio, D. Matthews, J. F. Medrano, D. R. Miller, G. Mittleman, B. A. Mock, J. S. Mogil, X. Montagutelli, G. Morahan, D. G. Morris, R. Mott, J. H. Nadeau, H. Nagase, R. S. Nowakowski, B. F. O'Hara, A. V. Osadchuk, G. P. Page, B. Paigen, K. Paigen, A. A. Palmer, H. J. Pan, L. Peltonen-

Palotie, J. Peirce, D. Pomp, M. Pravenec, D. R. Prows, Z. Qi, R. H. Reeves, J. Roder, G. D. Rosen, E. E. Schadt, L. C. Schalkwyk, Z. Seltzer, K. Shimomura, S. Shou, M. J. Sillanpaa, L. D. Siracusa, H. W. Snoeck, J. L. Spearow, K. Svenson, *et al.*, "The collaborative cross, a community resource for the genetic analysis of complex traits," *Nat Genet*, vol. 36, no. 11, pp. 1133–7, 2004.

[92] A. Roberts, F. Pardo-Manuel de Villena, W. Wang, L. McMillan, and D. W. Threadgill, "The polymorphism architecture of mouse genetic resources elucidated using genome-wide resequencing data: implications for qtl discovery and systems genetics," *Mamm Genome*, vol. 18, no. 6-7, pp. 473–81, 2007.

[93] R. E. Pachon, B. A. Scharf, D. E. Vatner, and S. F. Vatner, "Best anesthetics for assessing left ventricular systolic function by echocardiography in mice," *Am J Physiol Heart Circ Physiol*, vol. 308, no. 12, pp. H1525–9, 2015.

[94] X. H. Wehrens, S. Kirchhoff, and P. A. Doevendans, "Mouse electrocardiography: an interval of thirty years," *Cardiovasc Res*, vol. 45, no. 1, pp. 231–7, 2000.

[95] V. Mor-Avi, R. M. Lang, L. P. Badano, M. Belohlavek, N. M. Cardim, G. Derumeaux, M. Galderisi, T. Marwick, S. F. Nagueh, P. P. Sengupta, R. Sicari, O. A. Smiseth, B. Smulevitz, M. Takeuchi, J. D. Thomas, M. Vannan, J. U. Voigt, and J. L. Zamorano, "Current and evolving echocardiographic techniques for the quantitative evaluation of cardiac mechanics: Ase/eae consensus statement on methodology and indications endorsed by the japanese society of echocardiography," *Eur J Echocardiogr*, vol. 12, no. 3, pp. 167–205, 2011.

[96] S. Olejnik and J. Algina, "Generalized eta and omega squared statistics: measures of effect size for some common research designs," *Psychol Methods*, vol. 8, no. 4, pp. 434–47, 2003.

[97] D. M. Roth, J. S. Swaney, N. D. Dalton, E. A. Gilpin, and J. Ross, J., "Impact of anesthesia on cardiac function during echocardiography in mice," *Am J Physiol Heart Circ Physiol*, vol. 282, no. 6, pp. H2134–40, 2002.

[98] K. Kramer, S. A. van Acker, H. P. Voss, J. A. Grimbergen, W. J. van der Vijgh, and A. Bast, "Use of telemetry to record electrocardiogram and heart rate in freely moving mice," *J Pharmacol Toxicol Methods*, vol. 30, no. 4, pp. 209–15, 1993.

[99] X. P. Yang, Y. H. Liu, N. E. Rhaleb, N. Kurihara, H. E. Kim, and O. A. Carretero, "Echocardiographic assessment of cardiac function in conscious and anesthetized mice," *Am J Physiol*, vol. 277, no. 5, pp. H1967–74, 1999.

[100] J. M. Sonner, D. Gong, and n. Eger, E. I., "Naturally occurring variability in anesthetic potency among inbred mouse strains," *Anesth Analg*, vol. 91, no. 3, pp. 720–6, 2000.

[101] A. A. Chaves, D. M. Weinstein, and J. A. Bauer, "Non-invasive echocardiographic studies in mice: influence of anesthetic regimen," *Life Sci*, vol. 69, no. 2, pp. 213–22, 2001.

[102] A. Just, J. Faulhaber, and H. Ehmke, "Autonomic cardiovascular control in conscious mice," *Am J Physiol Regul Integr Comp Physiol*, vol. 279, no. 6, pp. R2214–21, 2000.

[103] P. V. Rasmussen, J. B. Nielsen, M. W. Skov, A. Pietersen, C. Graff, B. Lind, J. J. Struijk, M. S. Olesen, S. Haunso, L. Kober, J. H. Svendsen, and A. G. Holst, "Electrocardiographic pr interval duration and cardiovascular risk: Results from the copenhagen ecg study," *Can J Cardiol*, vol. 33, no. 5, pp. 674–681, 2017.

[104] S. Cheng, M. J. Keyes, M. G. Larson, E. L. McCabe, C. Newton-Cheh, D. Levy, E. J. Benjamin, R. S. Vasan, and T. J. Wang, "Long-term outcomes in individuals with prolonged pr interval or first-degree atrioventricular block," *JAMA*, vol. 301, no. 24, pp. 2571–7, 2009.

[105] A. Brenyo and W. Zareba, "Prognostic significance of qrs duration and morphology," *Cardiol J*, vol. 18, no. 1, pp. 8–17, 2011.

[106] T. J. Laboratory, "Multisystem phenotyping of 18 collaborative cross strains," 2019.

[107] J. Stypmann, M. A. Engelen, C. Epping, H. V. van Rijen, P. Milberg, C. Bruch, G. Breithardt, K. Tiemann, and L. Eckardt, "Age and gender related reference values for transthoracic doppler-echocardiography in the anesthetized cd1 mouse," *Int J Cardiovasc Imaging*, vol. 22, no. 3-4, pp. 353–62, 2006.

[108] K. Ashish, M. Faisaluddin, D. Bandyopadhyay, A. Hajra, and E. Herzog, "Prognostic value of global longitudinal strain in heart failure subjects: A recent prototype," *Int J Cardiol Heart Vasc*, vol. 22, pp. 48–49, 2019.

[109] Z. B. Popovic, J. P. Sun, H. Yamada, J. Drinko, K. Mauer, N. L. Greenberg, Y. Cheng, C. S. Moravec, M. S. Penn, T. N. Mazgalev, and J. D. Thomas, "Differences in left ventricular long-axis function from mice to humans follow allometric scaling to ventricular size," *J Physiol*, vol. 568, no. Pt 1, pp. 255–65, 2005.

[110] J. Wang, A. Huertas-Vazquez, Y. Wang, and A. J. Lusis, "Isoproterenol-induced cardiac diastolic dysfunction in mice: A systems genetics analysis," *Front Cardiovasc Med*, vol. 6, p. 100, 2019.

[111] A. Dorman, D. Baer, I. Tomlinson, R. Mott, and F. A. Iraqi, "Genetic analysis of intestinal polyp development in collaborative cross mice carrying the apc (min/+) mutation," *BMC Genet*, vol. 17, p. 46, 2016.

[112] J. A. Cichocki, S. Furuya, A. Venkatratnam, T. J. McDonald, A. H. Knap, T. Wade, S. Sweet, W. A. Chiu, D. W. Threadgill, and I. Rusyn, "Characterization of variability in toxicokinetics and toxicodynamics of tetrachloroethylene using the collaborative cross mouse population," *Environ Health Perspect*, vol. 125, no. 5, p. 057006, 2017.

[113] N. I. Lore, B. Sipione, G. He, L. J. Strug, H. J. Atamni, A. Dorman, R. Mott, F. A. Iraqi, and A. Bragonzi, "Collaborative cross mice yield genetic modifiers for pseudomonas aeruginosa infection in human lung disease," *mBio*, vol. 11, no. 2, 2020.

[114] J. R. Shorter, P. L. Maurizio, T. A. Bell, G. D. Shaw, D. R. Miller, T. J. Gooch, J. S. Spence, L. McMillan, W. Valdar, and F. Pardo-Manuel de Villena, "A diallel of the mouse collaborative cross founders reveals strong strain-specific maternal effects on litter size," *G3 (Bethesda)*, vol. 9, no. 5, pp. 1613–1622, 2019.

[115] E. Potter and T. H. Marwick, "Assessment of left ventricular function by echocardiography: The case for routinely adding global longitudinal strain to ejection fraction," *JACC*

Cardiovasc Imaging, vol. 11, no. 2 Pt 1, pp. 260–274, 2018.

[116] S. Karlsen, T. Dahlslett, B. Grenne, B. Sjoli, O. Smiseth, T. Edvardsen, and H. Brunvand, "Global longitudinal strain is a more reproducible measure of left ventricular function than ejection fraction regardless of echocardiographic training," *Cardiovasc Ultrasound*, vol. 17, no. 1, p. 18, 2019.

[117] T. Onishi, S. K. Saha, A. Delgado-Montero, D. R. Ludwig, T. Onishi, E. B. Schelbert, D. Schwartzman, and r. Gorcsan, J., "Global longitudinal strain and global circumferential strain by speckle-tracking echocardiography and feature-tracking cardiac magnetic resonance imaging: comparison with left ventricular ejection fraction," *J Am Soc Echocardiogr*, vol. 28, no. 5, pp. 587–96, 2015.

[118] C. Andersson and R. S. Vasan, "Epidemiology of heart failure with preserved ejection fraction," *Heart Fail Clin*, vol. 10, no. 3, pp. 377–88, 2014.

[119] B. J. Boukens, M. R. Rivaud, S. Rentschler, and R. Coronel, "Misinterpretation of the mouse ecg: 'musing the waves of mus musculus'," *J Physiol*, vol. 592, no. 21, pp. 4613–26, 2014.

[120] G. Quer, P. Gouda, M. Galarnyk, E. J. Topol, and S. R. Steinhubl, "Inter- and intraindividual variability in daily resting heart rate and its associations with age, sex, sleep, bmi, and time of year: Retrospective, longitudinal cohort study of 92,457 adults," *PLoS One*, vol. 15, no. 2, p. e0227709, 2020.

[121] C. D. Fryar, T. C. Chen, and X. Li, "Prevalence of uncontrolled risk factors for cardiovascular disease: United states, 1999-2010," *NCHS Data Brief*, no. 103, pp. 1–8, 2012.

[122] J. M. Gardin, R. McClelland, D. Kitzman, J. A. Lima, W. Bommer, H. S. Klopfenstein, N. D. Wong, V. E. Smith, and J. Gottdiener, "M-mode echocardiographic predictors of six- to seven-year incidence of coronary heart disease, stroke, congestive heart failure, and mortality in an elderly cohort (the cardiovascular health study)," *Am J Cardiol*, vol. 87, no. 9, pp. 1051–7, 2001.

[123] D. L. Aylor, W. Valdar, W. Foulds-Mathes, R. J. Buus, R. A. Verdugo, R. S. Baric, M. T. Ferris, J. A. Frelinger, M. Heise, M. B. Frieman, L. E. Gralinski, T. A. Bell, J. D. Didion, K. Hua, D. L. Nehrenberg, C. L. Powell, J. Steigerwalt, Y. Xie, S. N. Kelada, F. S. Collins, I. V. Yang, D. A. Schwartz, L. A. Branstetter, E. J. Chesler, D. R. Miller, J. Spence, E. Y. Liu, L. McMillan, A. Sarkar, J. Wang, W. Wang, Q. Zhang, K. W. Broman, R. Korstanje, C. Durrant, R. Mott, F. A. Iraqi, D. Pomp, D. Threadgill, F. P. de Villena, and G. A. Churchill, "Genetic analysis of complex traits in the emerging collaborative cross," *Genome Res*, vol. 21, no. 8, pp. 1213–22, 2011.

[124] R. Green, C. Wilkins, S. Thomas, A. Sekine, D. M. Hendrick, K. Voss, R. C. Ireton, M. Mooney, J. T. Go, G. Choonoo, S. Jeng, F. P. de Villena, M. T. Ferris, S. McWeeney, and J. Gale, M., "Oas1b-dependent immune transcriptional profiles of west nile virus infection in the collaborative cross," *G3 (Bethesda)*, vol. 7, no. 6, pp. 1665–1682, 2017.

[125] T. P. Tan, X. M. Gao, M. Krawczyszyn, X. Feng, H. Kiriazis, A. M. Dart, and X. J. Du, "Assessment of cardiac function by echocardiography in conscious and anesthetized mice: importance of the autonomic nervous system and disease state," *J Cardiovasc Pharmacol*, vol. 42, no. 2, pp. 182–90, 2003.

[126] J. A. Bouwknecht, T. H. Hijzen, J. van der Gugten, A. Dirks, R. A. Maes, R. Hen, M. A. Geyer, and B. Olivier, "Startle responses, heart rate, and temperature in 5-ht1b receptor knockout mice," *Neuroreport*, vol. 11, no. 18, pp. 4097–102, 2000.

[127] S. S. Khan, K. A. Kim, J. Peng, F. G. Aguilar, S. Selvaraj, E. E. Martinez, A. S. Baldridge, J. Sha, M. R. Irvin, U. Broeckel, D. K. Arnett, L. J. Rasmussen-Torvik, and S. J. Shah, "Clinical correlates and heritability of cardiac mechanics: The hypergen study," *Int J Cardiol*, vol. 274, pp. 208–213, 2019.

[128] K. Konganti, A. Ehrlich, I. Rusyn, and D. W. Threadgill, "gqtl: A web application for qtl analysis using the collaborative cross mouse genetic reference population," *G3 (Bethesda)*, vol. 8, no. 8, pp. 2559–2562, 2018.

[129] L. Gu, L. Wang, H. Chen, J. Hong, Z. Shen, A. Dhall, T. Lao, C. Liu, Z. Wang, Y. Xu, H. W. Tang, D. Chakraborty, J. Chen, Z. Liu, D. Rogulja, N. Perrimon, H. Wu, and Y. Shi, "Cg14906 (mettl4) mediates m(6)a methylation of u2 snrna in drosophila," *Cell Discov*, vol. 6, p. 44, 2020.

[130] Y. Fu, D. Dominissini, G. Rechavi, and C. He, "Gene expression regulation mediated through reversible m(6)a rna methylation," *Nat Rev Genet*, vol. 15, no. 5, pp. 293–306, 2014.

[131] P. Mathiyalagan, M. Adamiak, J. Mayourian, Y. Sassi, Y. Liang, N. Agarwal, D. Jha, S. Zhang, E. Kohlbrenner, E. Chepurko, J. Chen, M. G. Trivieri, R. Singh, R. Bouchareb, K. Fish, K. Ishikawa, D. Lebeche, R. J. Hajjar, and S. Sahoo, "Fto-dependent n(6)-methyladenosine regulates cardiac function during remodeling and repair," *Circulation*, vol. 139, no. 4, pp. 518–532, 2019.

[132] R. Knoll, M. Hoshijima, H. M. Hoffman, V. Person, I. Lorenzen-Schmidt, M. L. Bang, T. Hayashi, N. Shiga, H. Yasukawa, W. Schaper, W. McKenna, M. Yokoyama, N. J. Schork, J. H. Omens, A. D. McCulloch, A. Kimura, C. C. Gregorio, W. Poller, J. Schaper, H. P. Schultheiss, and K. R. Chien, "The cardiac mechanical stretch sensor machinery involves a z disc complex that is defective in a subset of human dilated cardiomyopathy," *Cell*, vol. 111, no. 7, pp. 943–55, 2002.

[133] C. Geier, K. Gehmlich, E. Ehler, S. Hassfeld, A. Perrot, K. Hayess, N. Cardim, K. Wenzel, B. Erdmann, F. Krackhardt, M. G. Posch, K. J. Osterziel, A. Bublak, H. Nagele, T. Scheffold, R. Dietz, K. R. Chien, S. Spuler, D. O. Furst, P. Nurnberg, and C. Ozcelik, "Beyond the sarcomere: Csrp3 mutations cause hypertrophic cardiomyopathy," *Hum Mol Genet*, vol. 17, no. 18, pp. 2753–65, 2008.

[134] X. Liao, R. Zhang, Y. Lu, D. A. Prosdocimo, P. Sangwung, L. Zhang, G. Zhou, P. Anand, L. Lai, T. C. Leone, H. Fujioka, F. Ye, M. G. Rosca, C. L. Hoppel, P. C. Schulze, E. D. Abel, J. S. Stamler, D. P. Kelly, and M. K. Jain, "Kruppel-like factor 4 is critical for transcriptional

control of cardiac mitochondrial homeostasis," *J Clin Invest*, vol. 125, no. 9, pp. 3461–76, 2015.

[135] G. A. Papadatos, P. M. Wallerstein, C. E. Head, R. Ratcliff, P. A. Brady, K. Benndorf, R. C. Saumarez, A. E. Trezise, C. L. Huang, J. I. Vandenberg, W. H. Colledge, and A. A. Grace, "Slowed conduction and ventricular tachycardia after targeted disruption of the cardiac sodium channel gene scn5a," *Proc Natl Acad Sci U S A*, vol. 99, no. 9, pp. 6210–5, 2002.

[136] T. King, Y. Bland, S. Webb, S. Barton, and N. A. Brown, "Expression of peg1 (mest) in the developing mouse heart: involvement in trabeculation," *Dev Dyn*, vol. 225, no. 2, pp. 212–5, 2002.

[137] Y. M. Tsutsumi, Y. T. Horikawa, M. M. Jennings, M. W. Kidd, I. R. Niesman, U. Yokoyama, B. P. Head, Y. Hagiwara, Y. Ishikawa, A. Miyanohara, P. M. Patel, P. A. Insel, H. H. Patel, and D. M. Roth, "Cardiac-specific overexpression of caveolin-3 induces endogenous cardiac protection by mimicking ischemic preconditioning," *Circulation*, vol. 118, no. 19, pp. 1979–88, 2008.

[138] V. S. Farook, S. Puppala, J. Schneider, S. P. Fowler, G. Chittoor, T. D. Dyer, H. Allayee, S. A. Cole, R. Arya, M. H. Black, J. E. Curran, L. Almasy, T. A. Buchanan, C. P. Jenkinson, D. M. Lehman, R. M. Watanabe, J. Blangero, and R. Duggirala, "Metabolic syndrome is linked to chromosome 7q21 and associated with genetic variants in cd36 and gnat3 in mexican americans," *Obesity (Silver Spring)*, vol. 20, no. 10, pp. 2083–92, 2012.

[139] Y. M. Zhang, J. Bo, G. E. Taffet, J. Chang, J. Shi, A. K. Reddy, L. H. Michael, M. D. Schneider, M. L. Entman, R. J. Schwartz, and L. Wei, "Targeted deletion of rock1 protects the heart against pressure overload by inhibiting reactive fibrosis," *FASEB J*, vol. 20, no. 7, pp. 916–25, 2006.

[140] S. Sunamura, K. Satoh, R. Kurosawa, T. Ohtsuki, N. Kikuchi, M. Elias-Al-Mamun, T. Shimizu, S. Ikeda, K. Suzuki, T. Satoh, J. Omura, M. Nogi, K. Numano, M. A. H. Sid-

dique, S. Miyata, M. Miura, and H. Shimokawa, "Different roles of myocardial rock1 and rock2 in cardiac dysfunction and postcapillary pulmonary hypertension in mice," *Proc Natl Acad Sci U S A*, vol. 115, no. 30, pp. E7129–E7138, 2018.

[141] K. Subramanian, D. Gianni, C. Balla, G. E. Assenza, M. Joshi, M. J. Semigran, T. E. Macgillivray, J. E. Van Eyk, G. Agnetti, N. Paolocci, J. R. Bamburg, P. B. Agrawal, and F. Del Monte, "Cofilin-2 phosphorylation and sequestration in myocardial aggregates: novel pathogenetic mechanisms for idiopathic dilated cardiomyopathy," *J Am Coll Cardiol*, vol. 65, no. 12, pp. 1199–1214, 2015.

[142] D. E. Arking, S. L. Pulit, L. Crotti, P. van der Harst, P. B. Munroe, T. T. Koopmann, N. Sotoodehnia, E. J. Rossin, M. Morley, X. Wang, A. D. Johnson, A. Lundby, D. F. Gudbjartsson, P. A. Noseworthy, M. Eijgelsheim, Y. Bradford, K. V. Tarasov, M. Dorr, M. Muller-Nurasyid, A. M. Lahtinen, I. M. Nolte, A. V. Smith, J. C. Bis, A. Isaacs, S. J. Newhouse, D. S. Evans, W. S. Post, D. Waggott, L. P. Lyytikainen, A. A. Hicks, L. Eisele, D. Ellinghaus, C. Hayward, P. Navarro, S. Ulivi, T. Tanaka, D. J. Tester, S. Chatel, S. Gustafsson, M. Kumari, R. W. Morris, A. T. Naluai, S. Padmanabhan, A. Kluttig, B. Strohmer, A. G. Panayiotou, M. Torres, M. Knoflach, J. A. Hubacek, K. Slowikowski, S. Raychaudhuri, R. D. Kumar, T. B. Harris, L. J. Launer, A. R. Shuldiner, A. Alonso, J. S. Bader, G. Ehret, H. Huang, W. H. Kao, J. B. Strait, P. W. Macfarlane, M. Brown, M. J. Caulfield, N. J. Samani, F. Kronenberg, J. Willeit, C. A. Consortium, C. Consortium, J. G. Smith, K. H. Greiser, H. Meyer Zu Schwabedissen, K. Werdan, M. Carella, L. Zelante, S. R. Heckbert, B. M. Psaty, J. I. Rotter, I. Kolcic, O. Polasek, A. F. Wright, M. Griffin, M. J. Daly, Dcct/Edic, D. O. Arnar, H. Holm, U. Thorsteinsdottir, M. C. e, J. C. Denny, D. M. Roden, R. L. Zuvich, V. Emilsson, A. S. Plump, M. G. Larson, C. J. O'Donnell, X. Yin, M. Bobbo, A. P. D'Adamo, A. Iorio, G. Sinagra, *et al.*, "Genetic association study of qt interval highlights role for calcium signaling pathways in myocardial repolarization," *Nat Genet*, vol. 46, no. 8, pp. 826–36, 2014.

[143] S. T. Turner, E. Boerwinkle, J. R. O'Connell, K. R. Bailey, Y. Gong, A. B. Chapman,

C. W. McDonough, A. L. Beitelshees, G. L. Schwartz, J. G. Gums, S. Padmanabhan, T. P. Hiltunen, L. Citterio, K. M. Donner, T. Hedner, C. Lanzani, O. Melander, J. Saarela, S. Ripatti, B. Wahlstrand, P. Manunta, K. Kontula, A. F. Dominiczak, R. M. Cooper-DeHoff, and J. A. Johnson, "Genomic association analysis of common variants influencing antihypertensive response to hydrochlorothiazide," *Hypertension*, vol. 62, no. 2, pp. 391–7, 2013.

[144] J. C. Braz, K. Gregory, A. Pathak, W. Zhao, B. Sahin, R. Klevitsky, T. F. Kimball, J. N. Lorenz, A. C. Nairn, S. B. Liggett, I. Bodi, S. Wang, A. Schwartz, E. G. Lakatta, A. A. DePaoli-Roach, J. Robbins, T. E. Hewett, J. A. Bibb, M. V. Westfall, E. G. Kranias, and J. D. Molkentin, "Pkc-alpha regulates cardiac contractility and propensity toward heart failure," *Nat Med*, vol. 10, no. 3, pp. 248–54, 2004.

[145] J. C. Mays, M. C. Kelly, S. L. Coon, L. Holtzclaw, M. F. Rath, M. W. Kelley, and D. C. Klein, "Single-cell rna sequencing of the mammalian pineal gland identifies two pinealocyte subtypes and cell type-specific daily patterns of gene expression," *PLoS One*, vol. 13, no. 10, p. e0205883, 2018.

[146] J. Mester-Tonczar, P. Einzinger, J. Winkler, N. Kastner, A. Spannbauer, K. Zlabinger, D. Traxler, D. Lukovic, E. Hasimbegovic, G. Goliasch, N. Pavo, and M. Gyongyosi, "Novel identified circular transcript of rcan2, circ-rcan2, shows deviated expression pattern in pig reperfused infarcted myocardium and hypoxic porcine cardiac progenitor cells in vitro," *Int J Mol Sci*, vol. 22, no. 3, 2021.

[147] M. Eijgelsheim, C. Newton-Cheh, N. Sotoodehnia, P. I. de Bakker, M. Muller, A. C. Morrison, A. V. Smith, A. Isaacs, S. Sanna, M. Dorr, P. Navarro, C. Fuchsberger, I. M. Nolte, E. J. de Geus, K. Estrada, S. J. Hwang, J. C. Bis, I. M. Ruckert, A. Alonso, L. J. Launer, J. J. Hottenga, F. Rivadeneira, P. A. Noseworthy, K. M. Rice, S. Perz, D. E. Arking, T. D. Spector, J. A. Kors, Y. S. Aulchenko, K. V. Tarasov, G. Homuth, S. H. Wild, F. Marroni, C. Gieger, C. M. Licht, R. J. Prineas, A. Hofman, J. I. Rotter, A. A. Hicks, F. Ernst, S. S. Najjar, A. F. Wright, A. Peters, E. R. Fox, B. A. Oostra, H. K. Kroemer, D. Couper, H. Volzke,

H. Campbell, T. Meitinger, M. Uda, J. C. Witteman, B. M. Psaty, H. E. Wichmann, T. B. Harris, S. Kaab, D. S. Siscovick, Y. Jamshidi, A. G. Uitterlinden, A. R. Folsom, M. G. Larson, J. F. Wilson, B. W. Penninx, H. Snieder, P. P. Pramstaller, C. M. van Duijn, E. G. Lakatta, S. B. Felix, V. Gudnason, A. Pfeufer, S. R. Heckbert, B. H. Stricker, E. Boerwinkle, and C. J. O'Donnell, "Genome-wide association analysis identifies multiple loci related to resting heart rate," *Hum Mol Genet*, vol. 19, no. 19, pp. 3885–94, 2010.

[148] P. Yu, M. Liu, B. Zhang, Y. Yu, E. Su, S. Xie, L. Zhang, X. Yang, H. Jiang, R. Chen, Y. Zou, and J. Ge, "Cardiomyocyte-restricted high-mobility group box 1 (hmgb1) deletion leads to small heart and glycolipid metabolic disorder through gr/pgc-1alpha signalling," *Cell Death Discov*, vol. 6, p. 106, 2020.

[149] R. A. Helmer, R. Martinez-Zaguilan, J. S. Dertien, C. Fulford, O. Foreman, V. Peiris, and B. S. Chilton, "Helicase-like transcription factor (hltf) regulates g2/m transition, wt1/gata4/hif-1a cardiac transcription networks, and collagen biogenesis," *PLoS One*, vol. 8, no. 11, p. e80461, 2013.

[150] S. Y. Lim, D. J. Hausenloy, S. Arjun, A. N. Price, S. M. Davidson, M. F. Lythgoe, and D. M. Yellon, "Mitochondrial cyclophilin-d as a potential therapeutic target for post-myocardial infarction heart failure," *J Cell Mol Med*, vol. 15, no. 11, pp. 2443–51, 2011.

[151] H. Q. Hong, J. Lu, X. L. Fang, Y. H. Zhang, Y. Cai, J. Yuan, P. Q. Liu, and J. T. Ye, "G3bp2 is involved in isoproterenol-induced cardiac hypertrophy through activating the nf-kappab signaling pathway," *Acta Pharmacol Sin*, vol. 39, no. 2, pp. 184–194, 2018.

[152] P. Liu, M. Sun, and S. Sader, "Matrix metalloproteinases in cardiovascular disease," *Can J Cardiol*, vol. 22 Suppl B, pp. 25B–30B, 2006.

[153] M. Quesnel-Vallieres, M. Irimia, S. P. Cordes, and B. J. Blencowe, "Essential roles for the splicing regulator nsr100/srrm4 during nervous system development," *Genes Dev*, vol. 29, no. 7, pp. 746–59, 2015.

[154] A. Pooryasin, M. Maglione, M. Schubert, T. Matkovic-Rachid, S. M. Hasheminasab, U. Pech, A. Fiala, T. Mielke, and S. J. Sigrist, "Unc13a and unc13b contribute to the decoding of distinct sensory information in drosophila," *Nat Commun*, vol. 12, no. 1, p. 1932, 2021.

[155] I. Augustin, C. Rosenmund, T. C. Sudhof, and N. Brose, "Munc13-1 is essential for fusion competence of glutamatergic synaptic vesicles," *Nature*, vol. 400, no. 6743, pp. 457–61, 1999.

[156] P. Z. Hang, H. Zhu, P. F. Li, J. Liu, F. Q. Ge, J. Zhao, and Z. M. Du, "The emerging role of bdnf/trkb signaling in cardiovascular diseases," *Life (Basel)*, vol. 11, no. 1, 2021.

[157] N. Feng, S. Huke, G. Zhu, C. G. Tocchetti, S. Shi, T. Aiba, N. Kaludercic, D. B. Hoover, S. E. Beck, J. L. Mankowski, G. F. Tomaselli, D. M. Bers, D. A. Kass, and N. Paolocci, "Constitutive bdnf/trkb signaling is required for normal cardiac contraction and relaxation," *Proc Natl Acad Sci U S A*, vol. 112, no. 6, pp. 1880–5, 2015.

[158] G. Fulgenzi, F. Tomassoni-Ardori, L. Babini, J. Becker, C. Barrick, S. Puverel, and L. Tessarollo, "Bdnf modulates heart contraction force and long-term homeostasis through truncated trkb.t1 receptor activation," *J Cell Biol*, vol. 210, no. 6, pp. 1003–12, 2015.

[159] M. T. Keating and M. C. Sanguinetti, "Molecular and cellular mechanisms of cardiac arrhythmias," *Cell*, vol. 104, no. 4, pp. 569–80, 2001.

[160] E. Marban, "Cardiac channelopathies," *Nature*, vol. 415, no. 6868, pp. 213–8, 2002.

[161] G. Salama and B. London, "Mouse models of long qt syndrome," *J Physiol*, vol. 578, no. Pt 1, pp. 43–53, 2007.

[162] D. Ho, X. Zhao, S. Gao, C. Hong, D. E. Vatner, and S. F. Vatner, "Heart rate and electrocardiography monitoring in mice," *Curr Protoc Mouse Biol*, vol. 1, pp. 123–139, 2011.

[163] S. Gao, D. Ho, D. E. Vatner, and S. F. Vatner, "Echocardiography in mice," *Curr Protoc Mouse Biol*, vol. 1, pp. 71–83, 2011.

[164] N. Ferri, P. Siegl, A. Corsini, J. Herrmann, A. Lerman, and R. Benghozi, "Drug attrition during pre-clinical and clinical development: understanding and managing drug-induced cardiotoxicity," *Pharmacol Ther*, vol. 138, no. 3, pp. 470–84, 2013.

[165] K. Kocadal, S. Saygi, F. B. Alkas, and S. Sardas, "Drug-associated cardiovascular risks: A retrospective evaluation of withdrawn drugs," *North Clin Istanb*, vol. 6, no. 2, pp. 196–202, 2019.

[166] A. Pruss-Ustun and C. Corvalan, "Preventing disease through healthy environments: Towards an estimate of the environmental burden of disease," *Geneva, Switzerland: World Health Organization*, 2006.

[167] R. Judson, A. Richard, D. J. Dix, K. Houck, M. Martin, R. Kavlock, V. Dellarco, T. Henry, T. Holderman, P. Sayre, S. Tan, T. Carpenter, and E. Smith, "The toxicity data landscape for environmental chemicals," *Environ Health Perspect*, vol. 117, no. 5, pp. 685–95, 2009.

[168] R. R. Maronpot, A. Nyska, J. E. Foreman, and Y. Ramot, "The legacy of the f344 rat as a cancer bioassay model (a retrospective summary of three common f344 rat neoplasms)," *Crit Rev Toxicol*, vol. 46, no. 8, pp. 641–75, 2016.

[169] S. C. Chang, S. Ren, C. D. Rau, and J. J. Wang, "Isoproterenol-induced heart failure mouse model using osmotic pump implantation," *Methods Mol Biol*, vol. 1816, pp. 207–220, 2018.

[170] M. Jelinek, C. Wallach, H. Ehmke, and A. P. Schwoerer, "Genetic background dominates the susceptibility to ventricular arrhythmias in a murine model of beta-adrenergic stimulation," *Sci Rep*, vol. 8, no. 1, p. 2312, 2018.

[171] C. Berthonneche, B. Peter, F. Schupfer, P. Hayoz, Z. Kutalik, H. Abriel, T. Pedrazzini, J. S. Beckmann, S. Bergmann, and F. Maurer, "Cardiovascular response to beta-adrenergic blockade or activation in 23 inbred mouse strains," *PLoS One*, vol. 4, no. 8, p. e6610, 2009.

[172] J. J. Wang, C. Rau, R. Avetisyan, S. Ren, M. C. Romay, G. Stolin, K. W. Gong, Y. Wang, and A. J. Lusis, "Genetic dissection of cardiac remodeling in an isoproterenol-induced heart failure mouse model," *PLoS Genet*, vol. 12, no. 7, p. e1006038, 2016.

[173] R. I. Fox, "Mechanism of action of hydroxychloroquine as an antirheumatic drug," *Semin Arthritis Rheum*, vol. 23, no. 2 Suppl 1, pp. 82–91, 1993.

[174] C. Chatre, F. Roubille, H. Vernhet, C. Jorgensen, and Y. M. Pers, "Cardiac complications attributed to chloroquine and hydroxychloroquine: A systematic review of the literature," *Drug Saf*, vol. 41, no. 10, pp. 919–931, 2018.

[175] N. L. Diny, X. Hou, J. G. Barin, G. Chen, M. V. Talor, J. Schaub, S. D. Russell, K. Klingel, N. R. Rose, and D. Cihakova, "Macrophages and cardiac fibroblasts are the main producers of eotaxins and regulate eosinophil trafficking to the heart," *Eur J Immunol*, vol. 46, no. 12, pp. 2749–2760, 2016.

[176] M. A. Kasinska, J. Drzewoski, and A. Sliwinska, "Epigenetic modifications in adipose tissue - relation to obesity and diabetes," *Arch Med Sci*, vol. 12, no. 6, pp. 1293–1301, 2016.

[177] I. Portig, F. Kliebe, C. Kliebe, V. Ruppert, and B. Maisch, "Hspa1b polymorphism in familial forms of inflammatory dilated cardiomyopathy," *Int J Cardiol*, vol. 133, no. 1, pp. 126–8, 2009.

[178] A. Riddell, M. McBride, T. Braun, S. A. Nicklin, E. Cameron, C. M. Loughrey, and T. P. Martin, "Runx1: an emerging therapeutic target for cardiovascular disease," *Cardiovasc Res*, vol. 116, no. 8, pp. 1410–1423, 2020.

[179] A. L. Chancey, G. L. Brower, J. T. Peterson, and J. S. Janicki, "Effects of matrix metalloproteinase inhibition on ventricular remodeling due to volume overload," *Circulation*, vol. 105, no. 16, pp. 1983–8, 2002.

[180] S. Sasagawa, Y. Nishimura, S. Okabe, S. Murakami, Y. Ashikawa, M. Yuge, K. Kawaguchi, R. Kawase, R. Okamoto, M. Ito, and T. Tanaka, "Downregulation of gstk1 is a common mechanism underlying hypertrophic cardiomyopathy," *Front Pharmacol*, vol. 7, p. 162, 2016.

[181] T. Yoshida, T. Fukuda, M. Hatano, H. Koseki, S. Okabe, K. Ishibashi, S. Kojima, M. Arima, I. Komuro, G. Ishii, T. Miki, S. Hirosawa, N. Miyasaka, M. Taniguchi, T. Ochiai, K. Isono,

and T. Tokuhisa, "The role of bcl6 in mature cardiac myocytes," *Cardiovasc Res*, vol. 42, no. 3, pp. 670–9, 1999.

[182] C. D. Rau, J. Wang, R. Avetisyan, M. C. Romay, L. Martin, S. Ren, Y. Wang, and A. J. Lusis, "Mapping genetic contributions to cardiac pathology induced by beta-adrenergic stimulation in mice," *Circ Cardiovasc Genet*, vol. 8, no. 1, pp. 40–9, 2015.

[183] M. Hernandez-Valladares, P. Rihet, and F. A. Iraqi, "Host susceptibility to malaria in human and mice: compatible approaches to identify potential resistant genes," *Physiol Genomics*, vol. 46, no. 1, pp. 1–16, 2014.

[184] G. M. Paganotti, B. C. Gallo, F. Verra, B. S. Sirima, I. Nebie, A. Diarra, M. Coluzzi, and D. Modiano, "Human genetic variation is associated with plasmodium falciparum drug resistance," *J Infect Dis*, vol. 204, no. 11, pp. 1772–8, 2011.

[185] C. Zaragoza, C. Gomez-Guerrero, J. L. Martin-Ventura, L. Blanco-Colio, B. Lavin, B. Mallavia, C. Tarin, S. Mas, A. Ortiz, and J. Egido, "Animal models of cardiovascular diseases," *J Biomed Biotechnol*, vol. 2011, p. 497841, 2011. Zaragoza, Carlos Gomez-Guerrero, Carmen Martin-Ventura, Jose Luis Blanco-Colio, Luis Lavin, Begona Mallavia, Benat Tarin, Carlos Mas, Sebastian Ortiz, Alberto Egido, Jesus eng Research Support, Non-U.S. Gov't Review J Biomed Biotechnol. 2011;2011:497841. doi: 10.1155/2011/497841. Epub 2011 Feb 16.

[186] G. R. Keele, W. L. Crouse, S. N. P. Kelada, and W. Valdar, "Determinants of qtl mapping power in the realized collaborative cross," *G3 (Bethesda)*, vol. 9, no. 5, pp. 1707–1727, 2019.

[187] F. A. Grimm, A. Blanchette, J. S. House, K. Ferguson, N. H. Hsieh, C. Dalaijamts, A. A. Wright, B. Anson, F. A. Wright, W. A. Chiu, and I. Rusyn, "A human population-based organotypic in vitro model for cardiotoxicity screening," *ALTEX*, vol. 35, no. 4, pp. 441–452, 2018.

[188] K. Blinova, J. Stohlman, J. Vicente, D. Chan, L. Johannesen, M. P. Hortigon-Vinagre, V. Zamora, G. Smith, W. J. Crumb, L. Pang, B. Lyn-Cook, J. Ross, M. Brock, S. Chvatal, D. Millard, L. Galeotti, N. Stockbridge, and D. G. Strauss, "Comprehensive translational assessment of human-induced pluripotent stem cell derived cardiomyocytes for evaluating drug-induced arrhythmias," *Toxicol Sci*, vol. 155, no. 1, pp. 234–247, 2017.

[189] K. Kolaja, "Stem cells and stem cell-derived tissues and their use in safety assessment," *J Biol Chem*, vol. 289, no. 8, pp. 4555–61, 2014.

[190] P. T. Lieu, A. Fontes, M. C. Vemuri, and C. C. Macarthur, "Generation of induced pluripotent stem cells with cytotune, a non-integrating sendai virus," *Methods Mol Biol*, vol. 997, pp. 45–56, 2013.

APPENDIX A

FIGURES

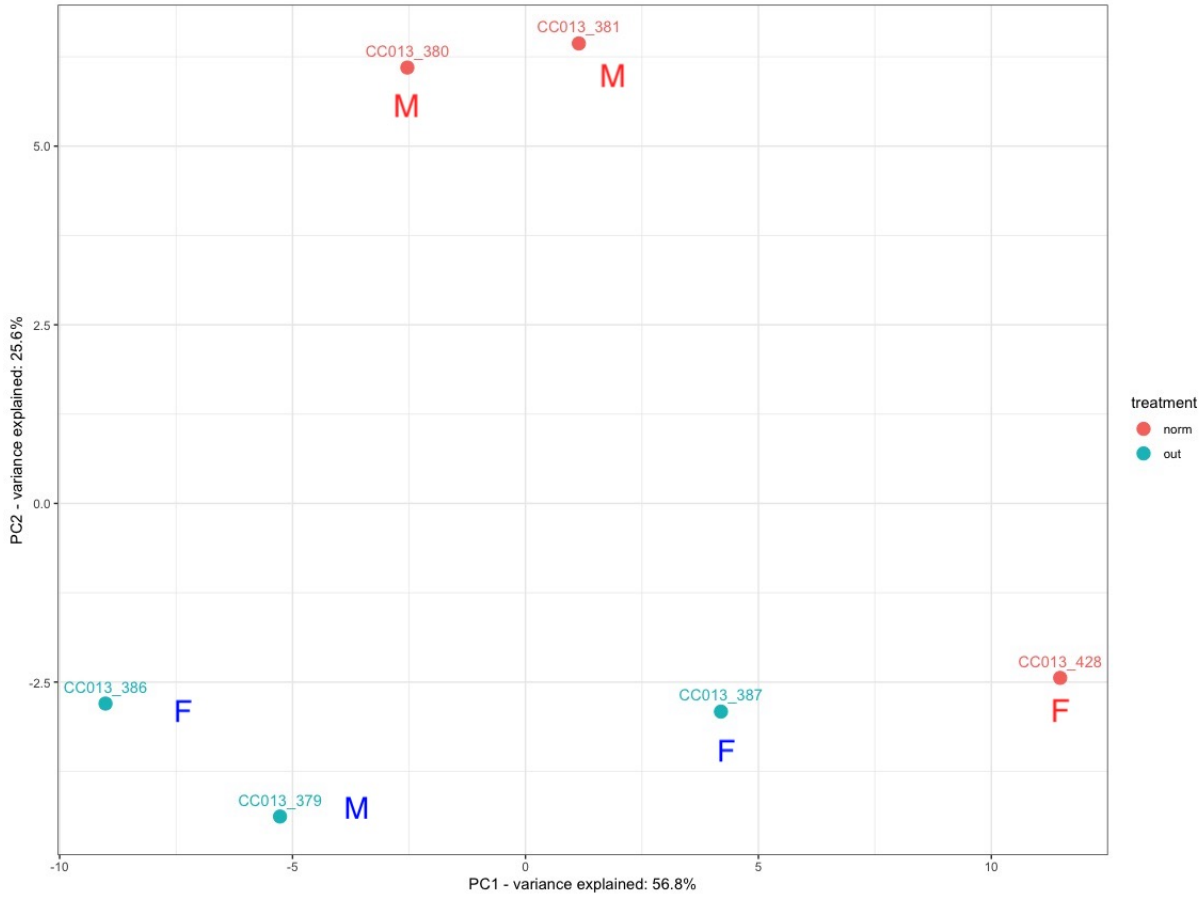

Figure A.1: Comparison of CC013 phenotypes. Dilated cardiomyopathic mice cluster in PCA

Text for the Appendix follows.

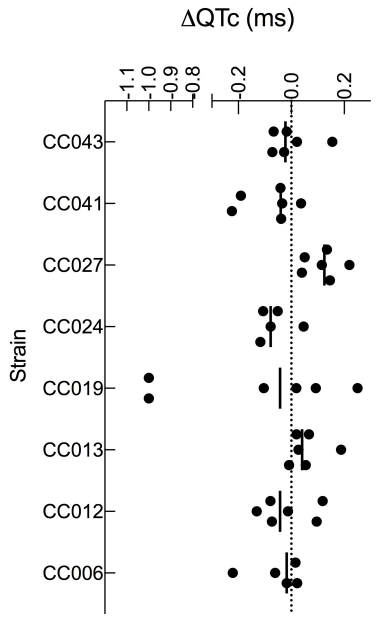

Figure A.2: Scatterplots of ΔQTc of isoproterenol treated mice. Horizontal bars represent median values for each strain.